Studies on Differentiation Mechanisms of Epithelial Cells in the Digestive System

Studies on Differentiation Mechanisms of Epithelial Cells in the Digestive System

A Dissertation Submitted to
the Graduate School of Life and Environmental Sciences,
the University of Tsukuba
in Partial Fulfillment of the Requirements
for the Degree of Doctor of Philosophy in Biological Science
(Doctoral Program in Biological Sciences)

Masakazu SUGIYAMA

Table of Contents

Abstract

Accumulation of genetic mutation in cancer cells and extracellular stimuli, for instance, cytokines released from the microenvironment such as chronic inflammation surrounding cancer cells, seem to trigger dedifferentiation resulting in gaining of stemness or epithelial-mesenchymal transition (EMT). It is hypothesized that this transition from differentiated epithelial cells is critical for the progression, recurrence, and drug resistance of gastrointestinal and liver cancer. Therefore, it is important to study the mechanisms underlying the transition of differentiation status in epithelial cells in order to explore novel strategies for drug discovery in cancer.

In the first part of this work, the transition of differentiation status between stem/progenitor cells and hepatocytes, which are differentiated epithelial cells from the adult mouse liver, was investigated. Moreover, the contribution of autophagy to the mechanism for the alteration of differentiation status between the stem/progenitor cells and hepatocytes was assessed. Adult stem/progenitor cells were isolated from the livers of mice with chemically-induced liver injury. The effect of autophagy on hepatic differentiation was investigated by silencing the gene encoding autophagy protein 5 (*ATG5)* using small interfering RNAs. *ATG5* silencing suppressed autophagy as observed by decreased active microtubule-associated protein light chain 3 (LC3) and increased p62 expression. Inhibition of autophagy promoted hepatic differentiation in the stem/progenitor cells. A mechanism suggested for the hepatic differentiation induced by inhibiting autophagy was the accumulation of intracellular p62 protein and activation of the mammalian target of rapamycin pathway by amino acids.

In the second part, I investigated the role of the Notch ligand, Jagged 1 (JAG1), and EMT in the prognosis and recurrence of human subjects with colorectal cancer (CRC).

The protein expression of JAG1 in CRC specimens was examined using immunohistochemistry. Moreover, EMT in CRC was evaluated based on the decreased protein expression levels of the well-differentiated epithelial cell marker, E-cadherin, using immunohistochemistry. The correlation of JAG1 expression with overall survival (OS), relapse-free survival (RFS), and E-cadherin expression was analyzed. JAG1 expression in cancerous tissues was graded as weak, moderate, or strong and higher JAG1 expression was associated with poorer prognostic outcomes. A correlation between high intensity of JAG1 staining and a low population of E-cadherin-positive cancer cells was detected in the analysis of JAG1 and E-cadherin expression. A mechanism for high JAG1 expression and EMT induction in CRC was suggested based on the significant correlation observed between JAG1 expression and KRAS status in groups stratified by high E-cadherin expression. *In vitro* studies using a colon cancer cell line supported the results from the human studies. Gene silencing using siRNA against JAG1 (siJAG1) indicated that JAG1 promotes EMT. An investigation using an MEK inhibitor suggested that the RAS-MEK-MAP pathway positively regulates JAG1 expression and EMT.

Taken together, I propose that suppression of autophagy and JAG1-Notch-related signaling could revert dedifferentiated epithelial cancer cells to a well-differentiated status in the gastrointestinal tract and in liver cancer. Further, elucidation of these regulation mechanisms for the transition of differentiation status in epithelial cells could lead to the discovery of new drug candidates to prevent the progression, recurrence, drug resistance, or metastasis of gastrointestinal and liver cancer.

Abbreviations

18s rRNA	18s ribosomal RNA
3-MA	3-methyladenine
AF	Alexa Fluor
ALB	albumin
ALK	anaplastic lymphoma kinase
Apc	adenomatous polyposis coli
APC	allophycocyanin
ATG5	autophagy-related gene 5
BCAA	branched chain amino acid
CD	cluster of differentiation
CI	confidence interval
CK	cytokeratin
CLiPs	chemically induced liver stem/progenitor cells
CMS	consensus molecular subtype
CRC	colorectal cancer
CSC	cancer stem cell
DDC	3,5-diethoxycarbonyl-1,4-dihydrocollidine
DLL	delta-like ligand
DMSO	dimethylsulfoxide
EGF	epidermal growth factor
EMT	epithelial-mesenchymal transition
EMT-TF	EMT-inducing transcription factors
ERK	extracellular signal-regulated kinase
FACS	fluorescence-activated cell sorting
FBP	fructose-1,6-bisphosphatase
GAPDH	glyceraldehyde-3-phosphate dehydrogenase
GSK	glycogen synthase kinase
HES	hairy and enhancer of split
HGF	hepatocyte growth factor
HNF	hepatocyte nuclear factor
HR	hazard ratio
IHC	immunohistochemistry
IL	interleukin

JAG	Jagged
KEAP	kelch like ECH associated protein
LC3	microtubule-associated protein light chain 3
Leu	leucine
LPC	liver stem/progenitiro cell
MAPK	mitogen-activated protein kinase
miRNA	micro-RNA
Mod	moderate
MSI	microsatellite instability
MSI-H	high MSI
MSI-L	low MSI
mTOR	mammalian target of rapamycin
mTORC	mTOR complex
NICD	notch intracellular domain
NRF	NF-E2-related factor
NS	nonspecific
NF	nuclear factor
OS	overall survival
OSM	oncostatin M
oval-cell-like	cells similar to oval cells
p53KO	$p53^{-/-}$ cells
pAKT	phosphorylated AKT
PBS	phosphate buffered saline
PCR	polymerase chain reaction
PDGF	platelet-derived growth factor
PE	phycoerythrin
pERK	phosphorylated ERK
PI3K	phosphoinositide 3-kinase
pS6	phosphorylated ribosomal S6 protein
qRT-PCR	quantitative RT-PCR
RFS	relapse-free survival
ROCK	Rho-associated, coiled-coil containing protein kinase
S.D.	standard deviations
siATG5	siRNAs against autophagic factor ATG5
siJAG1	siRNA against JAG1
si*SQSTM1*/p62	siRNA against *SQSTM1*/p62

siNON	non-targeting siRNA
siRNA	Small interfering RNA
SQSTM1	sequestosome 1
TGF	transforming growth factor
TP53	tumor protein p53
VIM	vimentin
Wt	Wild type
ZEB	zinc finger E-box-binding homeobox

General Introduction

Treatment strategies for human cancers such as surgery, drug treatment, radiotherapy, and a combination of these frequently produce failed results in clinical cases. Drug resistance and/or radioresistance, tumor recurrence, and metastasis are considered as the major reasons for treatment failure. Increasing evidence has shown that cancer stem cells (CSCs) are the root causes of tumor formation and recurrence (Gupta et al., 2009; Sato et al., 2016; Suresh et al., 2016; Zeuner et al., 2014). Moreover, epithelial-mesenchymal transition (EMT) plays a significant role in cancer progression. The acquisition of invasiveness in epithelial cancer cells is thought to be the first step that eventually leads to metastatic dissemination with life-threatening consequences. Activation of the EMT program has been proposed as the critical mechanism for the acquisition of an invasive phenotype and the subsequent systemic spread of epithelial cancer cells (Nieto, 2013; Sato et al., 2016; Thiery, 2002; Zheng and Kang, 2014). Therefore, to overcome the failed outcome and improve the efficacy of traditional anticancer therapies, it is important to understand the regulatory mechanisms underlying CSCs and EMT related processes.

The adult liver contains two main epithelial cell types, the hepatocytes and the bile duct epithelial cells. In the normal state without injury, cell turnover is very slow (Magami et al., 2002; Malato et al., 2011; Sell, 2001). However, the liver is a highly regenerative organ and can completely restore its mass after injury (Michalopoulos and DeFrances, 1997). The liver has been proposed to possess facultative stem cells that can become activated if any injury impairs the replication ability of the mature cells, particularly hepatocytes (Miyajima et al., 2014). These facultative stem cells are believed to exist near the portal region of the hepatic lobule in the canal of Hering

(Theise et al., 1999). After activation, these stem cells are thought to proliferate and produce progenitor cells called “oval cells,” which then differentiate into functional mature hepatocytes.

A previous study showed that Notch and Wnt are required for the differentiation of liver stem/progenitor cells (LPCs), and that their interaction is necessary for the appropriate delineation of hepatocellular versus biliary fate (Boulter et al., 2012). During the activation of LPCs in biliary disease, LPCs express Notch receptors, which are activated through interaction with Jagged 1 (JAG1) expressed by the surrounding fibroblasts.

The ductular reaction that occurs at the periphery of portal tracts is a response to the injury observed in liver diseases, including hepatitis C virus infection (Lowes et al., 1999). In chronic human liver disease, ductular proliferations containing cells similar to oval cells (oval-cell-like) are found frequently (Clouston et al., 2005; Richardson et al., 2007). Some recent experiments in mice indicated that oval-cell-like cells are transdifferentiated from hepatocytes through Notch-mediated cell lineage conversion rather than having a biliary origin (Sekiya and Suzuki, 2014; Tarlow et al., 2014; Yanger et al., 2013; Yimlamai et al., 2014). Thus, during oval-cell-inducing injury, hepatocytes could produce cells similar to LPCs if the injury was long-lived. Moreover, hepatocyte-derived-LPCs like cells have recently been shown to be capable of self-renewal, as well as differentiation into functional hepatocytes (Tarlow et al., 2014). This ductular plasticity of hepatocytes is also relevant to liver cancer, particularly cholangiocarcinoma (Deugnier et al., 1993; Prior, 1988; Tsukuma et al., 1993), which in the past was thought to be derived from proposed hepatic stem cells, but can in fact originate from hepatocytes (Fan et al., 2012; Sekiya and Suzuki, 2012). Thus,

identification of the signals that control cell plasticity transiting between a well-differentiated and a stem-like state in the liver, seems important to develop strategies for cancer therapy (Katsuda et al., 2017; Tarlow et al., 2014; Yimlamai et al., 2014).

To investigate liver cancers that are relevant to ductular reaction, experimental rodent models have been developed with chronic liver injury induced by potential carcinogens, including choline-deficient/ethionine-containing and 3,5-diethoxycarbonyl-1,4-dihydrocollidine (DDC)-containing diets (Preisegger et al., 1999; Shinozuka et al., 1978). In these models, biliary lineage cells that include oval cells appear and proliferate around the portal veins to regenerate the damaged liver tissues. Moreover, previous studies using these rodent models of chronic liver injury demonstrated their utility to study the progression of human primary liver cancers (Dumble et al., 2002; Suzuki et al., 2008). Thus, to develop therapeutic strategies for liver diseases, it is important to understand how oval-cell-containing biliary lineage cells emerge during the ductular reaction and contribute to the progression of chronic liver disease and liver cancer in these chronic liver injury models.

Autophagy, a process of degrading and recycling proteins and damaged cellular organs, has been shown to protect cells from nutritional deficiency and prevent cell death. Multiple studies have closely linked autophagy to many disease processes, especially cancers (Galluzzi et al., 2016; Gu et al., 2014; Lei et al., 2017; Li et al., 2017; Song et al., 2013). CSCs have characteristics similar to normal stem cells, such as self-renewal and differentiation. Autophagy might be involved in stemness maintenance of CSCs. Recently, researchers noted that elevated autophagic flux in CSCs could maintain metabolic homeostasis and cell viability, which facilitated CSCs to resist

microenvironmental stresses such as hypoxia, starvation, or anticancer treatment. Some studies found that inhibiting autophagy might be responsible in part, for the downregulation of stem cell markers, enhanced sensitivity to chemotherapeutics, and inhibition of CSCs self-renewal (Berardi et al., 2016; Zhang et al., 2016; Zhang et al., 2017). Thus, a pro-survival autophagic pathway may be critical for CSCs maintenance.

The aim of the present study was to investigate the role of autophagy inhibition and the related mechanism for hepatic differentiation from facultative LPCs or cells similar to LPCs potentially derived from mature hepatocytes collected from the liver during oval-cell inducing injury in a rodent model of chronic liver injury. I then discuss the role of autophagy and the related mechanism for maintaining stemness and cell plasticity transiting between stem/progenitor cells and differentiated cells.

Carcinogenesis arises from a series of genetic/epigenetic alterations and interactions with the microenvironment and growth factors that transform the normal intestinal mucosa into an aberrant phenotype (Becht et al., 2016; Carethers and Jung, 2015; Lampropoulos et al., 2012; Linnekamp et al., 2015; Markowitz and Bertagnolli, 2009; Zeuner et al., 2014). Tumor heterogeneity can be explained by the assembly of random genetic abnormalities as well as varying microenvironmental influences. A diverse population of subclones with different characteristics arises simultaneously. However, only selected clones can accumulate further mutations, resulting in a varying metastatic tumor from the primary lesion.

Intestinal homeostasis is regulated by the crosstalk of evolutionarily conserved pathways such as Wnt, Notch, and Hedgehog, which control the balance between proliferation, differentiation, migration, and renewal. Notch signaling is associated with multiple aspects of cancer biology (Espinoza and Miele, 2013). This pathway comprises

five canonical Notch ligands (Delta-like ligand 1 [DLL1], DLL3 and DLL4, and JAG1 and JAG2) and four Notch receptor paralogues (Notch1 – 4) (Gu et al., 2012). Unlike the DLL1/4 ligands, JAG1 was found to be dispensable for the homeostasis of normal intestinal stem cells (Pellegrinet et al., 2011); however, JAG1 has been shown to participate in multiple aspects of cancer biology including tumor angiogenesis, neoplastic cell growth, CSCs, EMT, the metastatic process, and resistance to therapy in several types of cancer. Importantly, JAG1 expression can be induced by signaling pathways such as transforming growth factor-β (TGF-β), Wnt-β-catenin, Interleukin-6 (IL-6), and Nuclear factor-κB (NF-κB), as well as by the Notch pathway itself (Chen et al., 2010; Rodilla et al., 2009; Sansone et al., 2007; Yamamoto et al., 2013; Zavadil et al., 2004).

The abilities of tumor cells to invade the surrounding tissues and to colonize distant organs (metastatic process) are key features of aggressive cancers. In order to escape their severe local environment, epithelial cells can use the reversible developmental program EMT, during which epithelial features are suppressed and mesenchymal traits acquired thus transforming tumor cells into cells with the potential for invasion, resisting apoptosis, dissemination, and acquiring stem cell features (Hanahan and Weinberg, 2011; Kong et al., 2011; Lamouille et al., 2014; Zheng and Kang, 2014). Several reports have described JAG1 involvement in EMT, invasive potential, and metastasis (Dai et al., 2014; Kim et al., 2013; Leong et al., 2007; Tanaka et al., 2012). Overall, JAG1-induced Notch signaling appears to be implicated in different steps of the invasive/metastatic process.

EMT is a biologic process that allows a polarized epithelial cell to undergo multiple biochemical changes enabling it to assume a mesenchymal cell phenotype. A number of

varying molecular processes are engaged in order to initiate an EMT and enable its completion. These include activation of transcription factors, expression of specific cell-surface proteins, reorganization and expression of cytoskeletal proteins, production of extracellular matrix-degrading enzymes, and changes in the expression of specific microRNAs (Kalluri and Weinberg, 2009). The full spectrum of signaling mediators that contribute to EMT in carcinoma cells remains unclear. One hypothesis is that the genetic and epigenetic alterations undergone by cancer cells during the course of primary tumor formation render them responsive to EMT-inducing signals derived from tumor-associated stroma. In many carcinomas, EMT-inducing signals released from the tumor-associated stroma, notably hepatocyte growth factor (HGF), epidermal growth factor (EGF), platelet-derived growth factor (PDGF), and TGF-β, appear to play a significant role in the induction or functional activation of a series of EMT-inducing transcription factors (EMT-TFs) like Snail, Slug, Zinc finger E-box-binding homeobox 1 (ZEB1), and Twist in cancer cells (Kokudo et al., 2008; Medici et al., 2008; Niessen et al., 2008; Shi and Massague, 2003; Thiery, 2002). The actual execution of the EMT program depends on a series of intracellular signaling networks involving signal-transducing proteins such as extracellular signal-regulated kinase (ERK), mitogen-activated protein kinase (MAPK), phosphoinositide 3-kinase (PI3K), AKT, SMADs, β-catenin, and RAS as well as cell surface proteins such as β4 integrins (Tse and Kalluri, 2007). EMT-associated changes in gene expression are mediated by EMT-TFs, all of which suppress the expression of E-cadherin. Conversely, EMT-TFs activate the expression of mesenchyme-associated genes such as those encoding N-cadherin, fibronectin, and vimentin.

The aim of the study in the second part was to investigate the role of the JAG1-Notch

pathway and EMT in poor prognosis and recurrence in colorectal cancer (CRC). I then discuss the role of JAG1-Notch pathway and EMT as an underlying mechanism for cancer progression and recurrence. I also discuss the contribution of major genetic changes, which are acquired by genetic mutations, and the promoted or suppressed activity of various signaling pathway to JAG1 expression/EMT in CRC.

Chapter 1: Role of Autophagy and p62 for Hepatic differentiation in Adult Liver Stem/Progenitor Cells

1. Abstract

Autophagy is a homeostatic process regulating the turnover of impaired proteins and organelles, and p62 (sequestosome-1, *SQSTM1*) functions as the autophagic receptor in this process. p62 also functions as a hub for intracellular signaling as in the mammalian target of rapamycin (mTOR) pathway. Liver stem/progenitor cells have the potential to differentiate into hepatocytes or cholangiocytes. In this study, I examined the effects of autophagy, p62, and associated signaling pathways on hepatic differentiation. Adult stem/progenitor cells were isolated from the livers of mice with chemically-induced liver injury. The effects of autophagy, p62, and related signaling pathways on hepatic differentiation were investigated by silencing the genes for autophagy protein 5 (*ATG5)* and/or *SQSTM1*/p62 using small interfering RNAs. Hepatic differentiation was assessed based on increased albumin and hepatocyte nuclear factor 4α as hepatocyte markers, and decreased cytokeratin 19 and SOX9 as stem/progenitor cell markers. These markers were measured using quantitative RT-PCR, immunofluorescence, and western blotting. *ATG5* silencing decreased the active LC3 and increased p62 levels, indicating the inhibition of autophagy. Inhibition of autophagy promoted hepatic differentiation in the stem/progenitor cells. Conversely, *SQSTM1*/p62 silencing impaired hepatic differentiation. A suggested mechanism for p62-dependent hepatic differentiation in my study was the activation of mTOR pathway by amino acids. Amino acid activation of mTOR signaling was enhanced by *ATG5* silencing and suppressed by *SQSTM1*/p62

silencing. My findings indicate that promoting the amino acid sensitivity of the mTOR pathway is dependent on p62 accumulated by the inhibition of autophagy and that this process plays an important role in the hepatic differentiation of stem/progenitor cells.

2. Introduction

Mammalian target of rapamycin (mTOR) is a nutrition sensor and a key molecule regulating autophagy. Suppressed mTOR activity in an environment of poor nutrition activates autophagy-related pathways. Autophagy plays an important role in maintaining intracellular homeostasis by regulating the turnover of impaired proteins and organelles (Mizushima and Komatsu, 2011). Autophagosome formation is the first step of the autophagy process, with autophagosomes engulfing abnormal protein aggregates or damaged organelles and fusing with lysosomes to form mature autolysosomes. The proteins sequestered in autolysosomes are the digested to amino acids by lysosomal enzymes (Kaur and Debnath, 2015). Through autophagy, intracellular proteins and organelles are reorganized and intracellular energy homeostasis is maintained.

The autophagic adaptor protein, p62 (sequestosome 1, *SQSTM1*), functions as an autophagy receptor for impaired proteins and organelles and is degraded along with these intracellular constituents in the autolysosome during the selective autophagic process (Rogov et al., 2014). Consistent with this, inhibition of autophagy induced intracellular p62 accumulation and the increased levels of p62 led to activation of p62-related signaling such as the Kelch like ECH associated protein 1 (KEAP1)–NF-E2-related factor 2 (NRF2) pathway (Komatsu et al., 2010). p62 was reported to regulate aspects of intracellular signaling such as the amino acid sensitivity of mTOR signaling activation (Duran et al., 2011). However, the physiological or pathological roles of mTOR activation through p62 have not been fully elucidated except for its involvement in cancer cell proliferation (Duran et al., 2011; Linares et al., 2015; Linares et al., 2013).

mTOR is a serine/threonine kinase, a master regulator that couples amino acid availability to cell proliferation and autophagy (Jewell et al., 2013). Leucine and

glutamine in particular, are potent mTOR stimulators, and detailed mechanisms of amino acid-induced mTOR activation have been described (Duran et al., 2011; Duran et al., 2012; Jewell et al., 2015). Under nutrient-rich conditions, mTOR promotes cell proliferation by stimulating biosynthetic pathways including protein synthesis and by inhibiting cellular catabolism through mechanisms such as repression of the autophagy pathway.

In the liver, mTOR activation by amino acids was shown to be important for the synthesis and secretion of albumin in hepatocytes (Ijichi et al., 2003; Okuno et al., 1995). In other reports, activation of mTOR signaling significantly affected the liver regeneration processes through the replication of hepatocytes in the liver (Espeillac et al., 2011; Zhang et al., 2015).

Although proliferation of hepatocytes is essential for liver regeneration after hepatectomy, proliferation and differentiation of LPCs are also implicated as important for supplying multiple cellular components to the mature organs during recovery from severe liver injury (Duncan et al., 2009; Turner et al., 2011). The liver contains two types of epithelial cells, hepatocytes and cholangiocytes. When the replication capacities of hepatocytes and/or cholangiocytes are exhausted, adult LPCs may be activated to supply these cell types (Furuyama et al., 2011; Huch et al., 2013).

A previous study in the laboratory to which I belonged, demonstrated the role of autophagy in liver regeneration after partial hepatectomy and the function of hepatocytes, using liver-specific knockouts of autophagy-related gene 5 (*ATG5*) (Toshima et al., 2014). However, the role of autophagy in LPCs has not been addressed yet.

Therefore, this study aimed to investigate the association of autophagy with hepatocyte differentiation in LPCs. This goal included elucidating the role of p62, and its associated

mTOR signaling in hepatic differentiation induced by autophagy inhibition.

3. Materials and Methods

3.1. Mouse experiments

Male C57BL/6 mice (Charles River, Yokohama, Japan) were maintained in a specific pathogen-free facility with a 12 h dark/light cycle. Mice, beginning at 8 wk of age, were fed a diet containing 0.1% DDC (Tokyo Chemical Industry, Tokyo, Japan) for 1 to 3 wk to induce the ductular reaction (Dorrell et al., 2011; Kitade et al., 2013; Okabe et al., 2009). All animal experiments were approved by the Kyushu University Animal Experiment Committee (A25-029, A27-248) and the care of the animals was in accordance with institutional guidelines.

3.2. Isolation of Epithelial cell adhesion molecule (EPCAM)$^{+}$ Cluster of differentiation (CD)133^{Low} cells

DDC-injured livers from the mice were digested using a two-step collagenase perfusion method. After eliminating hepatocytes by centrifugation at 50 ×g for 1 min, the cell suspension was centrifuged at 200 ×g for 5 min (fraction 1). The tissue remaining after two-step collagenase perfusion was further digested in collagenase solution. The cell suspension was centrifuged at 200 ×g for 5 min (fraction 2). The tissue remaining after digestion in collagenase solution was digested in collagenase/Accutase solution. The cell suspension was centrifuged at 200 ×g for 5 min (fraction 3). Cells derived from fractions 1, 2 and 3 were combined and treated with an anti-FcR antibody (BioLegend, San Diego, CA, USA) followed by incubation with an Alexa Fluor 488 (AF488)-conjugated anti-CD133 antibody (BD Biosciences, Franklin Lakes, NJ, USA), mouse lineage cocktail antibodies containing anti-CD3c, anti-CD11b, anti-CD45R, anti-TER-119 and anti-LY-6C/6G conjugated to biotin (BioLegend) and an allophycocyanin (APC)-conjugated anti- EPCAM antibody (BD Biosciences). Next, biotin-conjugated antibodies were labeled with phycoerythrin (PE)-conjugated

streptavidin (BD Biosciences). Lineage-negative, $EPCAM^{+}$ and $CD133^{High\ or\ Low}$ cells were isolated by fluorescence-activated cell sorting (FACS) using a FACS Aria II (BD Biosciences) or a SH800 (Sony, Tokyo, Japan). The antibodies used are detailed in Table 1- 1.

3.3. Cell culture and differentiation

Cells were seeded on collagen I-coated plastic dishes (AGC Techno Glass, Shizuoka, Japan) and cultured in William's E medium containing 10% fetal bovine serum, 10 mM HEPES, 1.25 mM N-acetylcysteine, 10^{-7} M dexamethasone, 1× insulin-transferrin-selenium (ThermoFisher Scientific, Waltham, MA, USA), 10 mM nicotinamide, 50 ng/mL murine EGF and 50 ng/mL murine HGF to maintain clonal proliferation (Dorrell et al., 2011; Kamiya et al., 2009; Kitade et al., 2013; Okabe et al., 2009).

Cells were subjected to differentiation toward hepatocytes, as previously described, but with modifications (Kitade et al., 2013; Okabe et al., 2009). Briefly, cells were plated at 50% confluence on a plastic tissue culture plate in standard culture medium. After 2 d, 20 ng/mL murine oncostatin M (OSM) and 1% dimethylsulfoxide (DMSO) were added to the confluent culture. On days 4 and 8 after plating, cells were treated with standard culture medium containing 20 ng/mL OSM, 1% DMSO and 5% Matrigel (growth factor-reduced, ThermoFisher Scientific). Then, at 2 wk after plating, the cultured cells were subjected to various analyses.

3.4. Small interfering RNA studies

Small interfering RNA (siRNA) studies were performed using the following siRNAs: *ATG5* siRNA (ThermoFisher Scientific; oligo ID MSS247019, MSS247021), *SQSTM1*/p62 siRNA (ThermoFisher Scientific; oligo ID MSS207329) or nonspecific (NS) small interfering RNA (siRNA; ThermoFisher Scientific oligo ID 12935–300). The siRNAs were transfected into cells using Lipofectamine RNAiMAX transfection regent

(ThermoFisher Scientific), administering them at 1 d before, on the same day, and at 4 and 8 d after the initiation of treatment, to induce hepatic differentiation. No signs of cell damage were observed following treatment with transfection reagent alone or the siRNAs transfection preparation (Figure 1- 5b).

3.5. Gene expression analysis

Total RNA was extracted from cultured cells or frozen liver tissue using an RNeasy Mini Kit (QIAGEN, Hilden, Germany) and reverse-transcribed using SuperScript III (ThermoFisher Scientific) following the manufacturers' instructions. Quantitative RT-PCR (qRT-PCR) was performed using TaqMan enzyme and a StepOne plus PCR system (Applied Biosystems, Waltham, MA, USA). The probes used are detailed in Table 1- 2. Expression levels were normalized to values for 18s ribosomal RNA (18s rRNA).

3.6. Western blot analysis

Liver tissue or cells were lysed in RIPA buffer. Lysate proteins were separated by SDS polyacrylamide gel electrophoresis and transferred to polyvinylidene difluoride membranes. The membranes were washed, blocked and incubated with primary antibodies, as indicated. After washing, membranes were incubated with the appropriate horseradish peroxidase-conjugated secondary antibody. The immunoreactive bands were visualized by enhanced chemiluminescence (Chemi-Lumi One Ultra: Nakarai Tesque, Kyoto, Japan) using an LAS3000 (Fuji Photo Film, Tokyo, Japan) or Amersham Imager 600 (GE Healthcare, Little Chalfont, UK). The relative densities of immunoreactive bands were determined using ImageJ software (National Institute of Health, Bethesda, MD, USA). The antibodies used are detailed in Table 1- 1.

3.7. Immunofluorescence analysis

Liver tissues isolated from normal- or DDC-fed mice were embedded in O.C.T.

compound (Sakura Finetek, Torrance, CA, USA) and frozen sections were prepared using a CM3050s cryostat (Leica Biosystems, Nussloch, Germany). Frozen sections were fixed in phosphate buffered saline (PBS) containing 3% paraformaldehyde at room temperature for 5 min. After permeabilization with 0.3% Triton X-100 and blocking with 3% bovine serum albumin, sections were incubated with primary antibodies listed in Supplementary Table S2 followed by Alexa Fluor dye-conjugated secondary antibodies (Jackson ImmunoResearch Laboratories, West Grove, PA, USA). To stain cells, they were first fixed in 90% methanol at 4°C for 30 min and then treated as described above for staining sections. Fluorescence images were obtained using a Biorevo BZ-900 microscope (Keyence, Osaka, Japan), an ImageXpress (Molecular Devices, Sunnyvale, CA, USA) and an A1Rsi confocal laser microscope (Nikon, Tokyo, Japan). Images were analyzed using MetaXpress Software (Molecular Devices). The antibodies used are detailed in Table 1- 1.

3.8. Statistical analysis

All values are presented as the means ± standard deviations (S.D.), with between-group differences assessed by Student's *t*-test. Statistical significant differences between groups were defined as **, $P < 0.01$ and *, $P < 0.05$.

4. Results

4.1. Isolation of adult LPCs from DDC-injured liver and generation of LPC lines

EPCAM was used as a marker for LPCs (Okabe et al., 2009). The DDC diet induced liver injury with a ductular reaction, causing $EPCAM^+$ cytokeratin 19 $(CK19)^+$ LPCs to be activated and expanded (Figure 1- 1a, Figure 1- 2a). Consistent with the expansion of $EPCAM^+$ $CK19^+$ cells in injured liver, *EPCAM* and *KRT19* mRNA expression increased and reached almost maximum expression at 2–3 wk after initiation of DDC treatment (Figure 1- 1b). LPC lines were generated from the livers of mice in which LPCs had been activated by consumption of the DDC diet for 3 wk. Primary LPCs were isolated at high purity by FACS after co-staining with cell-specific anti-EPCAM, anti-CD133 and lineage cocktail antibodies to exclude cells of hematopoietic origin (Figure 1- 1c). The "$EPCAM^+/CD133^{high}$ or $CD133^{low}/Lineage^-$" cells were then cultured (Figure 1- 1d). This enabled us to obtain CK19-positive LPCs with self-renewing capacity and hepatic differentiation potential, the latter illustrated by increased levels of albumin, a hepatocyte-specific marker, and decreased CK19, a cholangiocytic or progenitor marker. These markers were determined by immunofluorescence (Figure 1- 1e), qRT-PCR (Figure 1- 2b) and western blotting (Figure 1- 2c) in cells cultured under the differentiation conditions. Only cells derived from $EPCAM^+/CD133^{low}/Lineage^-$ cells had hepatic differentiation potential (Figure 1- 1e, Figure 1- 2b and c); those derived from $EPCAM^+/CD133^{high}/$ $Lineage^-$ cells did not (data not shown).

4.2. Inhibition of autophagy by ATG5 silencing induced hepatic differentiation

First, the effect of the autophagy inhibitor, 3-methyladenine (3-MA) (Seglen and Gordon, 1982), on hepatic differentiation in LPCs was examined (Figure 1- 3). Treatment of LPCs with 3-MA promoted hepatic differentiation, in a concentration-dependent

manner, as shown by increased albumin and hepatocyte nuclear factor 4α (HNF4α) and decreased CK19, by immunofluorescence. Next, to clarify the relationship between autophagy inhibition and hepatic differentiation, siRNAs against autophagic factor *ATG5* (si*ATG5*) were utilized to inhibit autophagy (Fujita et al., 2011; Ishida et al., 2009; Toshima et al., 2014). *ATG5* expression was decreased by si*ATG5*, compared with non-targeting siRNA (siNON), treatment. si*ATG5* also inhibited autophagy, as indicated by decreased microtubule-associated protein light chain 3 (LC3) active form (lower band) and increased p62 (Figure 1- 4) levels. Inhibition of autophagy induced a hepato-like phenotype in LPCs, as indicated by increased albumin and decreased CK19 by western blotting (Figure 1- 4), increased albumin and HNF4α by immunofluorescence (Figure 1- 5a, Figure 1- 6) and morphological appearance (Figure 1- 5b). *ATG5* silencing and inhibition of autophagy were maintained for 2 wk in cells under the differentiation conditions (Figure 1- 5c and d). The effects of si*ATG5* in promoting hepatic differentiation appeared at 5 d after initiation of treatment.

4.3. Autophagic adaptor protein p62 was significantly involved in hepatic differentiation

Inhibition of autophagy by si*ATG5* induced intracellular accumulation of p62 (Figure 1- 7a and Figure 1- 4). By immunofluorescence, HNF4α-positive differentiated hepatocytes had more intracellular p62 protein than CK19-positive differentiation-deficient cells, under siNON treatment (Figure 1- 7a). Furthermore, si*ATG5* treatment induced an increased number of p62- and HNF4α-double-positive cells (Figure 1- 7a).

To determine the contribution of p62 to hepatic differentiation in LPCs, the effects of siRNA against *SQSTM1*/p62 (si*SQSTM1*/p62) were investigated. Decreased *SQSTM1*

mRNA expression was observed at 2 wk after si*SQSTM1*/p62 treatment under the differentiation conditions (Figure 1- 7b). si*SQSTM1*/p62 suppressed mRNA expression of albumin (*ALB*) and fructose-1,6-bisphosphatase 1 (*FBP1*), both hepatocyte markers. In contrast, si*SQSTM1*/p62 increased mRNA expression of *KRT19* and *SOX9*, as progenitor and cholangiocyte markers, respectively (Figure 1- 7b). These results suggested that hepatic differentiation was impaired by p62 deficiency. Lower levels of p62 protein in cells treated with si*SQSTM1*/p62, compared with siNON, were associated with lower levels of albumin (Figure 1- 7d, Figure 1- 8b).

Immunofluorescence analysis also revealed that p62 existed primarily in the differentiated hepato-like cells, as indicated by their staining for the hepatocyte marker HNF4α, under siNON treatment (Figure 1- 7c). si*SQSTM1*/p62 decreased intracellular p62 protein levels and also decreased the numbers of HNF4α- and albumin-positive cells (Figure 1- 7c, Figure 1- 8a and b). Quantitative fluorescence analysis showed that si*SQSTM1*/p62 decreased p62 and albumin levels and increased CK19 levels (Figure 1- 8c). These results indicated that *SQSTM1*/p62 silencing impaired or delayed hepatic differentiation.

si*ATG5* induced hepatic differentiation, as indicated by upregulation of albumin and downregulation of SOX9. Increased p62 was also observed (Figure 1- 7d). with *siATG5* treatment. *ATG5* and *SQSTM1*/p62 were double-knocked down by siRNAs to determine whether hepatic differentiation induced by autophagy inhibition was dependent on p62 levels (Figure 1- 7d). Co-treatment of cells with si*ATG5* and si*SQSTM1*/p62 reduced ATG5 and p62 expression. siRNA co-treatment also led to lower albumin levels than with single si*ATG5* treatment. In contrast, the liver progenitor and cholangiocyte marker SOX9 showed the opposite changes with siRNAs co-treatment compared with single

si*ATG5* treatment. Albumin and SOX9 levels were similar with double siRNA as with siNON treatment. This showed that hepatic differentiation of LPCs was impaired or delayed by double knockdown of *ATG5* and *SQSTM1*/p62, more than with the single *ATG5* knockdown. That is, intracellular p62 levels influenced hepatic differentiation.

4.4. mTOR signaling activation was important for hepatic differentiation.

Western blot analysis showed increased p62 and albumin levels in cells treated with si*ATG5* under hepatic differentiation conditions (Figure 1- 7d and Figure 1- 9a). Activation of mTOR signaling was observed in these cells, as indicated by increasing levels of phosphorylated ribosomal S6 protein (pS6) under the hepatic differentiation conditions (Figure 1- 7d and Figure 1- 9a). PI3k–AKT signaling was decreased and MAP kinase signaling was nearly unchanged, compared with siNON treatment, as indicated by phosphorylated AKT (pAKT) and phosphorylated ERK (pERK), respectively (Figure 1- 9a). Conversely, under hepatic differentiation-deficient conditions induced with si*SQSTM1*/p62 treatment, p62 and albumin levels were decreased (Figure 1- 7d and Figure 1- 9a). si*SQSTM1*/p62, compared with siNON, treatment also decreased pS6 levels (Figure 1- 7d and Figure 1- 9a). Based on these results, I speculated that mTOR signaling activation was important for hepatic differentiation induced by autophagy inhibition and intracellular p62 accumulation.

Immunofluorescence results supported the significance of mTOR signaling for hepatic differentiation (Figure 1- 8a and b, Figure 1- 9b and c). At 2 wk after initiation of differentiation conditions by si*ATG5*, some cells displayed low or negative CK19 staining, showing that they were differentiated toward hepatocytes. mTOR activation, as indicated by pS6 staining, primarily existed in CK19-negative cells. The pS6-positive cells had higher levels of p62 protein. While si*ATG5* increased numbers of p62- and pS6-positive

cells, si*SQSTM1*/p62 had the opposite effect (Figure 1- 8a, Figure 1- 9b). As shown in Figure 1- 9c, pS6-positive cells were nearly all albumin-positive under siNON treated control conditions. Treatment with si*ATG5* increased pS6- and albumin-positive cells, while si*SQSTM1*/p62 treatment decreased both (Figure 1- 8b, Figure 1- 9c).

Rapamycin, an mTOR inhibitor, had several concentration-dependent effects. It inhibited pS6 signaling, without reducing p62 protein levels, decreased albumin and increased SOX9 levels (Figure 1- 10a). Rapamycin also decreased mRNA expression of the hepatocyte marker albumin, similar to the results of western blotting analysis (Figure 1- 10b).

These results suggested that mTOR signaling was significant for differentiation of LPCs into hepatocytes.

4.5. mTOR activation by amino acids was significant for hepatic differentiation.

I speculated that growth factors might not be significant as mTOR activators during hepatic differentiation of LPCs because, at higher concentrations of HGF, hepatic differentiation was suppressed, based on increased levels of CK19 and SOX9 (Figure 1- 11a and b). Because leucine and glutamine are more potent activators of mTOR signaling than other amino acids, their effects on differentiation were investigated. Furthermore, the effects of branched chain amino acids (BCAAs) were also investigated, because previous reports showed that they were important for stimulating albumin synthesis through mTOR activation in hepatocytes (Ijichi et al., 2003; Nishitani et al., 2004; Okuno et al., 1995). Immunofluorescence (Figure 1- 12a) and western blotting (Figure 1- 12b) revealed that removal of various amino acids from the differentiation medium suppressed or delayed hepatic differentiation of LPCs, compared with in normal differentiation medium, based on decreased albumin and increased CK19 levels. Differentiation medium

containing higher concentrations of leucine promoted differentiation, as indicated by decreased CK19 by immunofluorescence (Figure 1- 13a). Western blotting (Figure 1- 13b) gave similar results, showing decreased CK19 and SOX9. No effects on albumin levels were observed, but I speculated that the effects of leucine on albumin would be maximal anyway at the concentration (0.53 mM) in normal differentiation medium. qRT-PCR analysis supported the results from protein assessments (Figure 1- 12, Figure 1- 13) and also demonstrated the significant effects of BCAA containing leucine on hepatic differentiation (Figure 1- 14)

These results suggested that amino acids acted as mTOR activators for hepatic differentiation.

4.6. Possibility of enhanced amino acid sensing of mTOR by increased intracellular p62 levels under hepatic differentiation conditions.

Amino acid sensitivity of mTOR activation was examined in LPCs treated with siNON, si*ATG5* or si*SQSTM1*/p62. As shown in Figure 1- 15 a and b, the presence of leucine increased mTOR activation, based on pS6 staining in cells treated with si*ATG5*. In contrast, mTOR activation by leucine was almost completely abolished under *SQSTM1*/p62 knockdown conditions. The results of western blotting were consistent with the immunofluorescence (Figure 1- 15c). Leucine-induced increases in p62 and in S6 phosphorylation were observed under *ATG5* knockdown. Furthermore, with si*SQSTM1*/p62 treatment, p62 was downregulated and leucine-induced S6 phosphorylation was decreased. These results suggested that autophagy and intracellular p62 status influenced the amino acid sensitivity of mTOR activation.

5. Discussion

Figure 1- 16 present a model based on my study, which lead to five major novel findings. First, inhibition of autophagy induced hepatic differentiation in LPCs. Second, alteration of intracellular p62 levels affected hepatic differentiation. Third, mTOR activation promoted hepatic differentiation. Fourth, amino acids are important for differentiation toward a hepatic phenotype, through mTOR activation. Fifth, the amino acid sensitivity of mTOR activation is dependent on autophagy and intracellular p62 levels in LPCs. Together, these results suggest that p62 promotes amino acid sensitivity of the mTOR pathway and the differentiation of LPCs toward hepatocytes.

LPCs proliferate following chronic liver damage and numerous duct-like oval cells that could differentiate into either hepatocytes or bile ducts were observed around the portal vein in rodents with experimental liver injury (Lowes et al., 1999). EPCAM and CD133 have been used as markers to isolate adult-type LPCs (Okabe et al., 2009; Suzuki et al., 2008). Previous reports have indicated that large and small cell colonies were formed from cultured cells that were isolated as EPCAM- or CD133-positive. The large colonies were relatively committed toward hepatocytes, whereas the small colonies were committed toward cholangiocytes (Okabe et al., 2009; Suzuki et al., 2008). Isolation of cells expressing lower CD133 levels, among the EPCAM-positive cells by FACS appeared to select cells that were more committed toward hepatocytes in our study. Alternatively, it was suggested that these cells could be stem/progenitor-like cells derived from mature hepatocytes (Tarlow et al., 2014).

First, I examined the effects of autophagy inhibition on the hepatic differentiation of LPCs. I postulated that inhibition of autophagy by 3-MA or si*ATG5* would disturb intracellular homeostasis and impair hepatic differentiation in LPCs. Unexpectedly,

albumin levels were increased by autophagy inhibition, but these increased albumin levels were apparently not caused by inhibition of non-selective autophagic protein degradation. This was demonstrated by increased *ALB* mRNA and decreased CK19 protein expression. LPCs have a smaller size and fewer intracellular organelles than mature hepatocytes. A previous study showed that the diameter of LPCs was approximately 10 μm, which is a half to a third of that of hepatocytes (Tarlow et al., 2014). It was recently proposed that autophagy might maintain fewer organelles such as mitochondria by degrading them, resulting in a smaller cell size and preventing LPC differentiation (Tarlow et al., 2014).

Next, I hypothesized that increased intracellular p62 was a candidate mechanism for hepatic differentiation by autophagy inhibition because immunological analyses indicated that p62 levels were elevated in well-differentiated HNF4α-positive cells. The results of our experiment using si*SQSTM1*/p62 confirmed that p62 is a critical mediator of hepatic differentiation, because p62 protein deficiency did not induce or promote differentiation.

p62 is an adaptor protein that regulates various physiological and pathological intracellular signaling pathways (Duran et al., 2004; Martin et al., 2006; Rodriguez et al., 2006). Besides its function as an autophagy adaptor, p62 regulates osteoclastogenesis, T cell differentiation, and adipogenesis through various intracellular signaling pathways. Among the various functions of p62, I investigated its role in amino acid sensing via the mTOR pathway (Duran et al., 2011). mTOR activity is regulated by many intracellular mechanisms that sense the extracellular alterations in growth factors and amino acids. My pathway analysis demonstrated that the activity of mTOR pathway varied in accordance with p62 status. Other than PI3K–AKT pathway inactivation, no other signaling changes

were observed.

Generally, the mTOR pathway is activated through stimulation of the PI3K–AKT pathway in growth factor signaling. However, my results using si*ATG5* treatment, indicated that mTOR pathway activation was not associated with PI3K–AKT pathway activity. Therefore, I assumed that amino acids served as stimulators of mTOR signaling for differentiation. In fact, lower HGF concentrations promoted differentiation toward hepatocytes and removal of amino acids impaired or delayed differentiation. As reported previously, BCAAs prevented growth factor-induced hepatic tumor cell proliferation through mTOR activation and PI3K–AKT pathway inactivation because of the negative feedback from mTOR (Hagiwara et al., 2012). Furthermore, the same group of investigators reported that BCAAs also suppressed a hepatocellular cancer stem cell phenotype through a similar mechanism (Nishitani et al., 2013). From my results and the previously reported evidence, I speculated that mTOR activation by amino acids was important to suppress the stem cell phenotype and thereby, to promote differentiation toward hepatocytes.

Low BCAA/aromatic amino acid ratios reduced the biosynthesis and secretion of albumin in hepatocytes (Okuno et al., 1995) and were also associated with poor prognosis in patients with chronic liver disease (Steigmann et al., 1984). In addition, BCAAs are often used as a supplemental therapy to address protein malnutrition in patients with liver cirrhosis. BCAAs, particularly leucine, activated mTOR and regulated albumin synthesis, through mRNA translation in cultured rat hepatocytes (Ijichi et al., 2003; Okuno et al., 1995). Glutamine is another potent amino acid for mTOR activation and in combination with leucine, significantly activated mTOR signaling (Duran et al., 2012). My results demonstrated that BCAAs, leucine, and glutamine were significant for mTOR activation

and hepatic differentiation in LPCs. I further observed that a combination of leucine and glutamine was more effective than either amino acid alone. To my knowledge, this is the first report that amino acids contribute to hepatic differentiation through mTOR pathway activation.

LPCs undergo major expansion following chronic liver damage. In rodent experimental liver injury models, oval cells containing LPCs, which can differentiate into either hepatocytes or bile ducts, appeared around the portal vein (Lowes et al., 1999). Furthermore, in human diseases, the extent of biliary-like progenitor cell proliferation was consistently correlated with the degree of clinical impairment (Lowes et al., 1999; Sancho-Bru et al., 2012). As recently reported, mature hepatocytes could transdifferentiate into ductal biliary epithelial cells (Michalopoulos et al., 2005; Sekiya and Suzuki, 2014). Hepatocytes were also shown to be transformed into a cholangiocarcinoma, which is a biliary-cell-like tumor (Sekiya and Suzuki, 2012; Sekiya and Suzuki, 2014). Furthermore, as recently reported, hepatocyte-to-duct conversion was reversible and hepatocyte-derived progenitors could differentiate back to hepatocytes *in vivo* (Tarlow et al., 2014). One characteristic of mature hepatocyte-derived progenitors was a relatively lower expression of EPCAM and CD133 compared with that in biliary-derived cells, as described recently (Tarlow et al., 2014). In my study, the $CD133^{low}$ population among EPCAM-positive non-parenchymal cells could differentiate toward hepatocytes whereas the $CD133^{high}$ population could not. These results suggest that the cells described in my study were hepatocyte-derived progenitors.

Considering that hepatocyte-to-duct conversion is reversible, and that hepatocyte-derived progenitors could differentiate back to hepatocytes, pharmacological agents that improve the efficacy of progenitor-to-hepatocyte conversion might be novel

treatments to improve hepatic function and outcomes in some chronic liver injuries. For example, a recent study demonstrated that expression of autophagy-related genes such as *LC3B* was increased in the cirrhotic liver compared with that in the non-cirrhotic liver. Furthermore, LC3B localization was consistent with the cholangiocyte and liver progenitor marker CK19, in humans and rodents (Hung et al., 2015). This study also revealed that inhibition of autophagy attenuated the ductular reaction and fibrosis in the liver in a drug-induced cirrhotic model. My study suggests that in addition to autophagy inhibition, mTOR pathway activation by amino acids or enhancement of the amino acid sensitivity of mTOR activity by regulating the interaction between p62 and mTOR could be an effective medical treatment for the cirrhotic liver by attenuating the ductular reaction and promoting hepatic differentiation of biliary-like progenitors.

In conclusion, inhibition of autophagy and increased intracellular p62 positively coordinated hepatic differentiation through mTOR pathway activation. Moreover, my findings indicate that amino acids are important for hepatic differentiation. These results help to clarify the process by which LPCs differentiate into hepatocytes. Pharmacological agents or other treatment methods that improve the efficacy of LPC differentiation to hepatocytes may help improve hepatic function and outcomes in chronic liver damage.

6. Tables

Table 1- 1. List of antibodies used in immunological assays

Antibody	Source	Method	Dilution
Primary antibodies			
β actin	Cell signaling	WB	1:1000
AKT	Cell signaling	WB	1:1000
pAKT (S473)	Cell signaling	WB	1:1000
Albumin	Bethyl Laboratories	WB/ IF	1:2000/ 1:400
ATG5	Cell signaling	WB	1:1000
CD133	BD Biosciences	FACS	1:200
Cytokeratin 19	Developmental Studies Hybridoma Bank	WB/ IF	1:2000/ 1:200 or 300
EPCAM	BD Biosciences	FACS	1:160
ERK 1/2	Cell signaling	WB	1:2000
pERK 1/2 (T202/Y204)	Cell signaling	WB	1:1000
HNF4α	Santa Cruz Biotechnology	IF	1:50
LC3	Cell signaling	WB	1:1000
Lineage panel	BioLegend	FACS	1:250
p62	Progen	WB/ IF	1:1000/ 1:300
p62	MBL	WB	1:1000
S6	Cell signaling	WB	1:1000
pS6 (S240/244)	Cell signaling	WB/ IF	1:1000/ 1:400
SOX9	Millipore	WB	1:1000
2nd antibodies			
Anti rabbit - HRP	Abcam	WB	1:2000
Anti goat - HRP	Cappel	WB	1:5000
Anti rat - HRP	GE Healthcare	WB	1:5000
Anti guinea pig - HRP	Jackson ImmunoResearch	WB	1:10000
Anti goat - AF488	Jackson ImmunoResearch	IF	1:200
Anti guinea pig - AF488	Jackson ImmunoResearch	IF	1:300
Anti rat - AF594	Jackson ImmunoResearch	IF	1:400
Anti rabbit AF647	Jackson ImmunoResearch	IF	1:300 or 400

AF: Alexa Fluor

Table 1- 2. List of probes used in qRT-PCR

Target gene	Assay ID
18s rRNA	Mm03928990_g1
ALB	Mm00802090 m1
ATG5	Mm00504340_m1
EPCAM	Mm00493214_m1
FBP1	Mm00490181_m1
KRT19	Mm00492980_m1
SQSTM1/p62	Mm00448091_m1
SOX9	Mm00448840_m1
CPS1	Mm01256489_m1
CYP7A1	Mm00484150_m1
G6PC	Mm04209403_g1

7. Figures

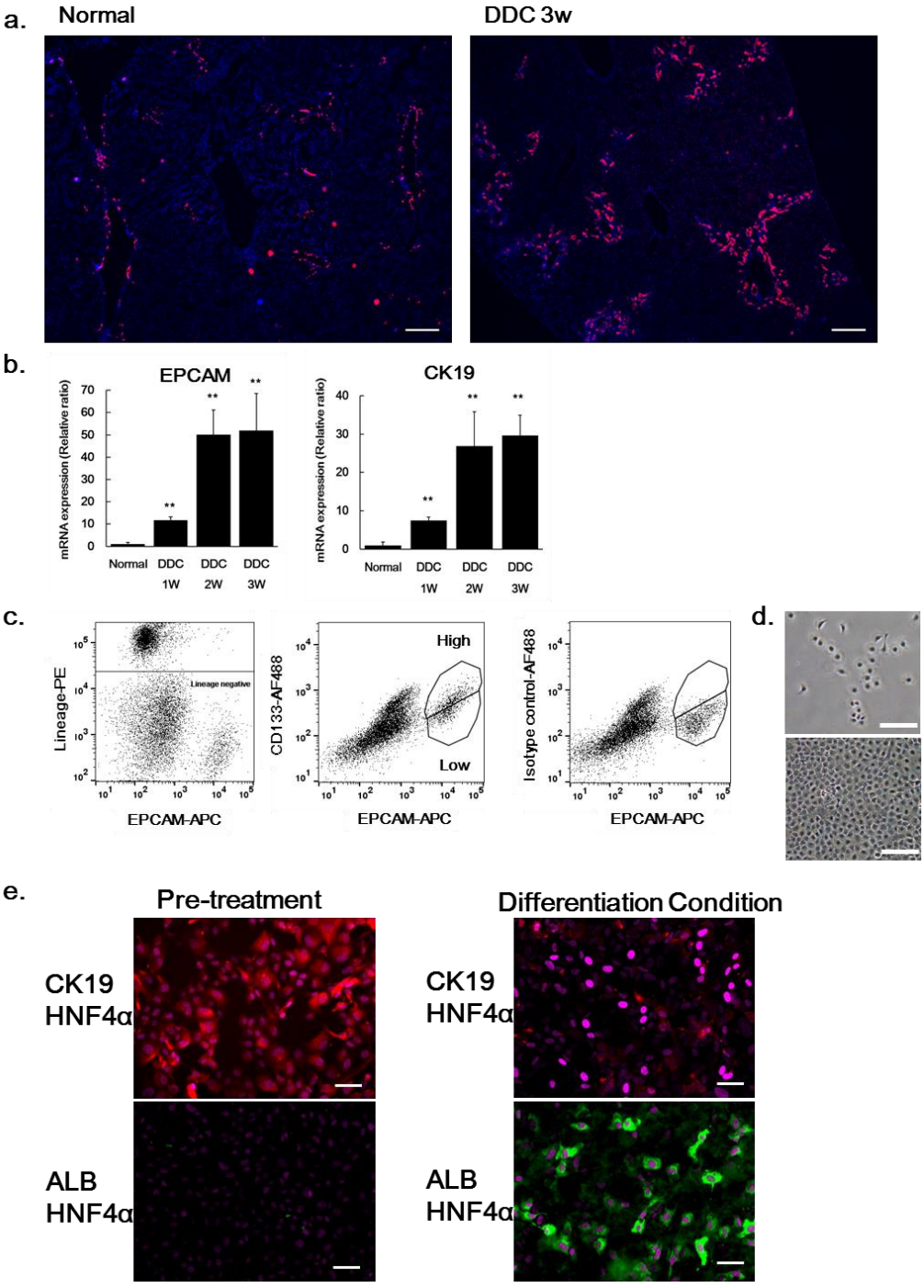

Figure 1- 1. Isolated mouse adult progenitor/stem cells (LPCs) from DDC-injured liver differentiated toward hepatocytes *in vitro*.

(a) $CK19^{+}$ cells underwent expansion in the livers of mice fed a DDC diet. Bars = 300 μm. (b) mRNA expression at different timepoints during DDC feeding. Expression levels at each timepoint were normalized to those in mice fed a normal diet and are means ± S.D.

of data from 4–5 mice. **, $P < 0.01$ versus normal diet, Student's *t*-test. These differences remained significant after correction for multiple testing by Bonferroni's inequality method. (c) Representative FACS plots and gates (boxed areas) used for sorting "CD133-Alexa Fluor (AF) 488^{High} or 488^{Low}/EPCAM-APC^{+}/Lineage-PE^{-}" liver stem/progenitor cells (LPCs). FACS plot showing staining with isotype controls. AF488 is on the right-hand side. (d) Cultured $CD133^{Low}$/$EPCAM^{+}$/$Lineage^{-}$ cells. Cells shown in the upper and lower panels are actively proliferating and confluent, respectively. Bars = 200 μm. (e) LPCs from DDC-injured liver differentiated into a hepato-like phenotype *in vitro*. Representative fluorescence microscopy images before (left panels) and at 2 wk after (right panels) exposure to differentiation conditions. Green, red, and magenta staining indicate albumin, CK19 and HNF4α, respectively. Bars = 50 μm.

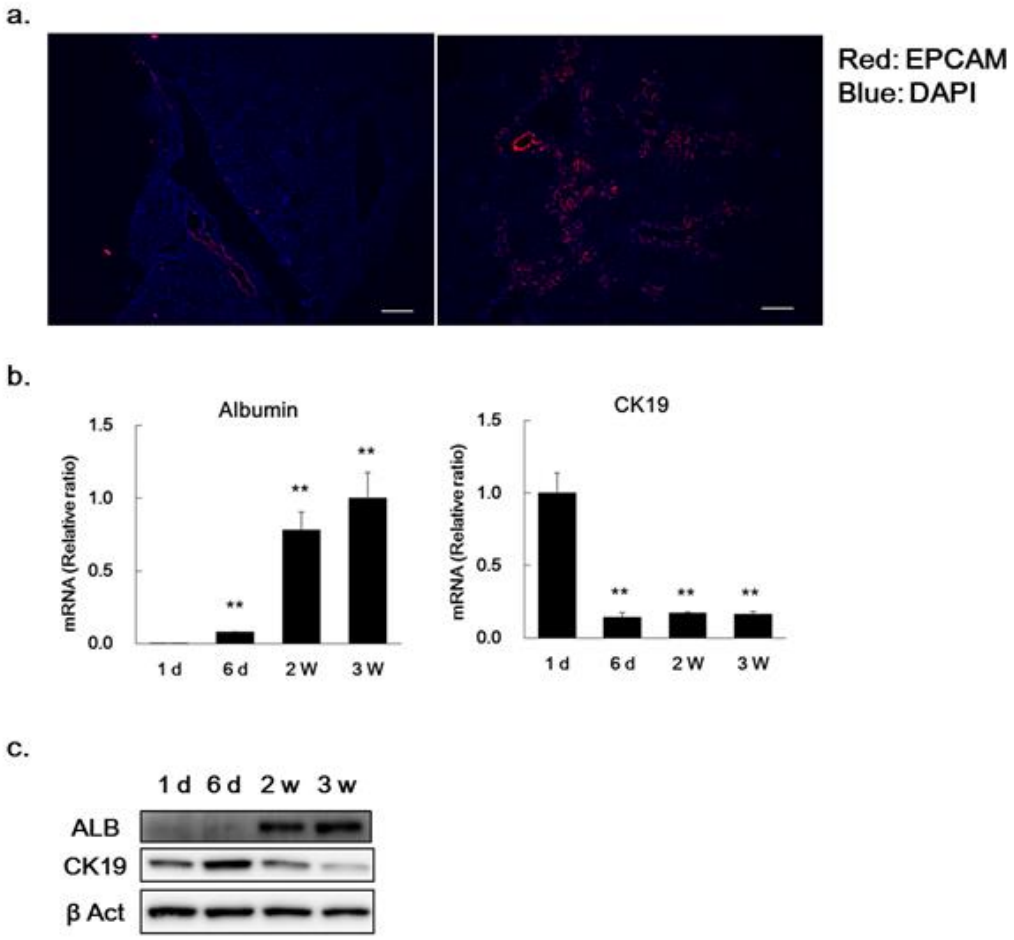

Figure 1- 2. Isolated mouse adult progenitor/stem cells (LPCs) from DDC-injured liver differentiated toward hepatocytes *in vitro*.

(a) Ductular reactions were induced in mice with a DDC diet. Ductular structures consisting of $EPCAM^+$ cells underwent expansion in the liver of mice fed the DDC diet. Bars = 300 μm. (b) mRNA expression at different timepoints under the hepatic differentiation conditions was analyzed by quantitative RT-PCR (qRT-PCR). Expression levels are shown as relative to those on day 1 after plating. Data are means ± S.D. of three wells at each timepoint. **, $P < 0.01$ versus day 1, Student's *t*-test. These differences remained significant after correction for multiple testing by Bonferroni's inequality method. (c) Protein levels at different timepoints during hepatic differentiation were determined by western blotting.

a.

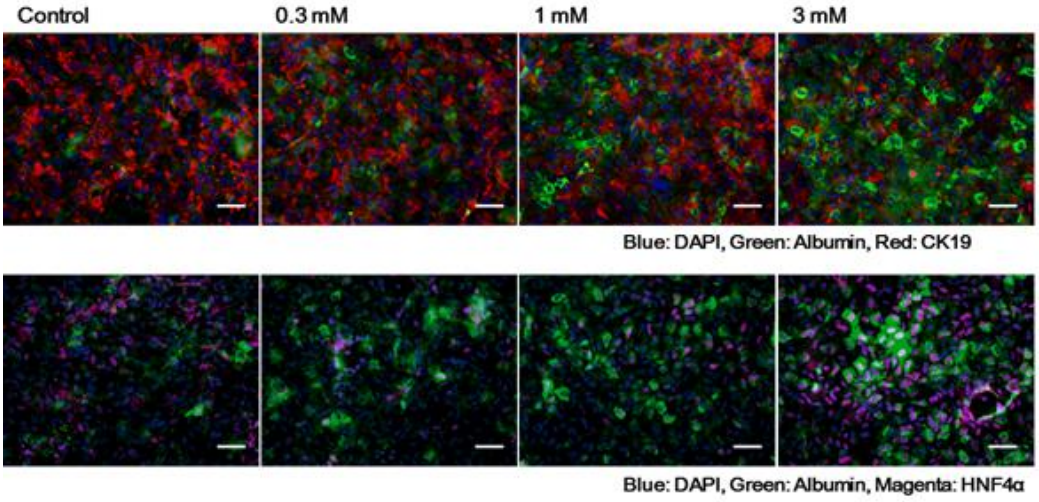

b.

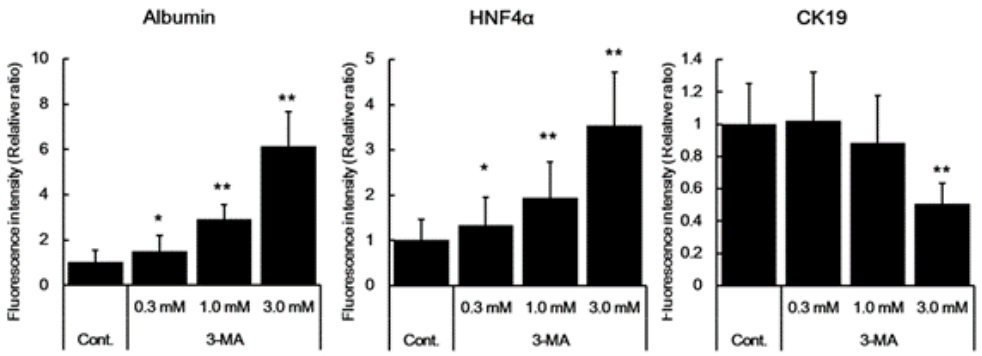

Figure 1- 3. Inhibition of autophagy by 3-methyladenine (3-MA) induced hepatic differentiation in LPCs.

Incubation with 0.3, 1 or 3 mM 3-MA was started on day 6 after plating under the differentiation conditions. Effects of 3-MA were analyzed by immunofluorescence at 1 wk 3-MA treatment. (a) Representative fluorescence microscopy images at 1 wk treatment. Bars = 50 μm. (b) Intensities of fluorescence microscopy images were analyzed. The data are means ± S.D. for 24 fields of view. *, $P < 0.05$; **, $P < 0.01$, versus control group, Student's *t*-test. Differences in albumin and HNF4α at 1 or 3 mM 3-MA and CK19 at 3 mM 3-MA remained significant after correction for multiple testing by Bonferroni's inequality method.

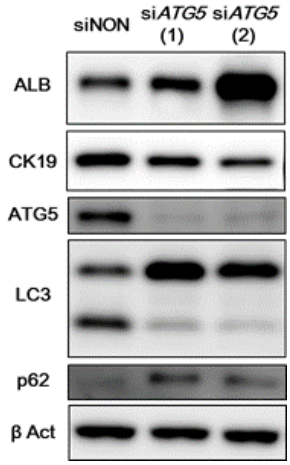

Figure 1- 4. Inhibition of autophagy by *ATG5* silencing induced hepatic differentiation in LPCs (western blotting).

Cells were incubated with either a non-targeting siRNA (siNON) or *ATG5*-specific siRNA (si*ATG5*) under the differentiation conditions. The effects of two types of si*ATG5* were analyzed by western blotting at 2 wk treatment.

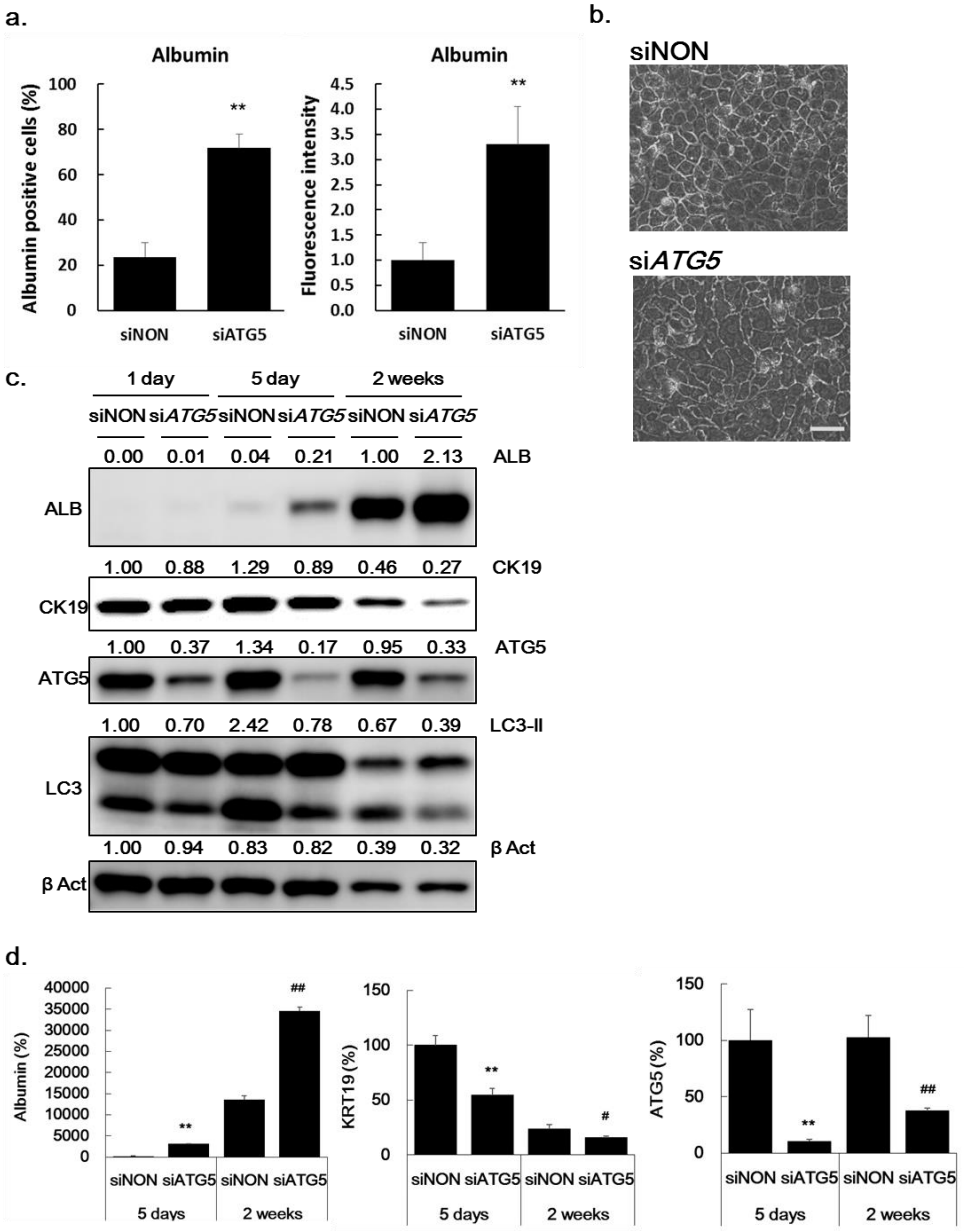

Figure 1- 5. Inhibition of autophagy by *ATG5* silencing induced hepatic differentiation.

(a) Either a non-targeting siRNA (siNON) or ATG5-specific siRNA (si*ATG5*) was incubated with cells under the differentiation conditions. The effects of si*ATG5* were analyzed at 2 wk by immunofluorescence, as shown in representative fluorescence microscopy images in Figure 1- 6. Arbitrary ratios of albumin-positive cells to total cells and the absolute fluorescence intensities were analyzed. Data are means ± S.D. measured in 24 fields of view. **, $P < 0.01$, versus siNON, Student's *t*-test. (b) Representative phase contrast microscopy image of differentiated LPCs after 2 wk siRNA treatment. Bar = 50 μm. (c) Effects of si*ATG5* on protein levels were analyzed by western blotting at 1

and 5 d and at 2 wk treatments. The relative densities of immunoreactive bands were quantified. Relative intensities are shown as ratios of the signals to those from cells given siNON at 1 d (CK19, ATG5, LC3, and βAct) or at 2 wk (ALB) (d) mRNA expression was analyzed by qRT-PCR at 5 d and 2 wk si*ATG5* treatment. Expression levels are shown as percentages of the values for cells treated with siNON, at 5 d. Data are means ± S.D. of three wells at each time point. **, $P < 0.01$, versus siNON at 5 d and $^{\#\#}$, $P < 0.01$; $^{\#}$, $P < 0.05$, versus siNON at 2 wk, Student's *t*-test. Data shown in (a), (c), (d) and Figure 1- 4 were from independent experiments.

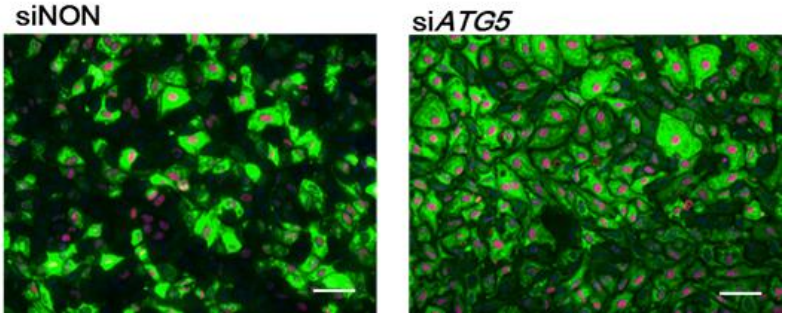

Figure 1- 6. Inhibition of autophagy by *ATG5* silencing induced hepatic differentiation in LPCs (immunofluorescence).

Cells were incubated with either a non-targeting siRNA (siNON) or ATG5-specific siRNA (si*ATG5*) under the differentiation conditions. Effect of si*ATG5*(2) were analyzed at 2 wk treatment by immunofluorescence. Representative fluorescence microscopy images at 2 wk after the initiation of treatment. Green and magenta show albumin and HNF4α, respectively. Bars = 50 μm.

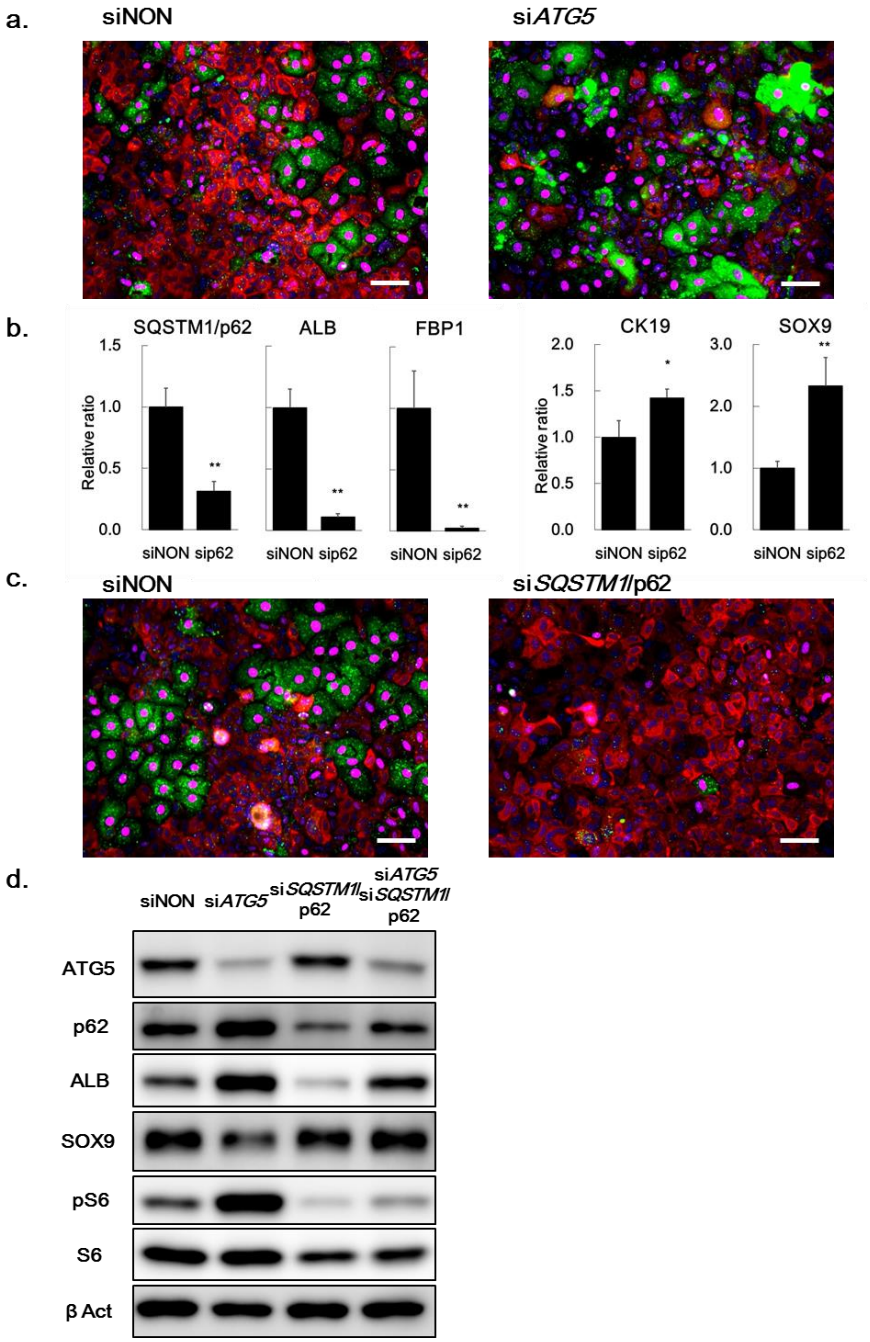

Figure 1- 7. Autophagic adaptor protein p62 significantly impacted hepatic differentiation.

(a) Representative fluorescence microscopy images at 2 wk treatment with siNON or si*ATG5*. Magenta, red, green and blue (DAPI) staining represent HNF4α, CK19, p62 and nuclei, respectively. (b) mRNA expression was analyzed by qRT-PCR at 2 wk treatment with either siNON or a *SQSTM1*/p62-specific siRNA (si*SQSTM1*/p62) during culture under the differentiation conditions. Expression levels are shown as relative to values in cells receiving siNON treatment. Data are means ± S.D. of three wells. **, $P < 0.01$; *, P

< 0.05 versus siNON, Student's *t*-test. (c) Representative fluorescence microscopy images at 2 wk treatment with siNON and si*SQSTM1*/p62. Magenta, red, green and blue (DAPI) staining represent HNF4α, CK19, p62 and nuclei, respectively. (d) Effects of a siNON, siATG5, si*SQSTM1*/p62 or si*ATG5*, given in combination with si*SQSTM1*/p62, on albumin, SOX9, ATG5, p62, S6 and pS6 protein levels was analyzed by western blotting at 2 wk treatment, during culture under hepatic differentiation conditions.

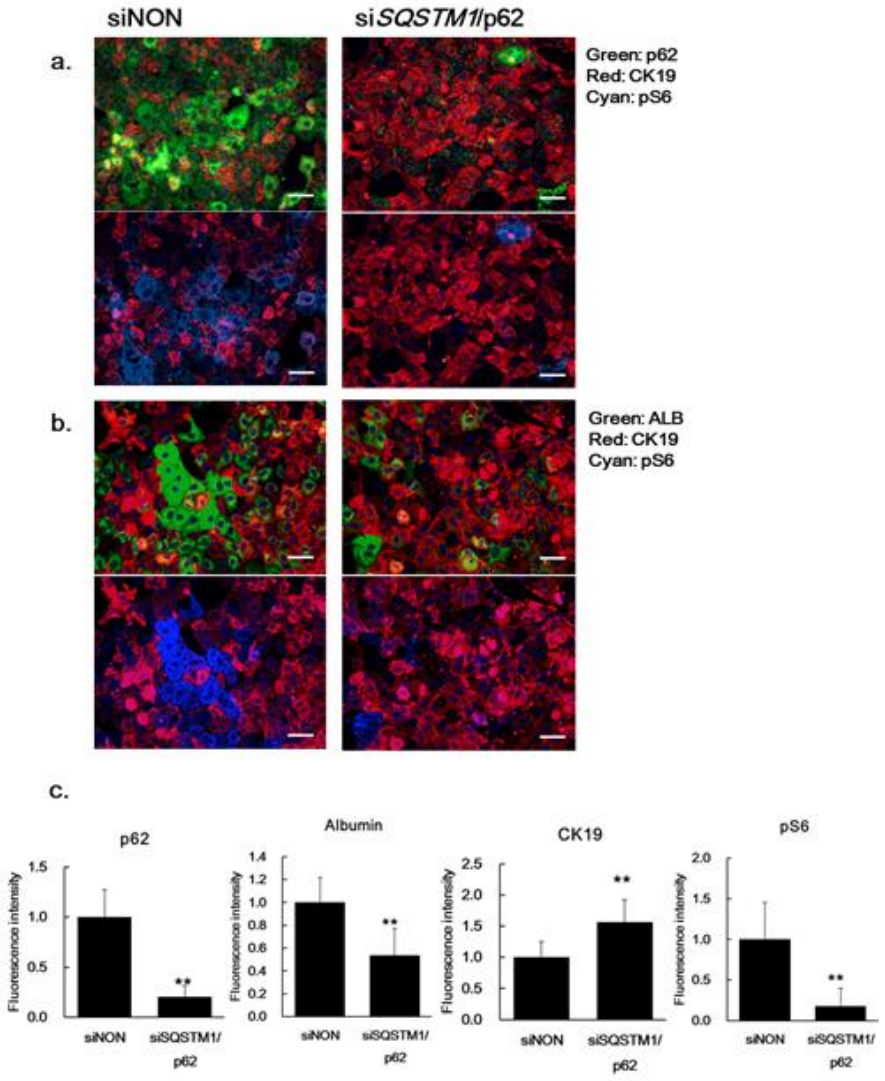

Figure 1- 8. Effect of si*SQSTM1*/p62 on hepatic differentiation of LPCs.

Cells were incubated with either siNON or *SQSTM1*/p62-specific siRNA (si*SQSTM1*/p62) during culture under hepatic differentiation conditions for 2 wk. (a), (b) Representative fluorescence microscopy images at 2 wk treatment with siNON (left) and si*SQSTM1*/p62 (right). These images were obtained in experiments independent from those shown in Figure 3. Bars = 50 μm. (a) Green, red and cyan staining represent p62, CK19 and pS6, respectively. (b) Green, red and cyan staining represent albumin, CK19 and pS6, respectively. (c) Intensity of fluorescence microscopy images. The data are means ± S.D. for 18 fields of view. **, $P < 0.01$, versus siNON, Student's *t*-test.

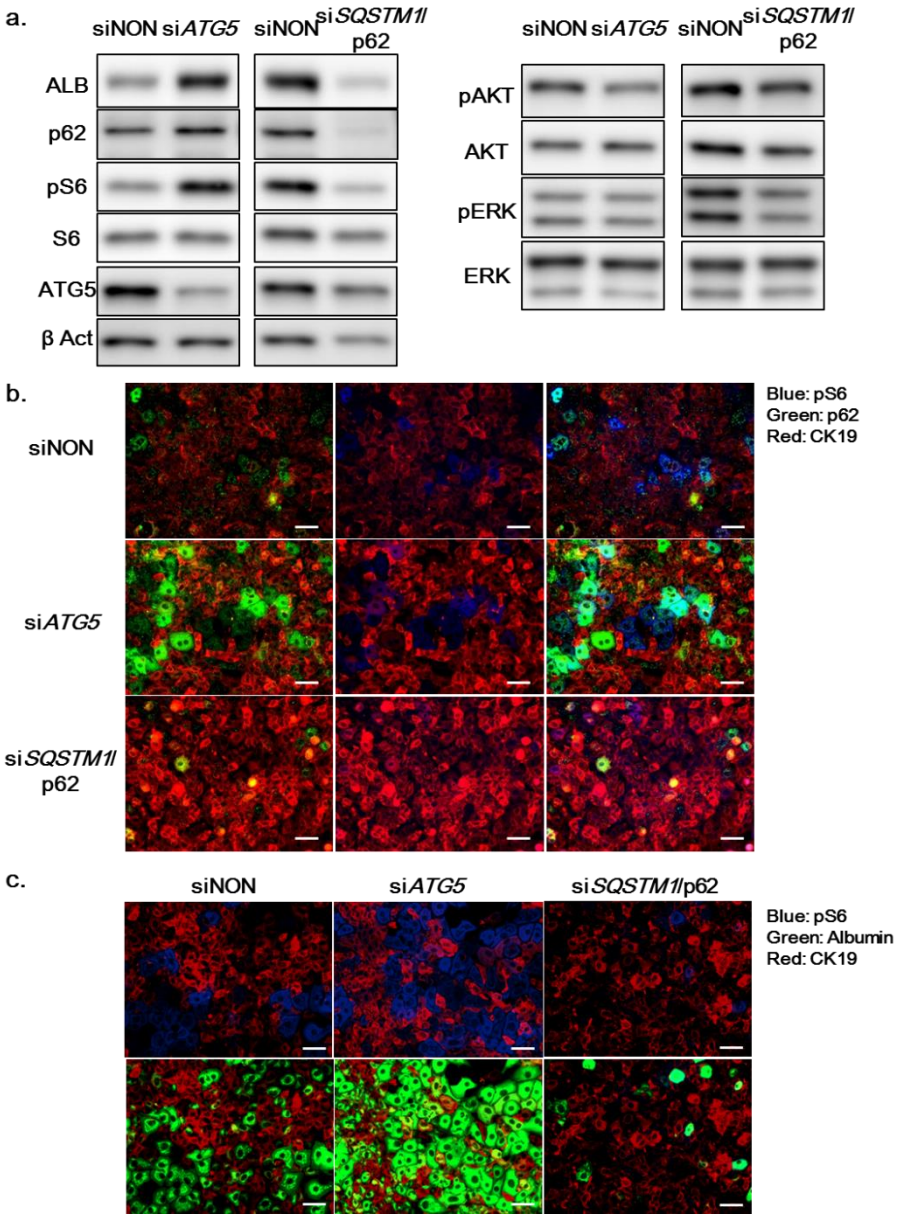

Figure 1- 9. Identification of intracellular signaling, dependent on intracellular p62, involved in hepatic differentiation.

(a) Total S6, pS6 (mTOR signaling), total AKT, pAKT (PI3k–AKT signaling), total ERK1/2, pERK1/2 (MAP kinase signaling), albumin, p62 and ATG5 levels were analyzed by western blotting following *ATG5* knockdown (KD) or *SQSTM1*/p62 KD in LPCs cultured under hepatic differentiation conditions. (b), (c) Representative fluorescence microscopy images at 2 wk siNON, si*ATG5* or si*SQSTM1*/p62 treatment. Red and blue staining show CK19 and phosphorylated S6 protein, respectively. Green staining shows p62 (b) and albumin (c).

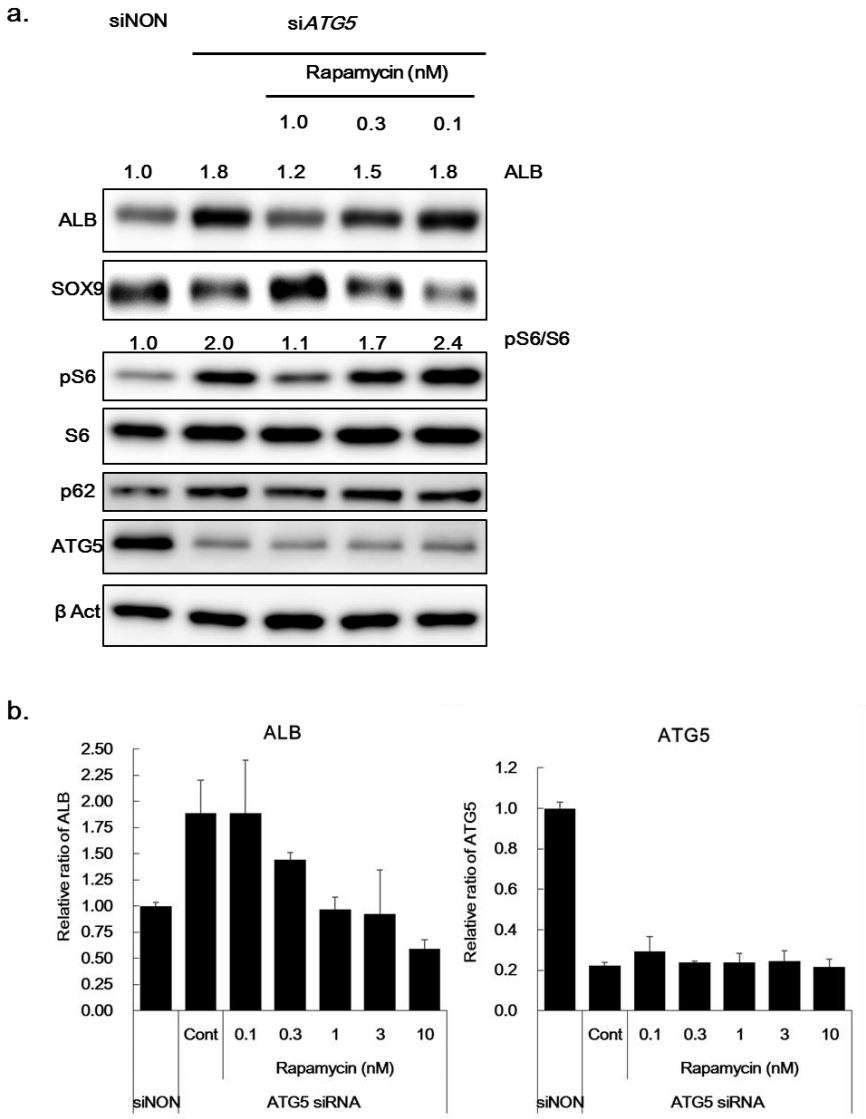

Figure 1- 10. mTOR signaling activation was important for hepatic differentiation.
(a) LPCs treated with si*ATG5* were incubated with rapamycin, an mTOR inhibitor, at the indicated concentrations under differentiation conditions. Albumin, SOX9, p62, total S6, pS6 and ATG5 levels were analyzed by western blotting. The relative density of immunoreactive bands for ALB, S6 and pS6 were quantified and the pS6/S6 ratio was calculated. Values for ALB or pS6/S6 ratios are shown relative to those in cells treated with siNON. (b) Effects of rapamycin were analyzed by qRT-PCR, to determine mRNA expression of *ALB* and *ATG5*. Expression levels are shown as relative to values in cells receiving siNON treatment. Data are means ± S.D. of two wells. The Jonckheere-Terpstra trend test was used to examine *ALB* mRNA expression trends across varying concentrations of rapamycin. The trends for decreased *ALB* mRNA expression with increased concentrations of rapamycin were significant ($P < 0.05$).

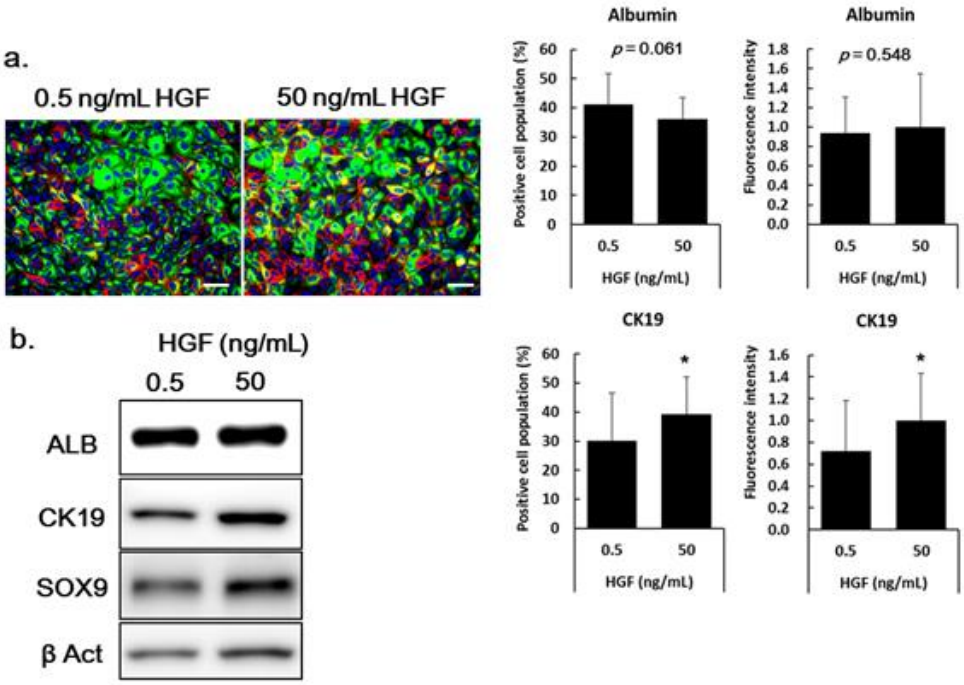

Figure 1- 11. Effect of HGF on hepatic differentiation of LPCs.

(a), (b) LPCs were cultured in differentiation medium containing 0.5 or 50 ng/mL HGF. (a) Representative fluorescence microscopy images for 0.5 or 50 ng/mL HGF treatment. Green, red and blue represent albumin, CK19 and nuclei, respectively. The arbitrary ratios of albumin- and CK19-positive cells to total cells and absolute fluorescence intensities were analyzed, as shown in right panels. Data are means ± S.D. for 27 fields of view. *, $P < 0.05$, Student's *t*-test. (b) Albumin, SOX9 and CK19 protein levels, analyzed by western blotting, in cells subjected to 0.5 or 50 ng/mL HGF treatment.

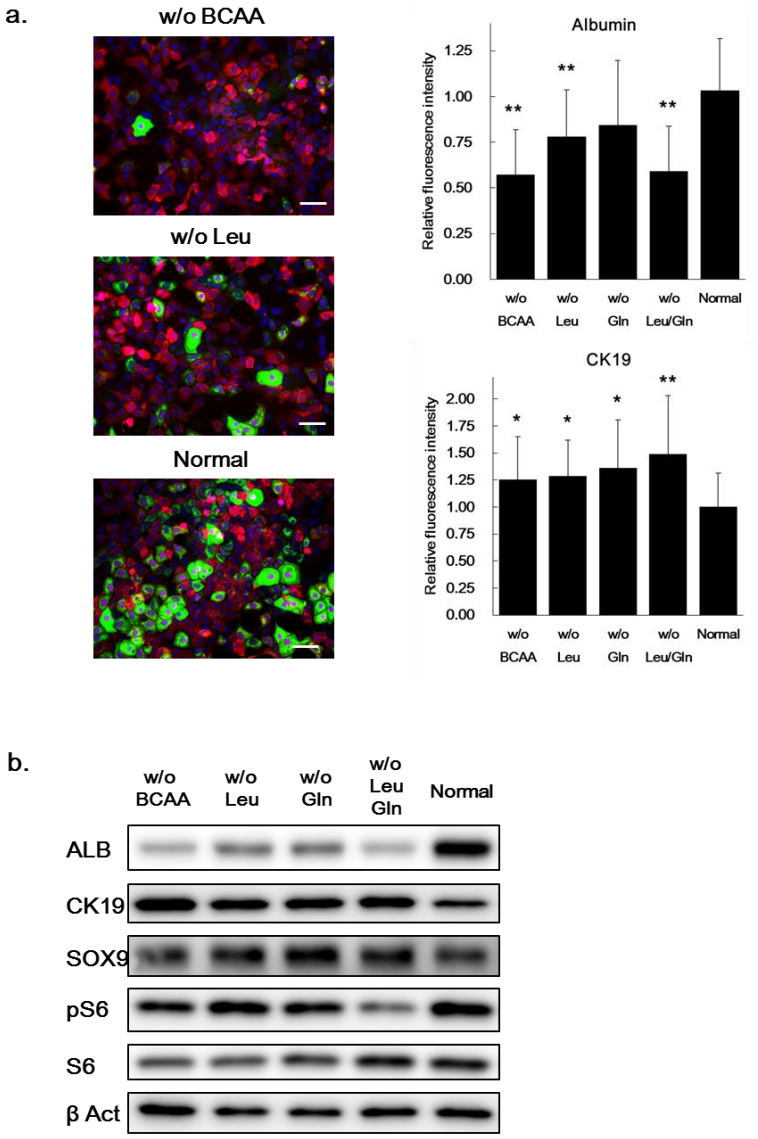

Figure 1- 12. mTOR activation by amino acids was important for hepatic differentiation.

(a), (b) LPCs were cultured in differentiation medium without (w/o) branched-chain amino acids (BCAAs), leucine (Leu), glutamine (Gln) or leucine plus glutamine. (a) Representative fluorescence microscopy images obtained in normal medium and medium without BCAA and leucine. Absolute fluorescence intensities for albumin or CK19 were analyzed, as shown in the right panel. Data are means ± S.D. obtained from 20 fields of view. **, $P < 0.01$; *, $P < 0.05$ versus normal medium, Student's *t*-test. Differences of w/o BCAA, w/o Leu, w/o Leu/Gln versus normal for albumin and differences of w/o Gln or w/o Gln/Leu versus normal for CK19 remained significant after correction for multiple testing by Bonferroni's inequality method. (b) Albumin, CK19, SOX9 and phosphorylated S6 protein were analyzed by western blotting.

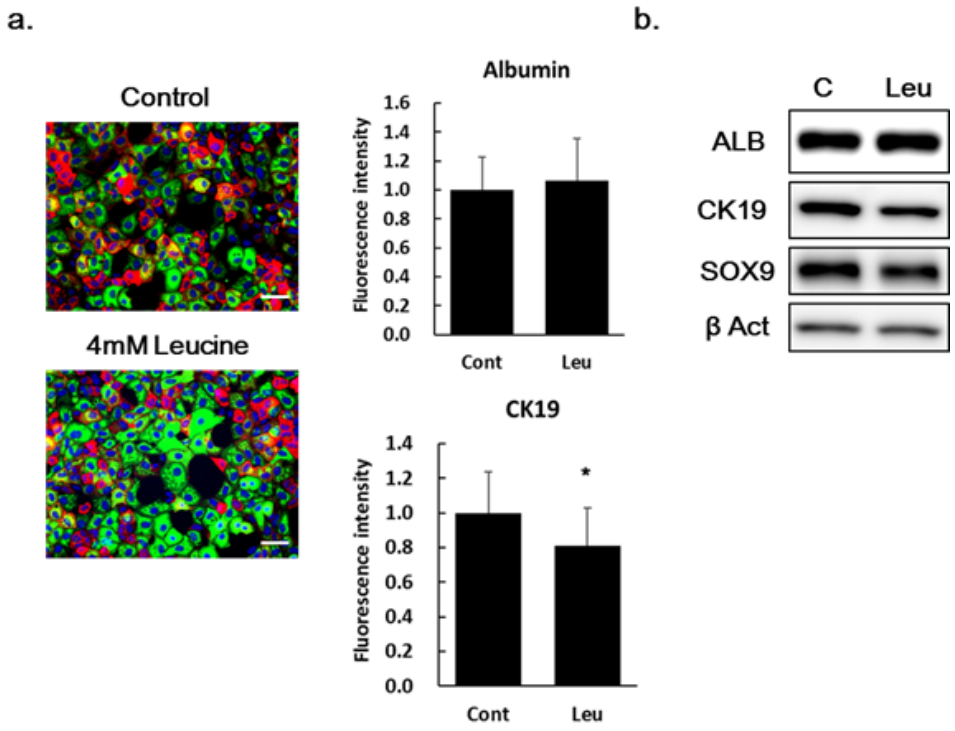

Figure 1- 13. Effect of leucine on hepatic differentiation of LPCs.

(a) Effects of leucine on hepatic differentiation were investigated by culture in differentiation medium containing 4 mM leucine. Representative fluorescence microscopy images. Green, red and blue represent albumin, CK19 and nuclei, respectively. Absolute fluorescence intensity for albumin and CK19 were analyzed, as shown in middle panels. The data are means ± S.D. for 18 fields of view. *, $P < 0.05$, Student's *t*-test. (b) Albumin, SOX9 and CK19 protein levels in cells cultured in normal medium or medium containing leucine (Leu), analyzed by western blotting.

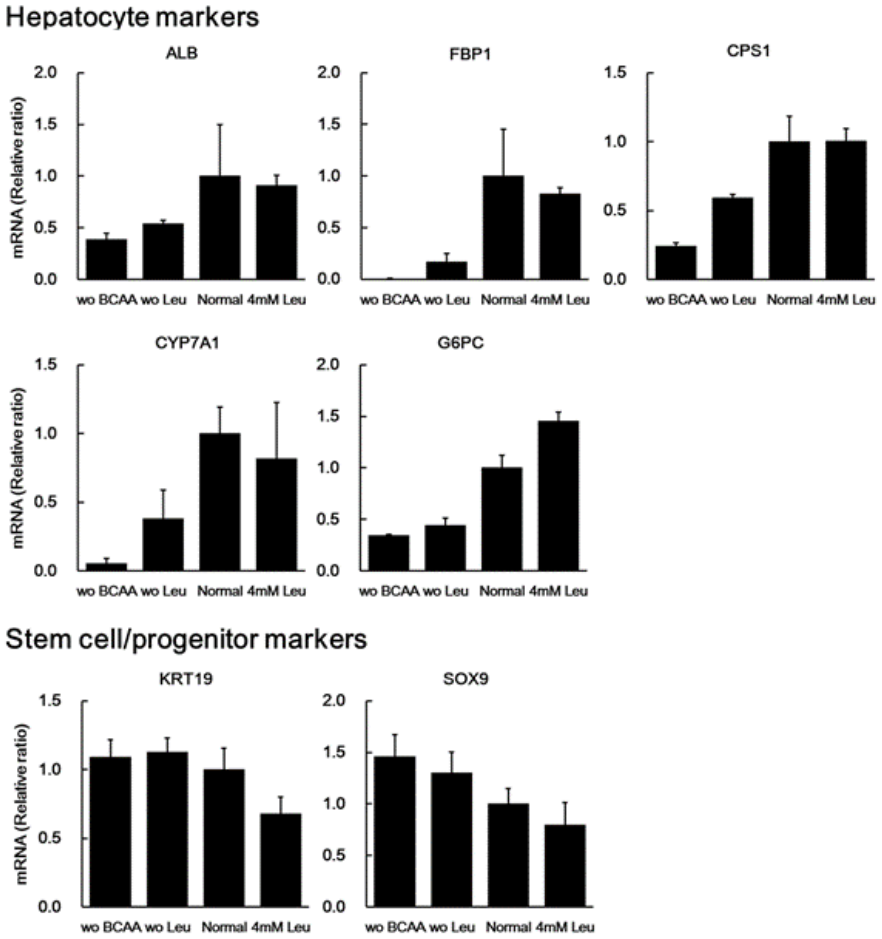

Figure 1- 14. Effect of branched chain amino acids or leucine on hepatic differentiation of LPCs.

Effect of branched chain amino acids (BCAA) or leucine (Leu) on hepatic differentiation was investigated by culture in differentiation medium without BCAA, without leucine or containing 4 mM leucine. mRNA expression levels of hepatocyte and stem cell/progenitor markers were analyzed by quantitative RT-PCR (qRT-PCR). Expression levels are relative to those in cells cultured in normal medium. Data are means ± S.D. of three wells, under each condition.

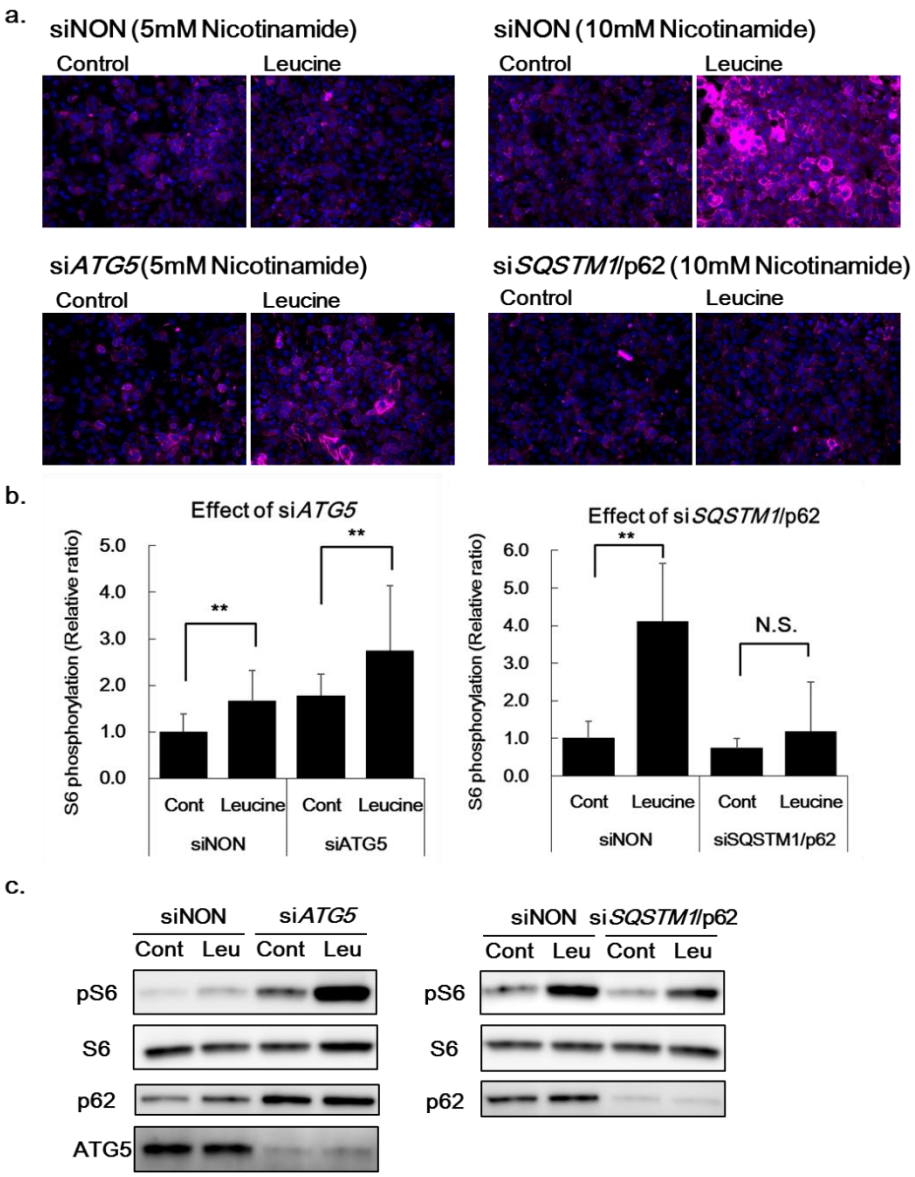

Figure 1- 15. Significance of enhanced amino acid sensitivity of mTOR by increased intracellular p62 levels.

LPCs were treated with siNON, si*ATG5* or si*SQSTM1*/p62 under hepatic differentiation conditions for 2 wk. Differentiation medium containing 5 and10 mM nicotinamide was used for si*ATG5* and si*SQSTM1*/p62, respectively. Starvation was induced in Hank's Balanced Salt Solution for 2 h followed by leucine treatment for 1 h. mTOR signaling was indicated by phosphorylation of S6 protein. (a) Representative fluorescence microscopy images. (b) Absolute fluorescence intensity for the pS6 staining. Data are means ± S.D. from 18 fields of view. **, $P < 0.01$; *, $P < 0.05$, Student's *t*-test. These differences remained significant after correction for multiple testing by Bonferroni's inequality method. (c) pS6, S6, p62 and ATG5 were analyzed by western blotting.

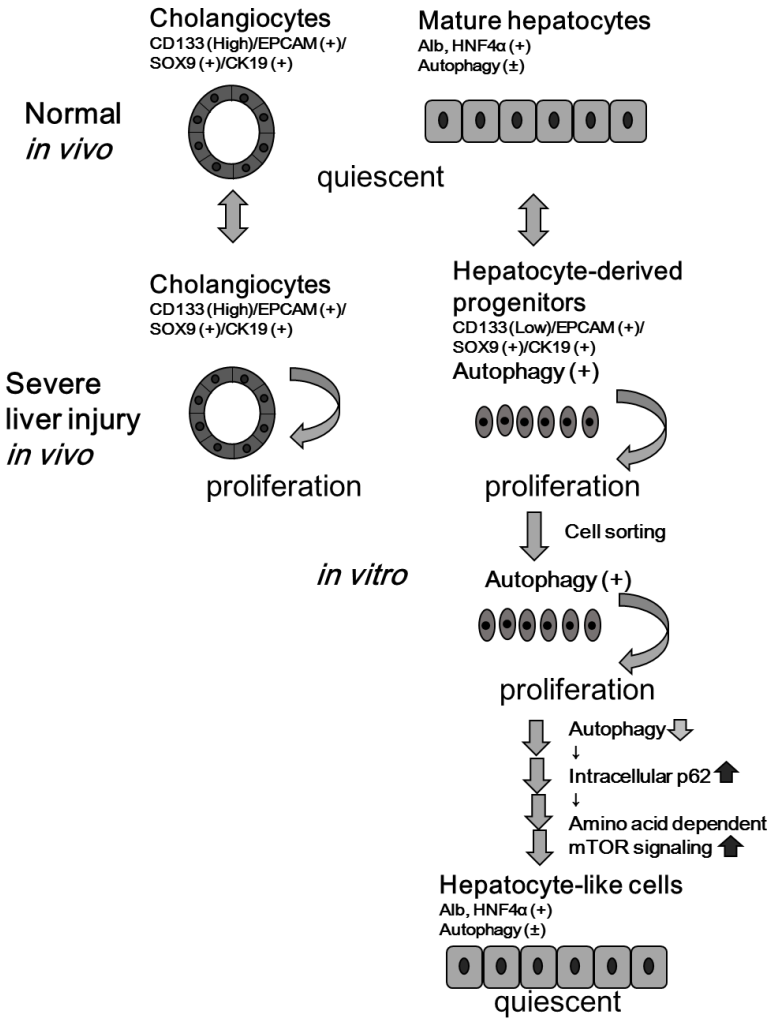

Figure 1- 16. A model based on my findings.

Chapter 2: Role of JAG1-Notch Signaling in Epithelial-Mesenchymal Transition and Poor Prognosis in Colorectal Cancer

1. Abstract

The importance of Notch signaling in colorectal cancer (CRC) development and progression has been presented previously. Increased expression of Jagged-1 (JAG1), a Notch ligand, in CRC has been demonstrated but the detailed prognostic significance of JAG1 in CRC has not been determined. JAG1 protein expression was examined by immunohistochemistry in 158 CRC specimens. Expression of JAG1 and E-cadherin and their association with clinicopathologic characteristics, overall survival (OS), and relapse-free survival (RFS) were evaluated. *In vitro* studies using compounds that regulate intracellular signaling and small interfering RNA that silence *JAG1* were performed on a colon cancer cell line. JAG1 expression in cancerous tissues was weak, moderate, or strong in 32%, 36%, and 32% of specimens, respectively, and correlated with the histologic type and T stage. In multivariate analysis, JAG1 expression, histologic type, and lymphatic invasion were independently correlated with OS and RFS. The combination of high JAG1 expression and low E-cadherin expression had an additive effect toward poorer OS and RFS compared with the low JAG1/high E-cadherin expression subtype. A significant correlation between JAG1 expression and KRAS status was detected in groups stratified by high E-cadherin expression. *In vitro* studies suggested that the RAS-MEK-MAP kinase and Wnt pathways positively regulated JAG1 expression. Gene silencing with siJAG1 indicated that JAG1 promotes epithelial to

mesenchymal transition and cell growth. Thus, high JAG1 expression is regulated by various pathways and is associated with a poor prognosis through promotion of epithelial to mesenchymal transition and cell proliferation or maintenance of cell survival in CRC.

2. Introduction

The Notch signaling pathway is important for intestinal epithelial stem/progenitor cell self-renewal and differentiation (Sancho et al., 2015). Four Notch receptors (Notch 1–4) and five Notch ligands (DLL1, DLL3, DLL4, JAG1, and JAG2) have been identified (Hori et al., 2013). JAG1, like the other ligands, binds to Notch receptors and induces activation through the cleavage of Notch receptor by γ-secretase and subsequent release of the Notch intracellular domain (NICD). NICD can translocate to the nucleus where it forms a complex with a transcriptional regulator and activates the transcription of target genes such as the hairy and enhancer of split (HES) gene family (Hori et al., 2013).

Accumulating evidence has shown that deregulation of the Notch pathway plays a significant role in the progression of several malignancies. Furthermore, high JAG1 expression levels are associated with enhanced progression and metastatic potential, recurrence, and poor overall survival (OS) in prostate cancer, breast cancer, glioma, head and neck cancers, and gastric cancer (Lin et al., 2010; Purow et al., 2005; Reedijk et al., 2005; Santagata et al., 2004; Sethi et al., 2011; Yeh et al., 2009).

Additionally, Notch signaling is shown to be strongly activated in primary human colorectal cancer (CRC) and has an important role in the initiation and progression of CRC through the regulation of apoptosis, proliferation, angiogenesis, and cell migration (Arcaroli et al., 2016; Chu et al., 2010; Ozawa et al., 2014; Serafin et al., 2011; Sikandar et al., 2010; Sonoshita et al., 2011). Recent reports also indicate that JAG1 mediates the activation of Notch signaling in CRC and induces CRC progression (Dai et al., 2014; Guilmeau et al., 2010; Kim et al., 2013; Lu et al., 2013; Rodilla et al., 2009). Thus, the JAG1-Notch pathway has been regarded an attractive target for CRC therapy.

Although high JAG1 expression and the prognostic implications of Notch receptors in

cancer cells have been described (Arcaroli et al., 2016; Chu et al., 2010; Dai et al., 2014; Guilmeau et al., 2010; Kim et al., 2013; Ozawa et al., 2014; Paiva et al., 2015; Rodilla et al., 2009; Serafin et al., 2011), the prognostic significance of high JAG1 expression in CRC has not been determined. Therefore, I investigated the association of JAG1 protein expression with survival and recurrence in CRC by immunohistochemistry (IHC) using postoperative specimens and survey information on CRC prognosis collected at the research institute where I was engaged in this research. I also examined E-cadherin expression as a marker of EMT to evaluate a possible relationship between JAG1 and EMT in the prognostic role of these factors in CRC. To my knowledge, the detailed clinical results of this study provide the first report of the poor prognostic implication of high JAG1 expression in CRC patients.

3. Methods

3.1. Patients and specimens

A total of 158 consecutive patients with CRC who underwent surgical resection at the Department of Surgery and Science, Kyushu University Hospital, between 1995 and 2002 were analyzed in this study. Histologic diagnosis was based on the World Health Organization Classification of Colorectal Carcinoma (Jass and Sobin, 1989). Pathologic staging was performed by the Department of Anatomic Pathology, Pathological Sciences, Kyushu University, Fukuoka, Japan, according to the tumor-node-metastasis classification system, as revised in 2002 (Sobin and Wittekind, 2002). Written informed consent was obtained from each patient prior to tissue acquisition. All fresh specimens were fixed in 10% formalin and embedded in paraffin. This study was conducted with the approval of the Ethics Committee of Kyushu University Hospital, Fukuoka, Japan, in accordance with the Declaration of Helsinki (Approval No. 27-193).

3.2. Immunohistochemistry

Tumor sections were assessed immunohistochemically using rabbit polyclonal antibody against an intracellular region of JAG1 (sc-8303, 1:200; Santa Cruz Biotechnology, CA, USA), rabbit monoclonal antibody against an extracellular region of JAG1 (2155, 1:100; Cell Signaling Technology, MA, USA) and mouse monoclonal antibody against E-cadherin (M106, 1:1,000; Takara Bio; Kyoto, Japan) with the horseradish peroxidase-labeled polymer secondary antibody Envision^{+} system (Dako, CA, USA). Briefly, 4-μm sections were deparaffinized and dehydrated. For antigen retrieval, the specimens were pretreated in an autoclave at 120°C for 15 min in 0.01 M citrate buffer, pH 6.0. The sections were incubated for 30 min in 0.3% hydrogen peroxidase in absolute methanol to deactivate endogenous peroxidases. After blocking of nonspecific binding with 10% goat serum, the specimens were incubated at 4°C with

primary antibodies overnight. After washing with Tris buffered Saline (pH 7.4), the sections were incubated with the Envision^{+} system (Dako) for 1 hour at room temperature. Color was developed with liquid DAB chromogen in Tris-buffered saline (pH 7.4) containing hydrogen peroxide. The sections were counterstained with hematoxylin. The immunoreactivity score was determined as described by Allred et al (Allred et al., 1998). Scoring was performed by the study investigators, which included general pathologists. The score for JAG1 was determined by the three grades of intensity ('weak' for no or weak staining; 'moderate'; or 'strong'). The score for E-cadherin was determined by adding the grades for intensity (1 for no or weak; 2 for moderate; 3 for strong) and the percentage of positive cells (1: 0–1%; 2: 1–10%; 3: 10–33%; 4: 33–66%; and 5: 66–100%).

3.3. *KRAS* and *BRAF* sequencing

Mutation of *KRAS* at codons at 12 and 13 or BRAF at codon 600 was determined by direct sequencing as previously described (Nakanishi et al., 2013; Zhao et al., 2008).

3.4. Microsatellite instability (MSI) analysis

MSI status was assessed using fluorescent-labeled primers and an automated DNA sequence, as previously described (Nakanishi et al., 2013; Zhao et al., 2008). Briefly, my collaborator amplified the microsatellite domain region by polymerase chain reaction (PCR) from cancerous and normal tissue. The fluorescent-labeled PCR product was loaded on ABI 310 sequencer and data was analyzed using Gene Scan software. High MSI (MSI-H) was defined as replication error in ≥2 markers. Low MSI (MSI-L) was defined as replication error in a single marker.

3.5. Cell culture and reagents

HCT-116 cells were purchased from the ATCC. HCT-116 p53$^{-/-}$ cells were kindly

provided by B. Vogelstein (Johns Hopkins University, Baltimore, MD, USA). These cells were authenticated in Ref. (Matsuoka et al., 2015). Caco-2 cells were purchased from the ECACC. Cell lines were passaged to prepare low-passage stocks, which were then cryopreserved in liquid nitrogen. Cell cultures were prepared from frozen stocks when the cells had undergone 1 month of continuous culture. HCT-116 cells were cultured in Dulbecco's modified Eagle's medium supplemented with 10% FBS, 100 U/mL penicillin, and 100 mg/mL streptomycin at 37°C in 5% CO_2. Caco-2 cells were cultured in the same medium for HCT-116, but Non-Essential Amino Acids was added. CHIR99021 and PD0325901 were purchased from Cayman Chemical (MI, USA).

3.6. Small interfering RNA (siRNA) studies

siRNA studies were performed using siRNA against JAG1 (siJAG1) (oligo ID HSS176255) or siNON (oligo ID 12935–112) purchased from Invitrogen (MA, USA). The siRNAs were transfected into cells using Lipofectamine RNAiMAX transfection regent (Invitrogen) according to the manufacturer's instructions.

3.7. Western blot analysis

Cells were lysed in RIPA buffer. Lysates were separated by sodium dodecyl sulfate polyacrylamide gel electrophoresis and transferred to polyvinylidene difluoride membranes. The membranes were washed, blocked, and incubated with the primary antibody. After washing, the membranes were incubated with horseradish peroxidase-conjugated secondary antibodies and immunoreactive bands were visualized by enhanced chemiluminescence (Chemi-Lumi One Ultra: Nakarai Tesque, Kyoto, Japan) using an Amersham Imager 600 (GE Healthcare, Little Chalfont, UK). The antibodies used were rabbit polyclonal antibody against JAG1 (sc-8303, 1:200), rabbit monoclonal antibody against E-cadherin (3195, 1:1,000; Cell Signaling Technology, MA,

USA), rat monoclonal antibody against Snail (61368, 1:4,000; Active Motif, Inc., CA, USA), mouse monoclonal antibody against β-catenin (610153, 1:1,000; BD Biosciences, New Jersey, USA), rabbit polyclonal antibody against phospho-p44/42 MAPK (Erk1/2) (Thr202/Tyr204) (9101, 1:1000; Cell Signaling Technology), rabbit polyclonal antibody against p44/42 MAPK (Erk1/2) (9102, 1:2000; Cell Signaling Technology), mouse monoclonal antibody against a-tubulin (T6199, 1:5,000; Sigma-Aldrich, MO, USA), and rabbit monoclonal antibody against glyceraldehyde-3-phosphate dehydrogenase (GAPDH) (GTX100118, 1:5,000; GeneTex, CA, USA).

3.8. Immunofluorescence analysis

Cells were fixed in 90% methanol at 4°C for 30 min. After permeabilization with 0.3% Triton X-100 and blocking with 3% bovine serum albumin, fixed cells were incubated with the following primary antibodies: rabbit polyclonal antibody against JAG1 (sc-8303, 1:50, or 1:100), mouse monoclonal antibody against E-cadherin (M106, 1:1,000), and rat monoclonal antibody against Snail (61368, 1:500 or 1:1,000). After washing, the cells were incubated with Alexa Fluor-conjugated secondary antibodies (Molecular Probes, MA, USA) for visualization.

3.9. Gene expression analysis

Total RNA was extracted from cultured cells using an RNeasy Mini Kit (QIAGEN, Hilden, Germany) and reverse-transcribed using SuperScript III (ThermoFisher Scientific, MA, USA) according to the manufacturers' instructions. qRT-PCR was performed using TaqMan enzyme and a StepOne plus PCR system (Applied Biosystems, MA, USA). The probes used were *JAG1* (Hs00164982_m1), *HES1* (Hs00172878_m1), *CDH1* (Hs01023894_m1), *VIM* (Hs00958111_m1) from Applied Biosystems. Expression levels were normalized to expression of *GAPDH*.

3.10. Statistical analysis

All statistical calculations were performed using JMP Pro 10 statistical software (SAS Institute Japan, Tokyo, Japan). Relationships among the clinicopathologic factors and JAG1 and E-cadherin staining were analyzed using χ^2 tests. Survival curves were plotted using the Kaplan–Meier method, and the log-rank test was used to determine associations between individual variables and survival. OS and relapse-free survival (RFS) were evaluated using the univariate or multivariate Cox proportional hazard model. Proportion data of recurrence were evaluated using the multivariate logistic regression model. Differences were considered significant at $P < 0.05$.

4. Results

4.1. JAG1 immunohistochemistry

Antibody against the intracellular region of JAG1 was used for immunohistochemical staining of CRC specimens. This antibody was relatively selective for JAG1 protein and had appropriate characteristics for analyzing the prognostic significance of JAG1 expression in the cancerous tissue and endothelium by IHC, as shown in Figure 2- 1 and Figure 2- 2.

Immunohistochemical analysis indicated that JAG1 was expressed by cancer cells and endothelium (Figure 2- 3). Weak (jcIHC-W), moderate (jcIHC-M), and strong (jcIHC-S) staining of cancerous tissues was detected in 51 (32%), 57 (36%), and 50 (32%) samples, respectively (Figure 2- 3, Table 2- 1). Weak (jeIHC-W), moderate (jeIHC-M), and strong (jeIHC-S) staining of endothelium was detected in 61 (39%), 54 (34%), and 43 (27%) samples, respectively (Figure 2- 3, Table 2- 1).

4.2. Correlation of JAG1 expression in cancer cells or endothelium with clinicopathologic characteristics and recurrence

The correlation between JAG1 expression and clinicopathologic characteristics is shown in Table 2- 1. JAG1 expression in cancer cells was correlated with histologic type ($P = 0.031$) and T stage ($P = 0.003$). JAG1 expression in cancer cells was also significantly associated with JAG1 expression in endothelium ($P < 0.001$) and rate of recurrence ($P = 0.009$). Moreover, JAG1 expression in endothelium was correlated with lymph node metastasis ($P = 0.035$) and venous invasion ($P = 0.039$). Moderate intensity of staining in the endothelium tended to be associated with poorer characteristics than the other staining groups.

4.3. Analysis of the association between JAG1 expression and survival outcome

The association between JAG1 expression in cancer cells and OS was evaluated in all patients (Figure 2- 4a). JAG1 expression was significantly associated with OS (P = 0.006). Evaluation of the association between JAG1 expression and RFS in 131 patients with stage 0–III CRC (ST_0-III) showed that JAG1 expression was also significantly associated with RFS (Figure 2- 4b; P = 0.010). Analysis of the prognostic significance of JAG1 expression as indicated by the 5-year survival rate calculated by Kaplan–Meier estimates and hazard ratio analyzed using the Cox proportional hazard model revealed that higher expression of JAG1 is associated with a poorer survival rate and larger hazard ratio (Figure 2- 5).

In univariate analysis for OS in all patients and for RFS in the ST_0-III subgroup, JAG1 expression was significantly correlated with both OS and RFS (Table 2- 2). In multivariate analysis, JAG1 expression, histologic type, and lymphatic invasion showed independent association with OS and RFS (Table 2- 2). Univariate analysis of the rate of recurrence in all patients by the logistic model (Table 2- 2) revealed a significant correlation of JAG1 expression with recurrence. Multivariate analysis showed that tumor stage and JAG1 expression were independently associated with recurrence (Table 2- 2).

The association between JAG1 expression in endothelium and OS or RFS was also analyzed (Figure 2- 6 a and b). The 5-year survival rate calculated by the Kaplan–Meier estimate is shown in Figure 2- 6c and prognostic analysis of JAG1 expression by the Cox proportional hazard model is shown in Figure 2- 6d. High expression of JAG1 in endothelium was more strongly associated with RFS than with OS.

4.4. Analysis of the association between JAG1 and E-cadherin expression

To investigate whether JAG1 expression is associated with the transition between

epithelial and mesenchymal characteristics, E-cadherin expression was analyzed as an epithelial marker by IHC (Figure 2- 7). E-cadherin expression was categorized by staining intensity (eIHC-In1–3) or the proportion of positive cells (eIHC-Pr1–5), as shown in Figure 2- 7 and Table 2- 3. High JAG1 expression (jcIHC-S vs. jcIHC-W/M) was significantly correlated with low E-cadherin expression in subgroup stratification by proportion (eIHC-Pr1-3 vs. eIHC-Pr4/5) (Table 2- 3, $P = 0.023$).

4.5. Analysis of JAG1 expression in patient samples stratified by E-cadherin expression

A significant poor prognosis of low E-cadherin expression for OS was detected by log-rank test in analysis according to staining intensity of 1 vs. 2/3 (Figure 2- 8a, $P = 0.038$). In this stratification, no correlation between JAG1 and E-cadherin expression was detected (Table 2- 3), therefore an additional prognostic impact of combined JAG1 and E-cadherin expression was expected. To investigate the significance of JAG1 expression on prognosis in samples stratified by intensity of E-cadherin staining, patients were divided into six groups as follows: (1) jcIHC-W/eIHC-In2/3; (2) jcIHC-M/eIHC-In2/3; (3) jcIHC-S/eIHC-In2/3; (4) jcIHC-W/eIHC-In1; (5) jcIHC-M/eIHC-In1; and (6) jcIHC-S/eIHC-In1 (Table 2- 4). The *P* value of the log-rank test for OS and RFS was 0.011 and 0.001, respectively (Figure 2- 9 a and b). OS and RFS in jcIHC-M/eIHC-In2/3, jcIHC-S/eIHC-In2/3, jcIHC-M/eIHC-In1, and jcIHC-S/eIHC-In1 groups were significantly shorter than those of the jcIHC-W/eIHC-In2/3 group (Figure 2- 9 a–d). Specifically, the jcIHC-S/eIHC-In1 group showed the poorest outcome of all groups: 3-year OS = 34.9% (HR = 10.08, 95% CI = 2.64–47.97, $P = 0.001$ [vs. jcIHC-W/eIHC-In2/3]); 3-year RFS = 33.3% (HR = 8.27, 95% CI = 2.49–31.67, $P = 0.001$ [vs. jcIHC-W/eIHC-In2/3]). The relationship between JAG1 expression and RFS

was notable in the group with moderate or strong intensity of E-cadherin staining (eIHC-In2-3). Namely, the 3-year RFS rate in jcIHC-S/eIHC-In2/3 (45.6%) was much lower than that in jcIHC-M/eIHC-In2/3 (68%), whereas the 3-year OS rate in jcIHC-S/eIHC-In2/3 (74.3%) was almost the same as that for jcIHC-M/eIHC-In2/3 (71.9%). This may indicate that high JAG1 expression is associated with shorter duration of recurrence rather than survival in the group with moderate or strong intensity of E-cadherin staining (eIHC-In2/3).

The correlation of JAG1 expression in cancer cells stratified by E-cadherin expression with clinicopathologic characteristics, JAG1 expression in endothelium, KRAS, BRAF, and MSI status was evaluated (Table 2- 4, Table 2- 5 and Figure 2- 10). Because of the retrospective analysis, data on KRAS, BRAF, and MSI status were available for only 78, 76, and 117 specimens of the 158 CRC patients, respectively. JAG1 expression in cancer cells stratified as high intensity of E-cadherin staining or large proportion of E-cadherin expression (eIHC-In2/3 or eIHC-Pr4/5) was significantly correlated with histologic type (Table 2- 4, Table 2- 5). And higher rate of KRAS mutation was observed in the jcIHC-S/eIHC-In2/3 group (48%) compared with the other groups (17% for jcIHC-W/eIHC-In2/3 and 23% for jcIHC-M /eIHC-In2/3) (Table 2- 4, Figure 2- 10). A significant correlation between JAG1 expression and KRAS status (P = 0.037, data not shown) was also observed in in the group with eIHC-Pr5 in stratification by eIHC-Pr1-4 (n = 79) versus eIHC-Pr5 (n = 79) based on the proportion of E-cadherin expression. These result suggested that one of the mechanism for high JAG1 expression in CRC was the enhancement of KRAS and its downstream pathway. There were not significant correlation between JAG1 expression and BRAF or MSI status in the group stratified as strong and moderate intensity of E-cadherin staining (eIHC-In2/3). On the other hand, in

the group of the other stratification in E-cadherin (eIHC-In1), strong intensity of JAG1 staining seemed to associate with MSI or BRAF status. However, I could not determine whether these associations for MSI or BRAF status were really significant because of too small sample size.

4.6. Mechanism of increasing JAG1 expression and JAG1-dependent promotion of epithelial–mesenchymal transition and proliferation in a colon cancer cell line

To investigate whether the KRAS-MEK-MAP kinase pathway regulates JAG1 expression and the transition between epithelial and mesenchymal status, the effect of the MEK inhibitor PD0325901 was examined in the HCT-116 colon cancer cell line. Treatment with MEK inhibitor decreased expression of JAG1 and the mesenchymal marker SNAIL (Figure 2- 11 a, b). Conversely, E-cadherin expression was increased after inhibition of MEK (Figure 2- 11 a, b). The effect of the MEK inhibitor PD325901 on JAG1 expression and transition toward mesenchymal phenotype was also investigated by western blotting in the HCT-116 (KRAS G13D) and Caco-2 (KRAS wild) colon cancer cell lines (Figure 2- 12). HCT-116 cells have lower level of E-cadherin and higher level of JAG1, SNAIL, phosphorylated ERK1/2 in the control condition than in Caco-2 cells. Inhibition of MEK kinase lead to suppression of phosphorylated ERK1/2, JAG1 and SNAIL level in HCT-116. Conversely, increasing of E-cadherin expression was observed by inhibition of MEK in HCT-116. On the other hand, there were no or little change about JAG1, E-cadherin, and SNAIL expression by inhibition of MEK in Caco-2.

I also detected the positive regulation of JAG1 expression and the EMT resulting from Wnt-β catenin pathway activation by the Glycogen synthase kinase (GSK) 3β inhibitor, CHIR-99021, in HCT-116 cells. Namely, treatment with CHIR-99021 increased JAG1 and SNAIL expression and decreased E-cadherin expression (Figure 2- 11c).

The effect of *JAG1* gene silencing on EMT in the colon cancer cell line was investigated using siJAG1. Western blot (Figure 2- 13a), qRT-PCR (Figure 2- 13b), and immunofluorescence (Figure 2- 14) analyses indicated that siJAG1 treatment increased expression of E-cadherin protein/mRNA, decreased expression of Snail protein and decreased expression of the mesenchymal marker vimentin mRNA compared with control siNON treatment. These results suggested that the colon cancer cell line transited into a more epithelial and less mesenchymal phenotype upon *JAG1* gene silencing.

I also examined the effect of siJAG1 on proliferation of HCT-116 cells and explored the possibility of crosstalk between the JAG1-Notch pathway and p53-related signaling by investigating the effects in HCT-116 $p53^{-/-}$ cells (p53KO). siJAG1 at the concentration of 30 nM decreased *JAG1* mRNA levels by more than 80% compared with siNON in both wild type (Wt) and p53KO cells (Figure 2- 13c). mRNA expression of *HES1*, one of the Notch signal target genes, was also decreased, suggesting suppression of intracellular Notch signaling (Figure 2- 13c). *JAG1* and *HES1* mRNA expression was significantly lower in p53KO than in Wt cells (Figure 2- 13c). JAG1 protein level was also suppressed by siJAG1 compared with siNON treatment (Figure 2- 13d). The lower expression level of JAG1 protein in p53KO than in Wt was concordant with the results of qRT-PCR analysis (Figure 2- 13c and d). Suppressed proliferation in Wt cells treated with siJAG1 compared with cells treated with siNON was evident 2 days after initiation of treatment (Figure 2- 13e). No obvious effect of siJAG1 on proliferation in p53 KO cells was observed (Figure 2- 13e).

5. Discussion

To my knowledge, this study is the first report of the prognostic significance of JAG1 expression in cancer cells from patients with CRC. Moreover, my data indicate a relationship between JAG1 and E-cadherin expression in the prognosis of CRC. Furthermore, I provide a novel insight into the correlation between KRAS status and JAG1 expression in CRC patients. Various studies have previously reported that a high JAG1 expression level was detected in cancer cells (Dai et al., 2014; Guilmeau et al., 2010; Kim et al., 2013; Pannequin et al., 2009; Rodilla et al., 2009), and was correlated with tumor grade (Kim et al., 2013) in human patients. However, the prognostic significance of JAG1 expression in CRC cells has not been determined. My study demonstrated that higher JAG1 expression in cancer cells of CRC patients is associated with a poorer survival rate and an increased risk of recurrence, and that the combination of high JAG1 expression with low E-cadherin expression might lead to severely poor outcome.

Three causes of the poor survival rate and increased risk of recurrence associated with high JAG1 expression have been proposed: increased cell proliferation or maintenance of survival, acquisition of a stem cell-like phenotype, and induction of an EMT-like phenotype in cancer cells. My study indicated that siRNA-mediated *JAG1* gene silencing in a colon cancer cell line resulted in delayed cell proliferation with a subsequent decrease in cell number. Similar results have been reported previously (Dai et al., 2014; Kim et al., 2013). The evidence from our *in vitro* study and the previous reports support the poor prognostic significance of high JAG1 expression in CRC.

The second possibility involves JAG1 protein expression associated with the endothelium. I found that a high expression of JAG1 protein in the endothelium was

associated with a high expression of JAG1 protein in cancer cells and a poor prognosis, especially an increased recurrence risk. This result might be associated with the acquisition of a stem cell-like phenotype in cancer cells through Notch pathway activation by JAG1 secreted from the endothelium in CRC, as described previously (Lu et al., 2013). While my study did not explore the mechanisms of high JAG1 expression in the endothelium, some mechanisms were speculated from previous reports (Gopinathan et al., 2015; Johnston et al., 2009). For instance, proinflammatory cytokines such as TNF-α and IL6 are possible inducers of JAG1 expression in the endothelium. JAG1 upregulation in colon cancer cell lines induced by forced Notch pathway activation also promotes stemness in the cancer cells themselves through positive feedback (Fender et al., 2015). My study indicates that JAG1 expression in cancer cells was strongly correlated with JAG1 expression in the endothelium and that a stronger intensity of JAG1 staining in the endothelium and cancer cells was associated with a poor prognosis. Thus, JAG1 secreted from the endothelium stimulates the Notch pathway in cancer cells, and JAG1 expression in cancer cells might be upregulated dependent on the activity of Notch pathway itself in cancer cells. JAG1-Notch signaling in cancer cells may then be amplified through a positive feedback. These findings suggest that the transition toward a cancer stem cell-like phenotype in cancer cells is promoted through an interaction between the endothelium and cancer cells, mediated by JAG1, leading to a poorer prognosis in CRC patients.

My study also demonstrates the significance of the JAG1-Notch pathway in EMT in human CRC. I detected a significant association between low E-cadherin and high JAG1 expression in clinical CRC samples and found that high JAG1 expression in CRC cells correlated with the histologic type (decreased differentiation status) and T stage (deep

invasion) among the clinicopathologic characteristics. This correlation may be caused by an EMT-like phenomenon induced by JAG1-Notch pathway activation. Induction of an EMT-like phenotype in cancer cells might facilitate their exit from the original site, migration to distant locations, and survival in a new microenvironment (Kalluri and Weinberg, 2009; Peinado et al., 2007). Notch signaling was reported to mediate EMT thorough upregulation of Snail protein (Sahlgren et al., 2008). Moreover, forced Notch pathway activation was shown to increase JAG1 expression and promote EMT through a positive feedback in a colorectal cancer cell line (Fender et al., 2015). My *in vitro* study demonstrated that although siRNA-mediated *JAG1* gene silencing induced transition to a more epithelial phenotype, activation of the Wnt pathway by inhibition of GSK-3β not only induced transition to a more mesenchymal phenotype but also increased JAG1 expression as predicted from the previously reported circumstantial evidence (Guilmeau et al., 2010; Pannequin et al., 2009; Rodilla et al., 2009; Zhou et al., 2004). Previous studies and my *in vitro* study support the significant role of JAG1-Notch pathway activation in poor prognosis for human CRC through EMT induction.

It was recently reported that concomitant Notch activation and p53 deletion triggers EMT and metastasis in a genetically engineered mouse model (Chanrion et al., 2014). I demonstrated that siJAG1 delayed or inhibited proliferation in the Wt cell line but had a less potent effect in a $p53^{-/-}$ cell line. Moreover, siJAG1 increased the expression of E-cadherin and decreased Snail protein in the Wt cell line, whereas a similar effect could not be detected in the $p53^{-/-}$ cell line (data not shown). These results indicate that JAG1-Notch signaling is important for the induction of an EMT-like phenotype as well as for proliferation through suppression of a p53-related pathway (Dotto, 2009). Alternatively, lower expression of JAG1 mRNA and protein in the $p53^{-/-}$ cell line

compared with that in Wt suggests a reciprocal relationship between JAG1 protein expression and p53 status (Dotto, 2009). This is an unexpected result and my studies could not validate a model in which concomitant Notch activation and p53 deletion triggers EMT (Chanrion et al., 2014). To address this issue, the effect of exogenous treatment with JAG1 in *p53*$^{-/-}$ cancer cells should be examined in the future. In the aspect of low JAG1 expression induced by p53 KO, my preliminary analysis in human clinical specimens indicated that low JAG1 expression was significantly associated with a high proportion of loss of heterozygosity in p53 status (data not shown). Thus, further studies on the association between JAG1 expression and p53 status in CRC patients might reveal the reciprocal relationship between p53 status and JAG1 expression.

My findings also suggest that EMT is induced by mediators other than JAG1-Notch signaling as indicated by the weak correlation between the low staining intensity of E-cadherin and high JAG1 expression. Consequently, I demonstrated an additive impact of the combination of high JAG1 and low E-cadherin expression on prognosis and found that the poorest survival rate for both OS and RFS was indicated by this combination. I could not find any association between JAG1 expression and clinicopathologic characteristics in groups stratified by low E-cadherin expression, and therefore it might be important to identify which downstream pathway of JAG1-Notch leads to poorer prognosis in these groups.

My study indicates a shorter recurrence free interval after surgery in patients with high JAG1 expression among the subgroup with an E-cadherin staining intensity of 2/3 (Figure 2- 9), and shows that this phenomenon might be associated with a high rate of mutation in KRAS (Table 2- 4, Figure 2- 10). It was previously reported that MEK inhibition suppresses JAG1 expression induced by growth factors in head and neck

squamous cell carcinoma (Zeng et al., 2005). In my study, the MEK inhibitor suppressed JAG1 expression as well as SNAIL expression and upregulated E-cadherin in a colon cancer cell line with a KRAS mutation and an possibly activated MAP kinase pathway (Ahmed et al., 2013). Therefore, activation of the MAP kinase pathway by the KRAS mutation might be partially upstream of JAG1 expression in CRC.

While this study presented a novel finding about the association among high JAG1 expression, KRAS status, and prognostic significance in CRC, there are some limitations including retrospective nature, sample size, various stages, and lack of enough information regarding molecular status. Multicenter prospective studies that enable investigation of a large sample size could validate my findings in this study.

In conclusion, this is the first report demonstrating the poor prognostic significance of high JAG1 expression in CRC. Moreover, my study revealed that low E-cadherin expression plays an additive role in the poor prognosis associated with high JAG1 expression in CRC. The results of my *in vitro* study support the poor prognostic impact associated with high JAG1 expression in CRC and suggest clues for the potential mechanisms involved in the complicated regulation of JAG1 expression and JAG1-Notch pathway-induced cancer development, as illustrated by the model in Figure 2- 15 Furthermore, this study implicates JAG1 and its related signaling pathways as a potential target for the development of new therapeutic approaches to reduce recurrence risk and cancer-related death after surgery for CRC.

6. Tables

Table 2- 1. Association between clinical characteristics and JAG1 expression in cancer cells and endothelium.

Characteristics	JAG1 (Cancer cells)			*P* value		JAG1 (Endothelium)			*P* value
	Weak	Mod	Strong			Weak	Mod	Strong	
Total	51 (32)	57 (36)	50 (32)			61 (39)	54 (34)	43 (27)	
Sex				0.352					0.877
Male	31 (61)	36 (63)	25 (50)			36 (59)	30 (56)	26 (60)	
Female	20 (39)	21 (37)	25 (50)			25 (41)	24 (44)	17 (40)	
Age (years)				*N.S.*					*N.S.*
Mean±SD	64.7 ± 10.8	64.6 ± 11.8	62.1 ± 13.9			63.0 ± 12.3	63.1 ± 10.1	65.9 ± 14.3	
Histologic type				0.031*					0.495
Well differentiated	38 (79)	34 (61)	26 (55)			41 (71)	32 (62)	25 (61)	
Mod/Poorly	10 (21)	22 (39)	21 (45)			17 (29)	20 (38)	16 (39)	
Others	3	1	3			3	2	2	
T stage				0.003**					0.080
T1	14 (27)	8 (14)	2 (4)			15 (25)	6 (11)	3 (7)	
T2	6 (12)	7 (12)	8 (16)			5 (8)	6 (11)	10 (23)	
T3	29 (57)	31 (55)	26 (53)			32 (54)	32 (59)	22 (51)	
T4	2 (4)	11 (19)	13 (27)			8 (13)	10 (19)	8 (19)	
Unknown			1			1			
Lymph node metastasis				0.242					0.035*
Negative	33 (65)	28 (49)	26 (53)			40 (67)	23 (43)	24 (56)	
Positive	18 (35)	29 (51)	23 (47)			20 (33)	31 (57)	19 (44)	
Unknown			1			1			
Stage of tumor				0.126					0.114
0–I	18 (35)	12 (21)	7 (14)			20 (33)	6 (11)	11 (25)	
II	12 (24)	14 (25)	15 (30)			16 (26)	13 (24)	12 (28)	
III	15 (29)	23 (40)	15 (30)			17 (28)	22 (41)	14 (33)	
IV	6 (12)	8 (14)	13 (26)			8 (13)	13 (24)	6 (14)	
Lymphatic invasion				0.136					0.436
Negative	39 (76)	34 (60)	31 (62)			43 (70)	32 (59)	29 (67)	
Positive	12 (24)	23 (40)	19 (38)			18 (30)	22 (41)	14 (33)	
Venous invasion				0.818					0.039*
Negative	32 (63)	33 (58)	27 (54)			39 (64)	24 (44)	29 (67)	
Positive	19 (37)	24 (42)	23 (46)			22 (36)	30 (56)	14 (33)	
JAG1 (Endothelium)				<0.001**	**JAG1 (Cancer)**				<0.001**
Weak	35 (69)	17 (30)	9 (18)		Weak	35 (57)	14 (26)	2 (5)	
Mod	14 (27)	24 (42)	16 (32)		Mod	17 (28)	24 (44)	16 (37)	
Strong	2 (4)	16 (28)	25 (50)		Strong	9 (15)	16 (30)	25 (58)	
Recurrence				0.009**					0.180
Absent	45 (90)	42 (76)	29 (64)			47 (78)	42 (84)	27 (68)	
Present	5 (10)	13 (24)	16 (36)			13 (22)	8 (16)	13 (32)	
Unknown	1	2	5			1	4	3	

Each value is presented as number (%) of specimens. χ^2 test: $^*P < 0.05$, $^{**}P < 0.01$

Mod moderate, *N.S.* not significant, *SD* standard deviation

Table 2- 2. Univariate and multivariate analysis of factors associated with overall survival or relapse-free survival.

Characteristics	Parameters	Univariate analysis			Multivariate analysis		
		HR	95% CI	*P* value	HR	95% CI	*P* value
Overall survival (All patients, Cox model)							
Sex	M vs. F	1.37	0.73–2.54	0.316	1.35	0.70–2.57	0.366
Age	< 65 vs. ≥ 65	0.96	0.52–1.78	0.906	0.99	0.51–1.93	0.980
Histologic type	Well vs. Others	4.51	2.38–9.00	< 0.001**	2.59	1.19–5.94	0.016*
T stage	T1,2 vs. T3,4	3.91	1.56–13.07	0.002**	1.47	0.51–5.31	0.497
Lymph node metastasis	− vs. +	3.93	2.02–8.23	< 0.001**	2.04	0.61–12.68	0.283
Stage of tumor	0/I/II vs. III/IV	4.08	2.03–9.08	< 0.001**	1.02	0.14–4.31	0.980
Lymphatic invasion	− vs. +	5.09	2.72–9.88	< 0.001**	3.88	1.81–8.63	< 0.001**
Venous invasion	− vs. +	2.18	1.18–4.09	0.013*	1.69	0.78–3.65	0.184
JAG1 (Cancer)	W vs. Mod/S	3.99	1.71–11.62	< 0.001**	2.62	1.10–7.74	0.027*
Relapse-free survival (Patients besides Stage IV, Cox model)							
Sex	M vs. F	1.58	0.78–3.13	0.226	1.21	0.54–2.63	0.643
Age	< 65 vs. ≥ 65	1.66	0.83–3.42	0.138	2.10	0.99–4.62	0.055
Histologic type	Well vs. Others	4.74	2.34–10.15	< 0.001**	2.71	1.09–6.91	0.032*
T stage	T1,2 vs. T3,4	2.40	1.06–6.44	0.035*	0.92	0.33–2.77	0.870
Lymph node metastasis	− vs. +	3.04	1.52–6.37	0.002**	1.60	0.25–31.32	0.660
Stage of tumor	0/I/II vs. III	3.16	1.56–6.76	0.001**	1.35	0.07–8.07	0.793
Lymphatic invasion	− vs. +	4.56	2.29–9.20	< 0.001**	4.47	1.76–11.57	0.002**
Venous invasion	− vs. +	2.07	1.03–4.12	0.033*	0.51	0.19–1.37	0.184
JAG1 (Cancer)	W vs. Mod/S	2.38	1.17–4.74	0.017*	2.65	1.16–5.95	0.021*
Recurrence (All patients, Logistic model)							
Sex	M vs. F			0.838			0.628
Age	< 65 vs. ≥ 65			0.369			0.080
Histologic type	Well vs. Others			0.003**			0.082
T stage	T1,2 vs. T3,4			0.272			0.354
Lymph node metastasis	− vs. +			0.006**			0.712
Stage of tumor	0/I/II vs. III/IV			0.005**			0.035*
Lymphatic invasion	− vs. +			0.031*			0.471
Venous invasion	− vs. +			0.191			0.846
JAG1 (Cancer)	W/Mod vs. S			0.011*			0.033*

*$P < 0.05$, **$P < 0.01$

HR, hazard ratio; *CI*, confidence interval; *M*, male; *F*, female; *W*, weak; *Mod*, moderate; *S*, strong

Table 2- 3. Associations between E-cadherin expression and clinical characteristics or JAG1 expression in cancer cells.

Characteristics	E-cadherin (Intensity)			E-cadherin (Proportion)		
	1	2/3	*P* value	1/2/3	4/5	*P* value
Total	39 (25)	119 (75)		44 (28)	114 (72)	
Sex			0.791			0.891
Male	22 (56)	70 (59)		18 (41)	48 (42)	
Female	17 (44)	49 (41)		26 (59)	66 (58)	
Age (Years)			0.462			0.608
< 65	18 (46)	63 (53)		24 (55)	57 (50)	
≥ 65	21 (54)	56 (47)		20 (45)	57 (50)	
Histologic type			0.007**			0.008**
Well differentiated	17 (44)	81 (68)		20 (45)	78 (68)	
Others	22 (56)	38 (32)		24 (55)	36 (32)	
T stage			< 0.001**			< 0.001**
T1, 2	1 (3)	44 (37)		4 (9)	41 (36)	
T3, 4	38 (97)	74 (63)		40 (91)	72 (64)	
Unknown		1			1	
Lymph node metastasis			0.014*			0.055
Negative	15 (38)	72 (61)		19 (43)	68 (60)	
Positive	24 (62)	46 (39)		25 (57)	45 (40)	
Unknown		1			1	
Stage of tumor			< 0.001**			0.002**
0/I/II	10 (26)	68 (57)		13 (30)	65 (57)	
III/IV	29 (74)	51 (43)		31 (70)	49 (43)	
Lymphatic invasion			0.003**			0.028*
Negative	18 (46)	86 (72)		23 (52)	81 (71)	
Positive	21 (54)	33 (28)		21 (48)	33 (29)	
Venous invasion			0.004**			0.100
Negative	15 (38)	77 (65)		21 (48)	71 (62)	
Positive	34 (62)	42 (35)		23 (52)	43 (38)	
JAG1 (Cancer)						
Weak	11 (28)	40 (34)	0.527	14 (32)	37 (32)	0.939
Mod/Strong	28 (72)	79 (66)		30 (68)	77 (68)	
Weak/mod	26 (67)	82 (69)	0.795	24 (55)	84 (74)	0.023*
Strong	13 (33)	37 (31)		20 (45)	30 (26)	

Each value is presented as number (%) of specimens. χ^2 test: *$P < 0.05$, **$P < 0.01$

Mod, Moderate

Table 2- 4. JAG1 expression in cancer cells stratified by E-cadherin expression (based on intensity of staining) and correlation with clinicopathologic characteristics, JAG1 expression in endothelium, and KRAS status

Characteristics	E-cadherin intensity (1) JAG1			*P* value	E-cadherin intensity (2/3) JAG1			*P* value
	Weak	Mod	Strong		Weak	Mod	Strong	
Total	11 (28)	15 (38)	13 (33)		40 (34)	42 (35)	37 (31)	
Sex				0.899				0.149
Male	6 (55)	8 (53)	8 (62)		25 (62)	28 (67)	17 (46)	
Female	5 (45)	7 (47)	5 (38)		15 (38)	14 (33)	20 (54)	
Age (years)				0.321				0.683
< 65	3 (27)	8 (53)	7 (54)		22 (55)	20 (48)	21 (57)	
≥ 65	8 (73)	7 (47)	6 (46)		18 (45)	22 (52)	16 (43)	
Histologic type				0.475				0.045*
Well differentiated	5 (45)	8 (53)	4 (31)		33 (83)	26 (62)	22 (59)	
Others	6 (55)	7 (47)	9 (69)		7 (17)	16 (38)	15 (41)	
T stage				0.377				0.110
T1, T2	0 (0)	1 (7)	0 (0)		20 (50)	14 (33)	10 (28)	
T3, T4	11 (100)	14 (93)	13 (100)		20 (50)	28 (67)	26 (72)	
Unknown							1	
Lymph node metastasis				0.480				0.348
Negative	5 (45)	4 (27)	6 (46)		28 (70)	24 (57)	20 (56)	
Positive	6 (55)	11 (73)	7 (54)		12 (30)	18 (43)	16 (44)	
Unknown							1	
Stage of tumor				0.800				0.226
0/I/II	3 (27)	3 (20)	4 (31)		27 (68)	23 (55)	18 (49)	
III/IV	8 (73)	12 (80)	9 (69)		13 (32)	19 (45)	19 (51)	
Lymphatic invasion				0.998				0.070
Negative	5 (45)	7 (47)	6 (46)		34 (85)	27 (64)	25 (68)	
Positive	6 (55)	8 (53)	7 (54)		6 (15)	15 (36)	12 (32)	
Venous invasion				0.822				0.724
Negative	5 (45)	5 (33)	5 (38)		27 (68)	28 (67)	22 (59)	
Positive	6 (55)	10 (67)	8 (62)		13 (32)	14 (33)	15 (41)	
JAG1 (Endothelium)				0.052				< 0.001**
Weak/Moderate	10 (91)	10 (67)	6 (46)		39 (98)	31 (74)	19 (51)	
Strong	1 (9)	5 (33)	7 (54)		1 (2)	11 (26)	18 (49)	
KRAS status				0.527				0.048*
Total	6	8	9		12	22	21	
Wild type	3 (50)	5 (63)	7 (78)		10 (83)	17 (77)	11 (52)	
Mutant	3 (50)	3 (37)	2 (22)		2 (17)	5 (23)	10 (48)	
BRAF status				0.111				0.863
Total	5	8	9		11	22	21	
Wild type	4 (80)	8 (100)	6 (67)		10 (91)	21 (95)	20 (95)	
Mutant	1 (20)	0 (0)	3 (33)		1 (9)	1 (5)	1 (5)	
MSI status				0.007**				0.977
Total	10	12	11		22	33	29	
MSS or MSI-L	10 (100)	12 (100)	7 (64)		19 (86)	29 (88)	25 (86)	
MSI-H	0 (0)	0 (0)	4 (36)		3 (14)	4 (12)	4 (14)	

Each value is presented as number (%) of specimens. χ^2 test: $^*P < 0.05$, $^{**}P < 0.01$

Mod, moderate

Table 2- 5. JAG1 expression in cancer cells stratified by E-cadherin expression (based on proportion of positive staining) and correlation with clinicopathologic characteristics, JAG1 expression in endothelium, and KRAS status

Characteristics	E-cadherin proportion (1–3) JAG1			*P* value	E-cadherin proportion (4–5) JAG1			*P* value
	Weak	Mod	Strong		Weak	Mod	Strong	
Total	14 (32)	10 (23)	20 (45)		37 (32)	47 (41)	30 (26)	
Sex				0.778				0.143
Male	9 (64)	5 (50)	12 (60)		22 (59)	31 (66)	13 (43)	
Female	5 (36)	5 (50)	8 (40)		15 (41)	16 (34)	17 (57)	
Age (years)				0.417				0.976
< 65	6 (43)	5 (50)	13 (65)		19 (51)	23 (49)	15 (50)	
≥ 65	8 (57)	5 (50)	7 (35)		18 (49)	24 (51)	15 (50)	
Histologic type				0.102				0.029*
Well differentiated	7 (50)	7 (70)	6 (30)		31 (84)	27 (57)	20 (67)	
Others	7 (50)	3 (30)	14 (70)		6 (16)	20 (43)	10 (33)	
T stage				0.643				0.166
T1, T2	2 (14)	1 (10)	1 (5)		18 (49)	14 (30)	9 (31)	
T3, T4	12 (86)	9 (90)	19 (95)		19 (51)	33 (70)	20 (69)	
Unknown							1	
Lymph node metastasis				0.599				0.599
Negative	7 (50)	3 (30)	9 (45)		26 (70)	25 (53)	17 (59)	
Positive	7 (50)	7 (70)	11 (55)		11 (30)	22 (47)	12 (41)	
Unknown							1	
Stage of tumor				0.686				0.133
0/I/II	4 (29)	2 (20)	7 (35)		26 (70)	24 (51)	15 (50)	
III/IV	10 (71)	8 (80)	13 (65)		11 (30)	23 (49)	15 (50)	
Lymphatic invasion				0.907				0.075
Negative	8 (57)	5 (50)	10 (50)		31 (84)	29 (62)	21 (70)	
Positive	6 (43)	5 (50)	10 (50)		6 (16)	18 (38)	9 (30)	
Venous invasion				0.671				0.915
Negative	8 (57)	4 (40)	9 (45)		24 (65)	29 (62)	18 (60)	
Positive	6 (43)	6 (60)	11 (55)		13 (35)	18 (38)	12 (40)	
JAG1 (Endothelium)				0.001**				< 0.001**
Weak/Moderate	14 (100)	9 (90)	11 (55)		35 (95)	32 (68)	14 (47)	
Strong	0 (0)	1 (10)	9 (45)		2 (5)	15 (32)	16 (53)	
KRAS status				0.191				0.064
Total	6	3	12		12	27	18	
Wild type	3 (50)	0 (0)	9 (75)		10 (83)	19 (70)	10 (56)	
Mutant	3 (50)	3 (100)	3 (25)		2 (17)	8 (30)	8 (44)	

Each value is presented as number (%) of specimens. χ^2 test: *$P < 0.05$, **$P < 0.01$

Mod, moderate

7. Figures

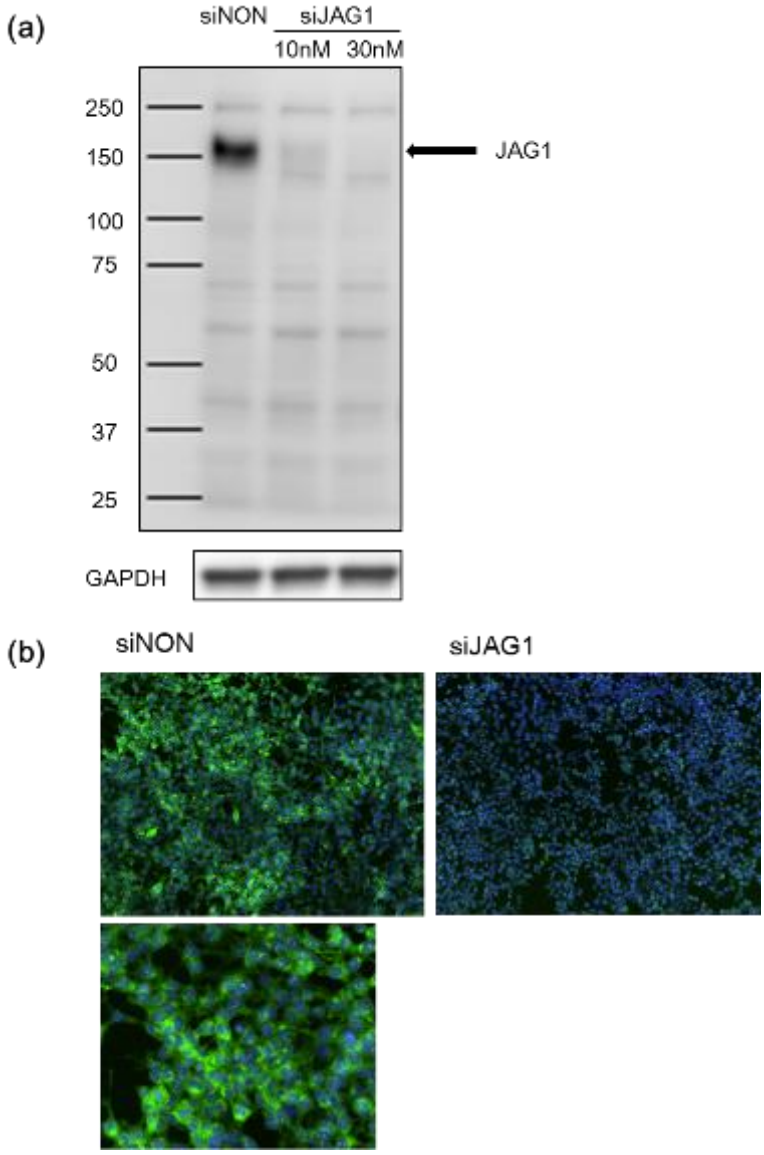

Figure 2- 1. Verification of anti-JAG1 antibody for immunohistochemical staining to analyze the prognostic value of JAG1 expression in human CRC.

(a) Effect of small interfering RNA (siRNA) specific for JAG1 (siJAG1) on JAG1 protein expression in HCT-116 cells at 2 days after siJAG1 treatment analyzed by western blotting. JAG1 protein was detected as a protein of approximately 150 kDa that was knocked down by siJAG1. (b) Representative fluorescence microscopy images of HCT-116 cells 2 days after treatment with siNON or siJAG1. Blue staining indicates the nucleus and green staining shows JAG1 protein expression. Staining for JAG1 was observed in the plasma membrane and this signal was decreased by siJAG1 treatment.

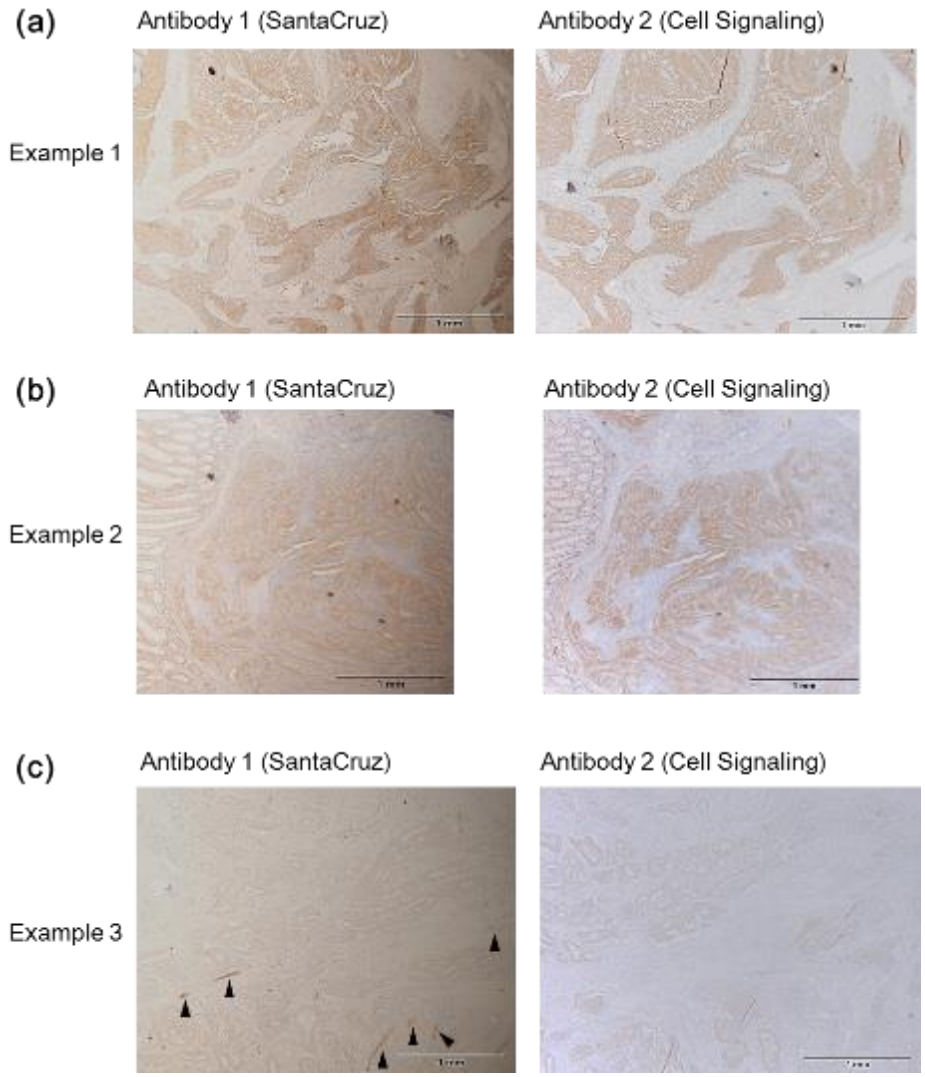

Figure 2- 2. Comparison between anti-JAG1 antibodies for immunohistochemical staining in human CRC (original magnification × 50, scale bars represent 1 mm).

(a, b) Examples of cancer cell staining with two types of anti-JAG1 antibody. Both antibodies showed a similar intensity and localization of staining. (c) Example of no or weak staining in cancer by two anti-JAG1 antibodies. Staining in the endothelium (arrowhead) was detected in the sample treated with antibody 1 (left panel) but not with antibody 2 (right panel). Antibody 1 detects the intracellular region of JAG1 protein whereas antibody 2 detects the extracellular region of JAG1 protein. The lack of staining for endothelium with antibody 2 suggests that the extracellular region of JAG1 was released by shedding, as described in reference (Lu et al., 2013).

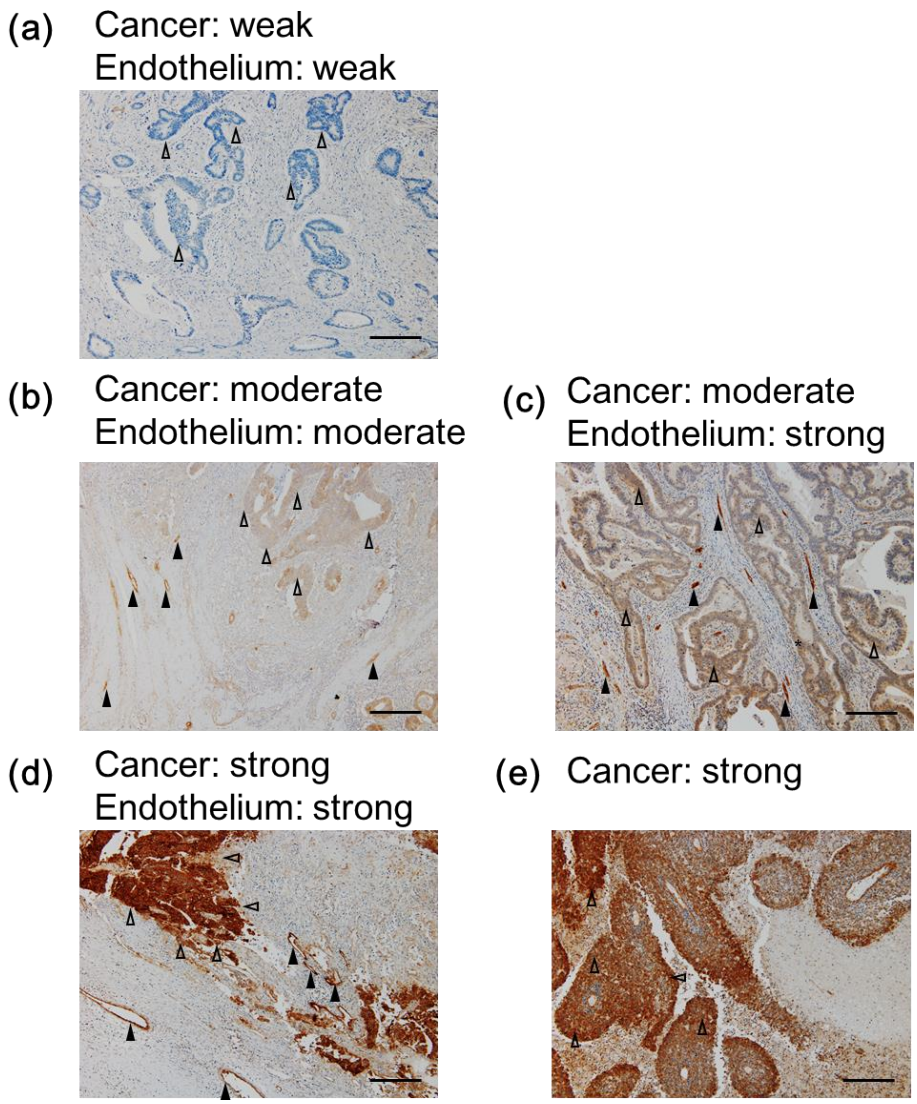

Figure 2- 3. Representative immunohistochemical staining of JAG1 expression in human colorectal cancer tissues (original magnification ×100, scale bars represent 0.25 mm).

(a) Example of cancer and endothelium tissue with weak intensity of staining (jcIHC-W, jeIHC-W). (b) Example of cancer and endothelium with moderate intensity of staining (jcIHC-M, jeIHC-M). (c) Example of cancer and endothelium with moderate and strong intensity of staining, respectively (jcIHC-M, jeIHC-S). (d) Example of cancer and endothelium with strong intensity of staining (jcIHC-S, jeIHC-S). (e) Example of poorly differentiated carcinoma with a strong intensity of staining. Representative each 5 regions in cancer or endothelium were indicated by open or filled arrow-heads, respectively.

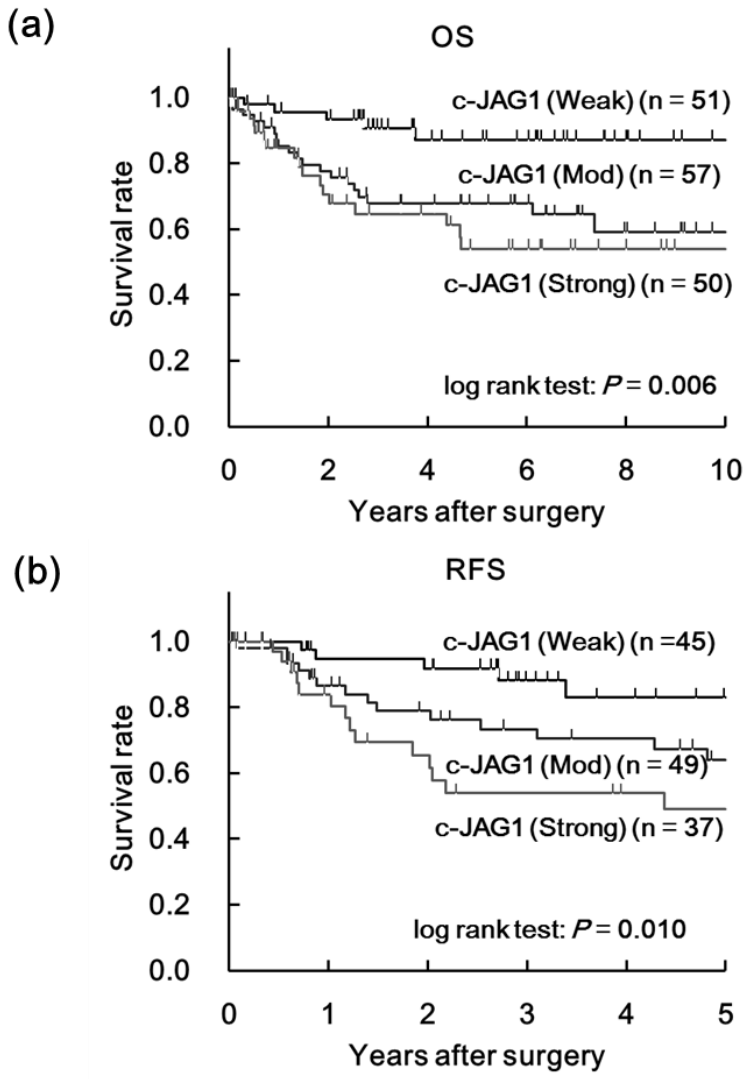

Figure 2- 4. Prognostic significance of JAG1 expression in cancer cells by analysis of Kaplan–Meier estimates.

(a) Kaplan–Meier estimates of 10-year overall survival (OS) in all CRC patients and (b) 5-year recurrence-free survival (RFS) in patients except for Stage IV CRC according to staining intensity. *Mod* indicates moderate.

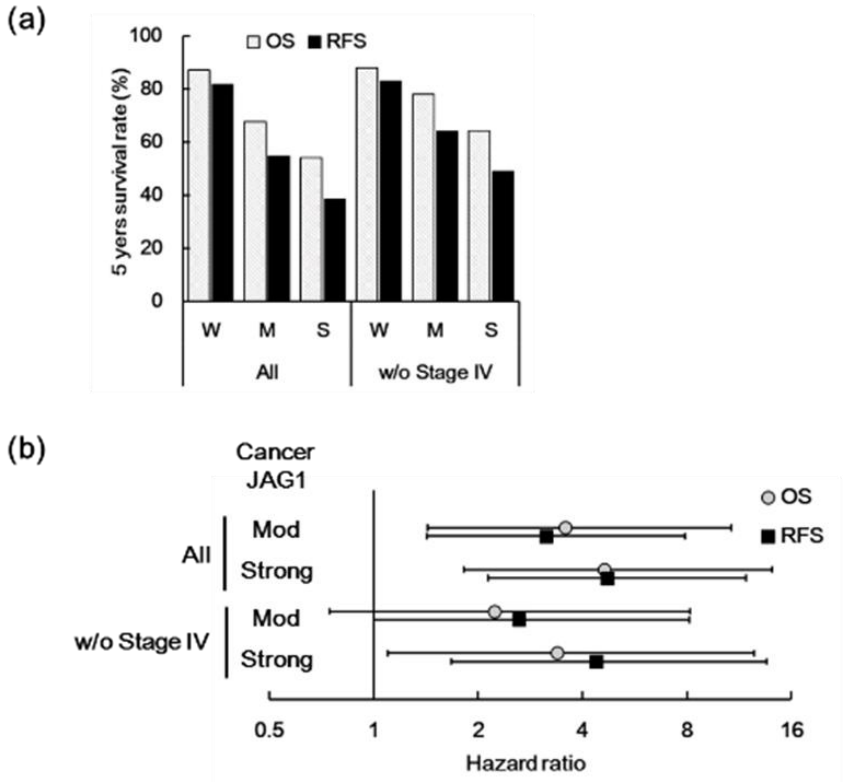

Figure 2- 5. Prognostic significance of JAG1 expression in cancer cells for all CRC patients and patients with stage 0–III disease (i.e., excluding stage IV).

(a) Five-year survival rate calculated by analysis of Kaplan–Meier estimates as shown in Fig. 2 (W, Weak; M, Moderate; S, Strong). (b) Hazard ratio (HR) and 95% confidence interval (CI) for overall survival (OS) and relapse-free survival (RFS) analyzed by Cox proportional hazard model. Higher expression of JAG1 was associated with a larger hazard ratio. A significant HR for OS and RFS in all patients was detected for Mod vs. Weak (P = 0.005 for OS, *P* = 0.004 for RFS) and Strong vs. Weak (*P* = 0.001 for OS, *P* < 0.001 for RFS) staining. A significant HR for OS and RFS in stages 0–III was detected for Mod vs. Weak (*P* = 0.050 for RFS) and Strong vs. Weak (*P* = 0.033 for OS, *P* = 0.002 for RFS) staining.

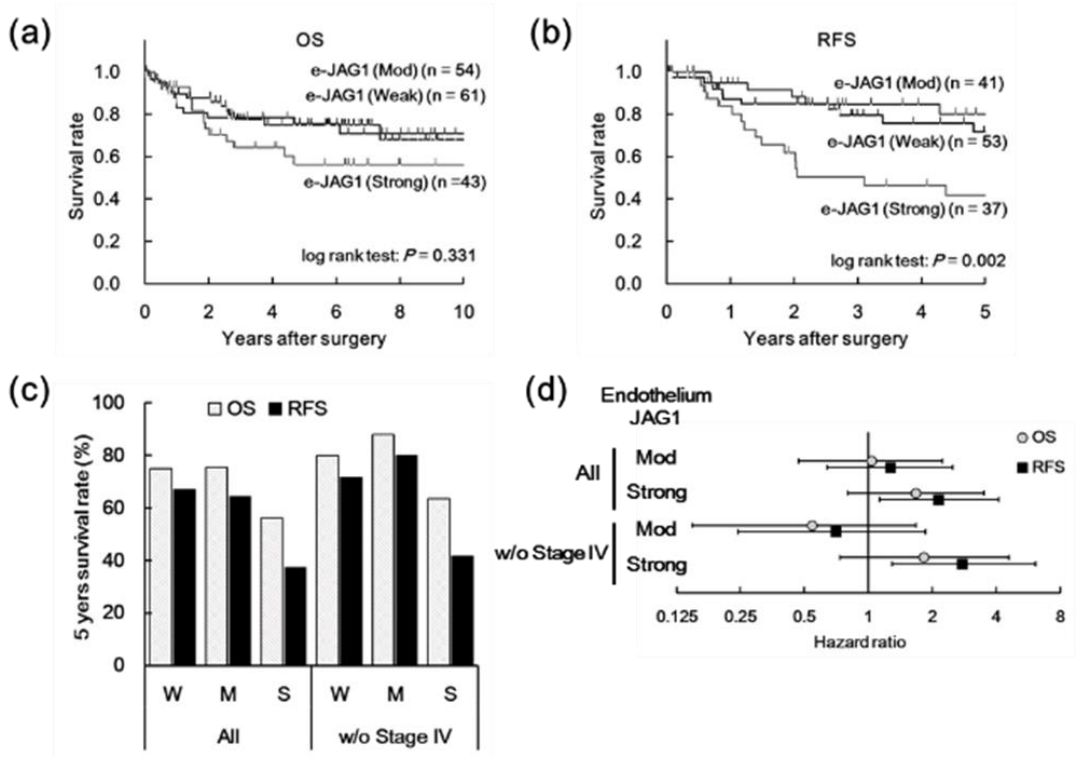

Figure 2- 6. Prognostic significance of JAG1 expression in endothelium by analysis of Kaplan–Meier estimates and Cox proportional hazards model.

Kaplan–Meier estimates of (a) 10-year overall survival (OS) in all CRC patients, and (b) 5-year recurrence-free survival (RFS) in CRC patients excluding stage IV, according to staining intensity. Mod indicates moderate staining. JAG1 expression was significantly associated with RFS (P = 0.002). (c) Five-year survival rate calculated by analysis of Kaplan–Meier estimates (W, Weak; M, Moderate; S, Strong). A lower survival rate was observed for RFS than for OS. (d) Hazard ratio and 95% confidence interval for Moderate or Strong vs. Weak staining intensity of JAG1 expression analyzed by Cox proportional hazards model. A significant HR for RFS was detected for Strong vs. Weak (P = 0.020 for all patients, P = 0.009 for stages 0–III).

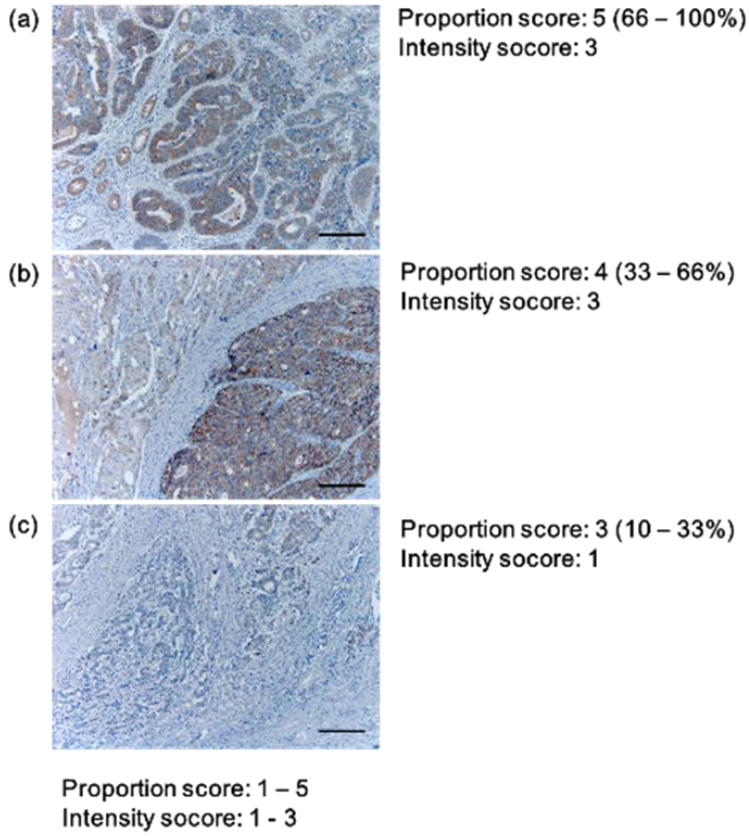

Figure 2- 7. Representative immunohistochemical staining of E-cadherin expression in human CRC tissues (original magnification × 100, scale bars represent 0.25 mm). (a) Example showing proportion score 5 (eIHC-Pr5) and intensity score 3 (eIHC-In3) staining in cancer cells. (b) Example showing proportion score 4 (eIHC-Pr4) and intensity score 3 (eIHC-In3) staining in cancer cells. (c) Example of proportion score 3 (eIHC-Pr3) and intensity score 1 (eIHC-In1) staining in cancer cells. Intensity score 1 (eIHC-In1), 2 (eIHC-In2), and 3 (eIHC-In3) for staining was detected in 39 (25%), 63 (40%), and 56 (35%) samples, respectively. Proportion scale 1–5 (eIHC-Pr1–eIHC-Pr5) of positive cells was detected in seven (4%), 16 (10%), 21 (14%), 35 (22%), and 79 (50%) patients respectively (Table S1).

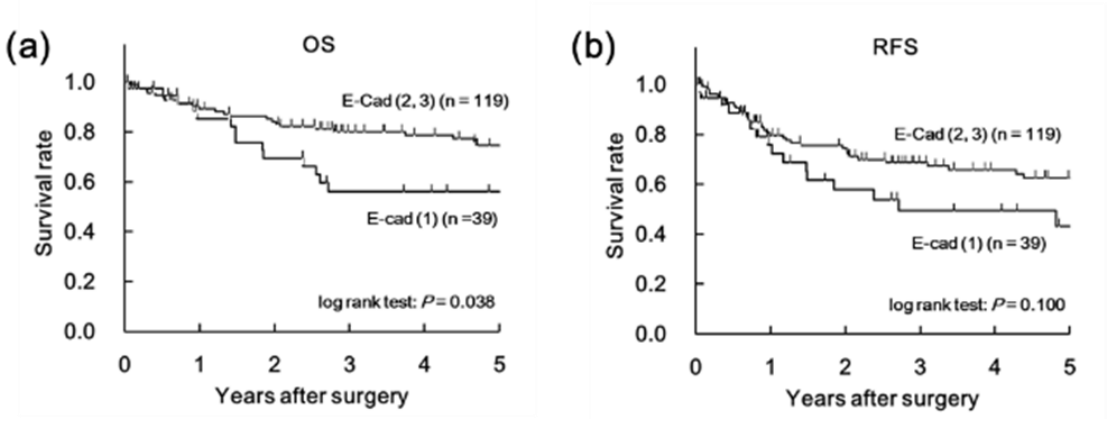

Figure 2- 8. Prognostic significance of E-cadherin expression by analysis of Kaplan–Meier estimates.

Kaplan–Meier estimates of (a) 5-year overall survival (OS) in all CRC patients and (b) 5-year recurrence-free survival (RFS) according to staining intensity of E-cadherin. Prognostic significance for OS of E-cadherin expression in CRC was also analyzed by log-rank test in another stratification (data not shown). The *p* value of eIHC-In-1/2 vs. eIHC-In3, eIHC-Pr1/2/3 vs. eIHC-Pr4/5, and eIHC-Pr1/2/3/4 vs. eIHC-Pr5 was 0.281, 0.194, and 0.157, respectively. E-cadherin expression was not significantly correlated with RFS.

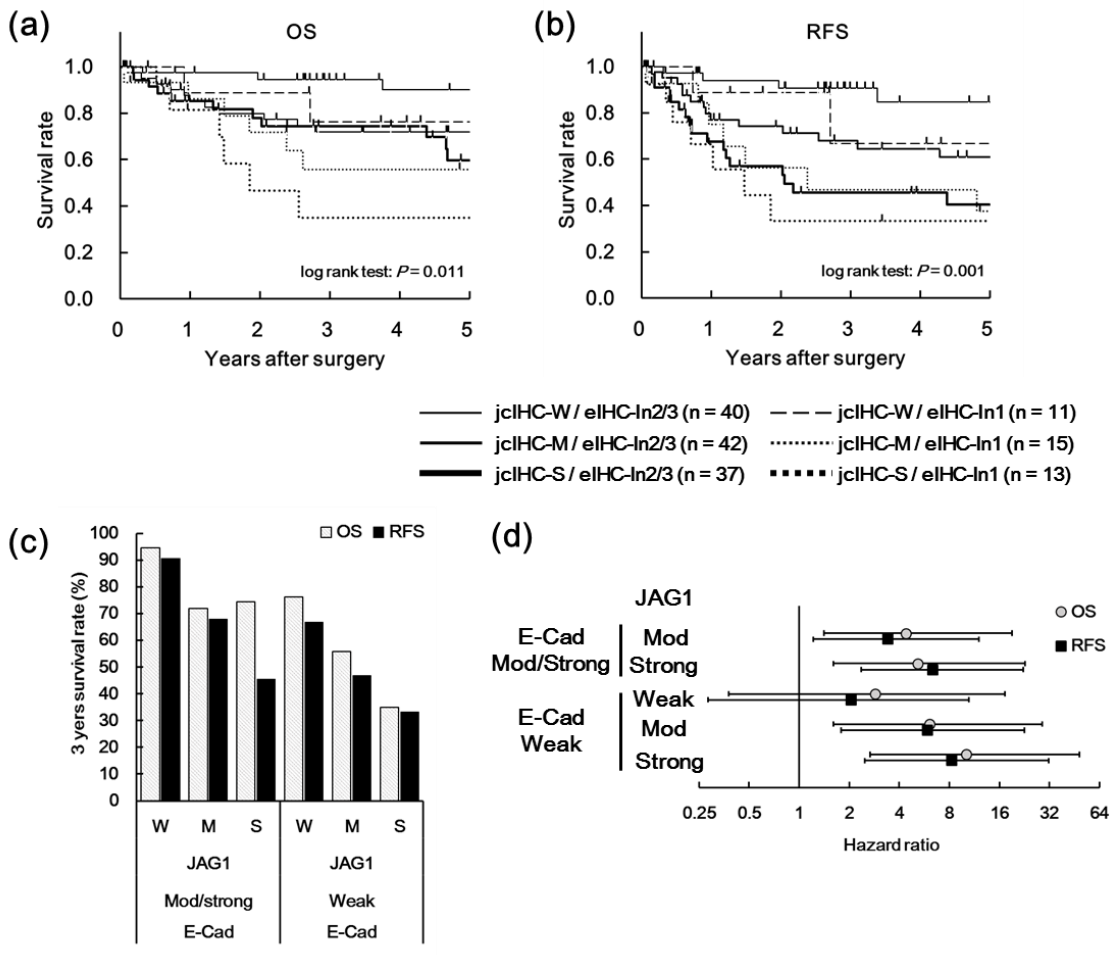

Figure 2- 9. Prognostic significance of JAG1 expression in cancer cells stratified by E-cadherin expression (based on intensity of staining) shown by analysis of Kaplan–Meier estimates and Cox proportional hazards model.

(a, b) Kaplan–Meier estimate of 5-year OS (a) and 5-year RFS (b) in CRC patients according to staining intensity of JAG1 expression in cancer cells stratified by E-cadherin expression. jcIHC-W, -M, -S indicate weak, moderate, and strong intensity of staining of JAG1 expression in cancer cells, respectively. eIHC-In2/3 and eIHC-In1 indicate staining intensity of 2/3 and 1 for E-cadherin expression, respectively. (c) 3-year survival rate calculated by analysis of the Kaplan–Meier estimates shown in (a) and (b). (d) Hazard ratio (HR) and 95% confidence interval (CI) of JAG1 and E-cadherin expression analyzed by Cox proportional hazards model versus jcIHC-W/eIHC-In2/3 group.

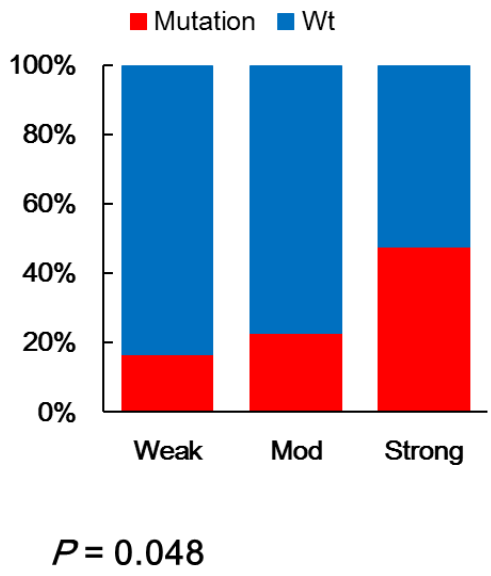

Figure 2- 10. Correlation between KRAS status and JAG1 expression in CRC patients with staining intensity 2/3 for E-cadherin expression.

Proportion of KRAS mutation as shown in Table 4 is presented as a red bar. Relationship between the KRAS status and JAG1 expression was statistically analyzed using the χ^2 test.

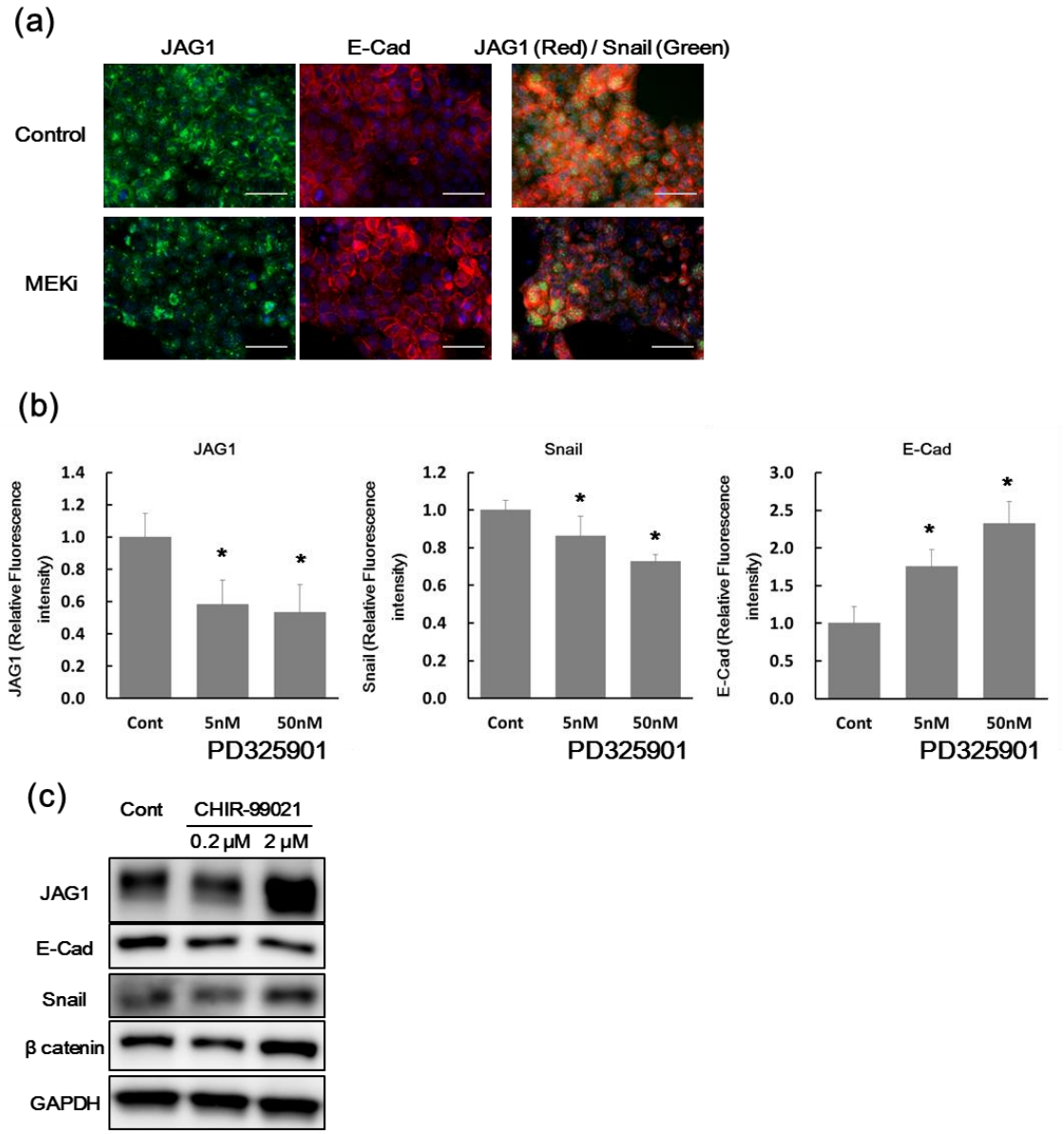

Figure 2- 11. Mechanisms of regulation of JAG1 expression based on *in vitro* study.
(a) The effect of inhibition of RAS-MEK-MAP kinase pathway on JAG1 expression and induction of EMT-like phenotype was examined using the MEK inhibitor PD325901 in the colon cancer cell line HCT-116. In the left panel, blue staining indicates the nucleus and green staining indicates JAG1 protein. In the middle panel, blue staining indicates the nucleus and red staining indicates E-cadherin protein. In the right panel, blue, green, and red staining indicate the nucleus, SNAIL, and JAG1 protein, respectively. Scale bars represent 50 μm. (b) Fluorescence intensity of JAG1, Snail, and E-cadherin was analyzed. Data are presented as mean ± S.D. of 20 fields of view. *, $P < 0.05$, Student's t-test. (c) Effects of Glycogen synthase kinase (GSK3) β inhibitor on JAG1 protein expression and EMT-like phenotype. JAG1, E-cadherin, and SNAIL protein expression was analyzed by

western blotting.

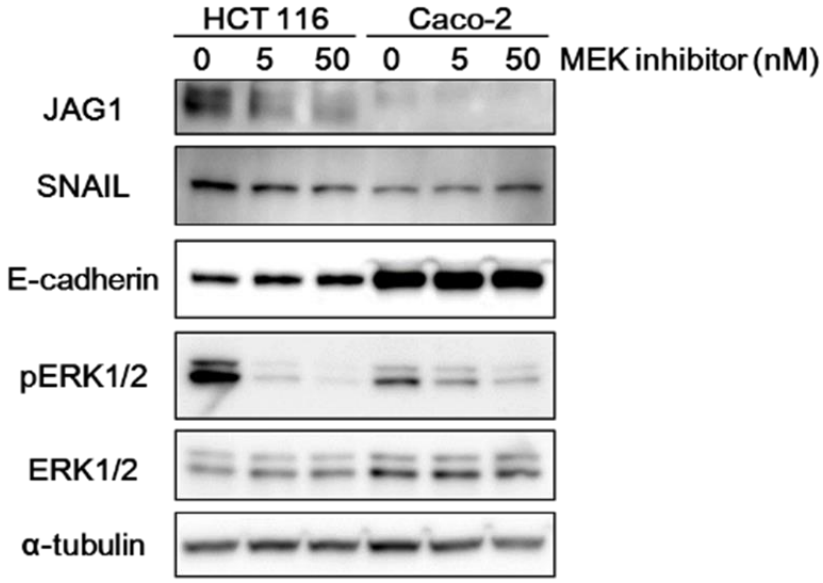

Figure 2- 12. Effect of inhibition of RAS-MEK-MAP kinase pathway on JAG1, SNAIL and E-cadherin protein level in the cancer cell lines HCT-116 and Caco-2. JAG1, SNAIL, E-cadherin, and, total or phosphorylated ERK1/2 level were analyzed by western blotting in HCT-116 (KRAS G13D) and Caco-2 (KRAS wild) cells. PD325901 was used to inhibit MEK activity. Activation of MAP kinase pathway was detected by the extent of phosphorylation of ERK1/2.

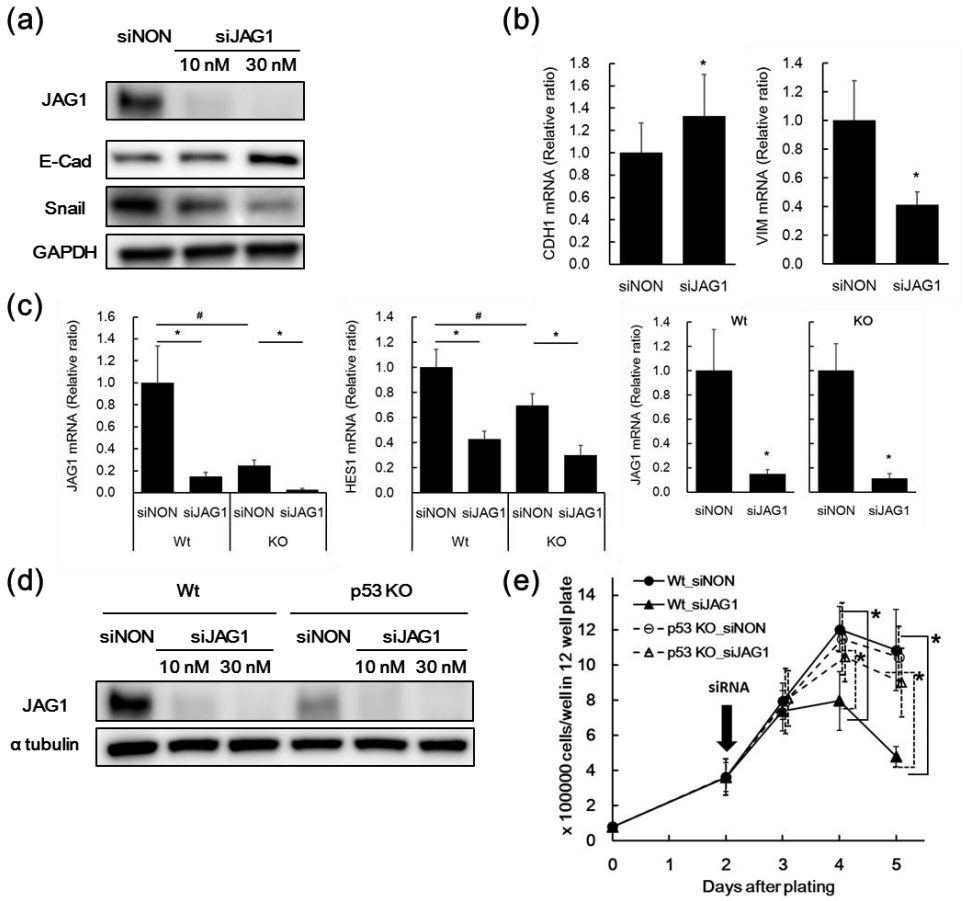

Figure 2- 13. Effect of *JAG1* gene silencing on proliferation and epithelial mesenchymal transition (EMT)-like phenotype based on *in vitro* study.

(a, b) Effect of small interfering RNA for JAG1 (siJAG1) on JAG1 expression and EMT-like phenotype. E-cadherin and SNAIL protein expression (a) or E-cadherin (*CDH1*) and vimentin (*VIM*) mRNA expression (b) were analyzed by western blotting and qRT-PCR respectively. Non-targeting siRNA (siNON) was used as a negative control. Expression levels of mRNA are indicated relative to expression with siNON treatment. Data are mean ± S.D. of nine wells. (c) Effect of siJAG1 on *JAG1* and *HES1* mRNA expression in $p53^{-/-}$ and wild type (Wt) HCT-116 cells. mRNA expression was presented as a ratio relative to expression in Wt cells treated with siNON in the left two panels. *JAG1* mRNA expression in Wt or $p53^{-/-}$ cells treated with siJAG1 was also presented as a ratio relative to expression in Wt or *p53-/-* cells treated with siNON in the right panels. Data are mean ± S.D. of nine wells. (d) Effect of siJAG1 on JAG1 protein expression in $p53^{-/-}$ and Wt cells analyzed by western blotting. (e) Effect of siJAG1 on cell growth in $p53^{-/-}$ and Wt cells. siJAG1 treatment was initiated 2 days after plating. Data are presented as mean ± S.D. of six wells for each time point (result from three independent experiments). Statistical analysis was performed by Student's *t*-test. * or $^{\#}$, $P < 0.05$.

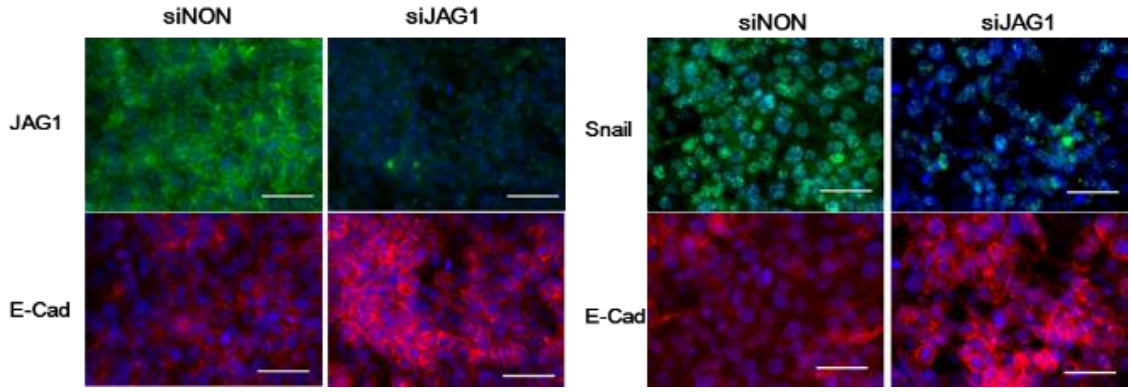

Figure 2- 14. Effect of *JAG1* gene silencing on epithelial–mesenchymal transition in HCT116 cancer cell line.

Representative fluorescence microscopy images at 2 days of siNON and siJAG1 treatment are shown. In the left panels, blue, green, and red staining indicates the nucleus, JAG1, and E-cadherin, respectively. In the right panels, blue, green, and red staining indicates the nucleus, SNAIL, and E-cadherin respectively. Scale bars represent 50 μm.

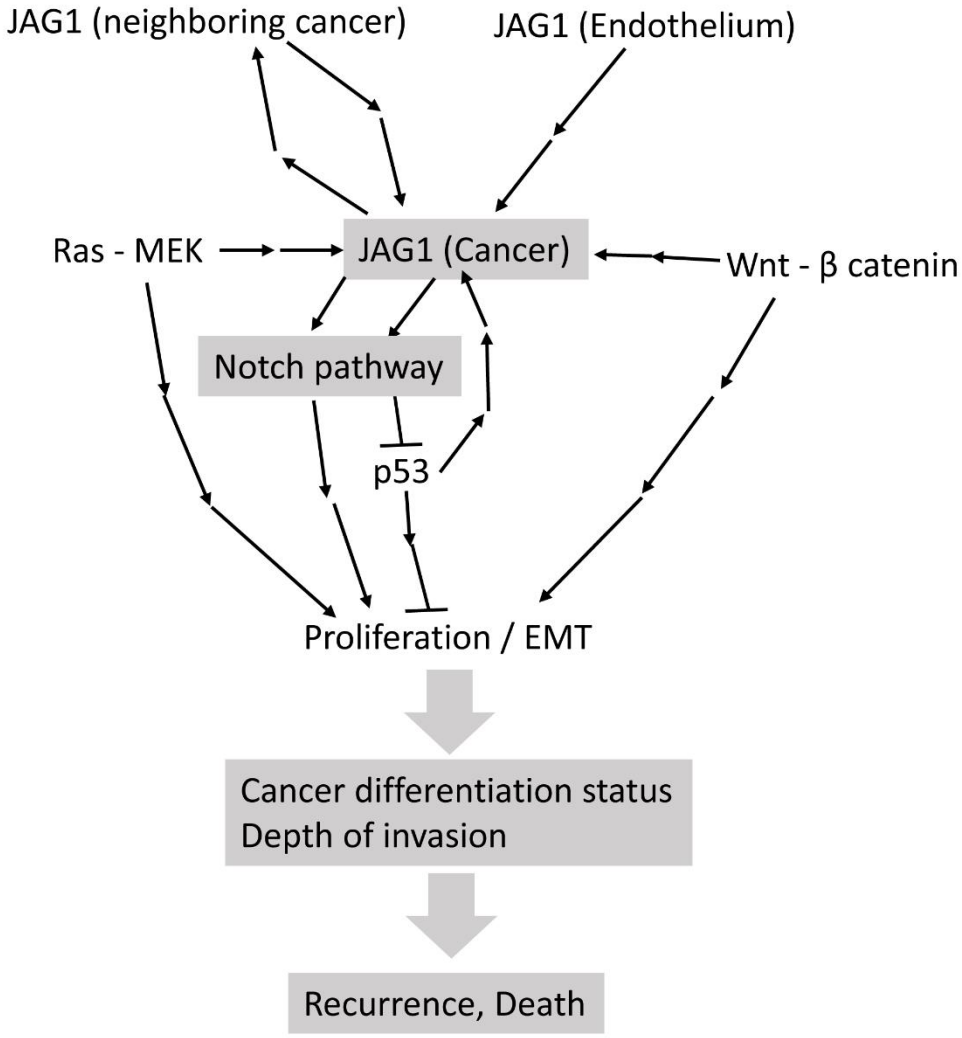

Figure 2- 15 Hypothesized mechanisms of cancer recurrence or death induced by JAG1-Notch pathway activation following increased JAG1 expression regulated by various factors.

General Discussion

In the two studies described above, I explored mechanisms for the transition of differentiation status in LPCs and CRC. Acquisition of a stem cell phenotype and/or mesenchymal characteristics seem to play an important role in epithelial cancer cell survival in severe environments such as starvation, hypoxia, attacks from immune cells or anticancer treatment, and escape from the severe environment. The acquisition of stem cell phenotype and/or mesenchymal characteristics could then contribute to drug resistance and/or radioresistance, tumor recurrence, and metastasis. Therefore, it seems important to understand the mechanisms underlying these transitions in epithelial cancer cells for overcoming the malignant phenotype. Moreover, exploring methods for converting these stem or mesenchymal status into a well-differentiated status potentially leads to new strategies for anticancer treatment. First, I investigated the role of autophagy and the related signaling pathways as the mechanism for transition towards differentiated hepatocytes in normal LPCs collected from a mouse liver injury model (part 1). Second, I evaluated the prognostic function of the JAG1-Notch pathway and EMT in CRC. Moreover, I investigated the related mechanism *in vitro* using a colon cancer cell line.

In the first part, I found that autophagy inhibition promotes hepatic differentiation in LPCs. Although normal stem/progenitor cells were used in my work, this new insight from my work could be beneficial for research on CSCs and for anticancer treatment in the liver.

LPCs and/or cells similar to LPCs potentially derived from mature hepatocytes were isolated from the liver during oval-cell inducing injury in a rodent model with chronic liver injury. Tarlow et al. reported that 8.7–39.3% of cells expressing liver

stem/progenitor marker proteins were derived from mature hepatocyte in this DDC injury and that about 35% of these cells could differentiate into mature hepatocytes after about 4 weeks of recovery from a diet with DDC (Tarlow et al., 2014). Progenitors originated from hepatocytes were characterized by a relatively low expression of some stem/progenitor marker proteins such as EPCAM, CD133, and CK19 compared to cells of biliary origin (Tarlow et al., 2014). In my work, I isolated cells expressing EPCAM and divided these cells into two fractions by CD133 expression levels. Only cells with low expression levels of CD133 could undergo hepatic differentiation under the differentiation conditions in my work. While progenitors originating from cells with low CD133 expression levels were examined for the effect of autophagy inhibition on hepatic differentiation, the cells used in my work might have originated from mature hepatocytes. Oval-cell-inducing liver injuries that induce a ductular reaction are associated with an increased risk of primary liver cancers (Deugnier et al., 1993; Prior, 1988; Tsukuma et al., 1993). Moreover, injured hepatocytes could dedifferentiate toward cells similar to LPCs under the ductular plasticity during oval-cell-inducing liver injury in chronic liver diseases, which could be relevant to liver cancer, particularly cholangiocarcinomas (Fan et al., 2012; Sekiya and Suzuki, 2012). Therefore, the new insight obtained from my work with regard to hepatic differentiation from LPCs might provide clues to clarify the mechanisms for ductular plasticity of hepatocytes during oval-cell-inducing injury. Further methods to differentiate hepatocytes from hepatocyte-derived progenitors may lead to new strategies for anticancer treatment in liver cancer.

Recently, conversion of mature hepatocytes to bipotent stem/progenitor cells *in vitro* using a cocktail of small molecules was reported (Katsuda et al., 2017). These

chemically induced liver stem/progenitor cells (CLiPs) could differentiate into both mature hepatocytes and biliary epithelial cells. This report provides strong *in vitro* evidence supporting the mature hepatocyte reprogramming theory. The small molecules used in this paper were Y-27632 (Rho-associated, coiled-coil containing protein kinase [ROCK] inhibitor), A-83-01 (inhibitor of TGF-β type I receptor kinase (Anaplastic lymphoma kinase [ALK] 5), activin type IB receptor (ALK4), nodal type I receptor (ALK7), and CHIR99021 (GSK3 inhibitor), but the detailed molecular mechanisms for the mature hepatocyte plasticity have not been described yet. In the future, studying the role of autophagy, p62, and related signaling pathways for this mature hepatocyte reprogramming regimen as shown in the previous report could lead to further clarification of the detailed mechanism underlying ductular plasticity of hepatocytes during oval-cell-inducing injury.

Next, I would like to address the effect of amino acid-sensitive mTOR signaling pathway activation on hepatic differentiation in LPCs. It has been accepted that long-term treatment with BCAAs is an effective preventive treatment for improving the clinical outcome of cirrhotic patients by reducing the occurrence of liver failure (Kawaguchi et al., 2011; Marchesini et al., 2003; Muto et al., 2005). Moreover, recent reports describe that BCAA suppresses the incidence of hepatocellular carcinoma in cirrhotic patients (Muto et al., 2006; Nishikawa and Osaki, 2014; Tada et al., 2014). Supporting these findings, several mouse experiments have demonstrated that BCAAs reduce the incidence of chemically induced hepatocellular carcinoma (Iwasa et al., 2010; Ohno et al., 2008; Takegoshi et al., 2017; Yoshiji et al., 2009). Moreover, recent report showed that suppression of mTOR complex (mTORC) 1 signaling in Raptor knockout mice rendered them more susceptible to chemically induced hepatic fibrosis

and hepatocellular carcinoma (Umemura et al., 2014). In my work, I indicated that amino acids, including BCAAs, play an important role for hepatic differentiation in LPCs. The new insight from my study that BCAA could promote a return from hepatocyte-derived progenitor to hepatocytes, might provide a possible mechanism for decreasing the incidence of hepatocellular carcinoma in chemically-induced or non-alcoholic steatohepatitis induced liver injury in a mouse model. Further studies are needed to clarify the association between the beneficial effect of BCAAs on the incidence of hepatocellular carcinoma and the promoting effect of BCAAs on hepatic differentiation in LPCs.

In the second part, I mainly investigated the association of JAG1 expression in cancerous tissues with prognostic impact, clinical characteristics, JAG1 expression levels in the endothelium, and EMT status (the extent of decreased E-cadherin expression) in CRC patients. I found that a high JAG1 expression in cancerous tissues was partly associated with EMT status. My study also suggested that JAG1 expression levels in cancer cells could be regulated exogenously by JAG1 itself expressed in the endothelium, and that JAG1 expression levels in cancer cells were also regulated intracellularly by Wnt-β catenin signaling, KRAS status, and p53 status in cancer cells. Moreover, my study also suggests that JAG1 expression levels are associated with EMT status *in vitro*. Therefore, although studies in the second part mainly concerned JAG1 expression, I believe that increased JAG1 expression in cancer cells is nearly equivalent to acquisition of mesenchymal characteristics to a varying extent.

In my work, I obtained results about the correlation between both JAG1 expression levels in cancer cells and in the endothelium. This is important for understanding the underlying mechanism in malignancy of cancer cells through interactions between cancer

cells and the microenvironment. The Notch signaling pathway is important for normal intestinal epithelial stem/progenitor self-renewal and differentiation under healthy conditions (Sancho et al., 2015), and DLL1 and DLL4 function as physiological ligands for Notch receptors (Pellegrinet et al., 2011). Unlike in healthy conditions, JAG1 might be released as an angiocrine factor from endothelial cells and functions as a Notch ligand to induce the cancer stem cell phenotype in CRC (Lu et al., 2013). My work indicates that JAG1 expression in cancer cells is strongly correlated with its expression in the endothelium. This suggests that high JAG1 expression in the endothelium promotes acquisition of a cancer stem cell-like phenotype in cancer cells and leads to poor prognosis in humans. Further investigations will be needed to clarify the mechanisms of acquiring a stem cell phenotype and mesenchymal characteristics in cancer cells through the interaction between cancer cells and the surrounding tumor vasculature via JAG1 and other factors.

Mutations in the adenomatous polyposis coli (Apc) tumor suppressor gene are common and induce Wnt activation in CRC (85% in sporadic cancer), and tumors often acquire heterogeneous Wnt activity through an additional regulation. Mutations in the Apc gene, β-catenin, or in Wnt pathway regulatory proteins result in continuous activation of this signaling pathway (Haegebarth and Clevers, 2009). Thereby, I examined the effect of the GSK3β inhibitor CHIR-99021, on JAG1 and EMT marker expression *in vitro*. My investigation suggested that Wnt-β-catenin pathway activation increases JAG1 expression and induces EMT in CRC.

Inactivation of the p53 pathway by mutation of the tumor protein p53 (*TP53*) is the second key genetic step in colorectal cancer development (35-55% in sporadic cancer). Wild-type p53 mediates cell-cycle arrest and a cell-death checkpoint, which can be

activated by multiple cellular stresses (Markowitz and Bertagnolli, 2009). Moreover, p53 loss-of-function mutation seems to exacerbate EMT dependent on Notch pathway activation through increasing EMT-TF. This increased expression of EMT-TF occurs via a decrease in micro-RNA (miRNA)-34 levels that are positively regulated by p53 (Chanrion et al., 2014; Kim et al., 2011). My work suggested that JAG1-Notch signaling is important for the transition toward a mesenchymal phenotype as well as for proliferation in a colon cancer cell line through suppression of the p53-related pathway. On the other hand, lower expression of JAG1 mRNA and protein in a $p53^{-/-}$ cell line than that in the Wt cell line was unexpected. This might indicate that deficiency of p53 reduces JAG1 expression due to unknown negative feedback mechanisms against facilitating activate notch signaling via the miRNA-34 related mechanism in cancer cells. To clarify the detailed mechanisms for this reciprocal regulation between JAG1 expression and p53 status, further investigations will be necessary in the future.

Oncogenic mutations of RAS and BRAF, which activate the MAPK signaling pathway, occur in 37% and 13% of colorectal cancers, respectively. My work suggested that epithelial populations with relatively high E-cadherin expression levels among CRC patients showed an association between JAG1 expression and the proportion of KRAS mutations. Recently, a large-scale consortium of leading scientists within the colorectal field reported a consensus molecular subtype (CMS) as four subtypes for CRC (Guinney et al., 2015). Among the four CMSs, CMS3 was reported as the subtype which had metabolic characteristics and was associated with KRAS mutations. Moreover, this subtype had more epithelial characteristics (Guinney et al., 2015). An association between the proportion of KRAS mutation and high JAG1 expression in the more epithelial group demonstrated in my work could predict that patients with KRAS

mutations among the CMS3 could show high JAG1 expression and a relatively more mesenchymal phenotype compared to patients without KRAS mutations even in the patients group with a more epithelial phenotype. In my work, a colon cancer cell line with KRAS mutations and high phosphorylated Erk1/2 levels was more sensitive to an MEK inhibitor with regard to JAG1 and Snail expression levels than a colon cancer cell line without KRAS mutation. Altogether, because it seems that a clinical subtype with more epithelial characteristics such as CMS3 has little or no exogenous influence from invading inflammatory or stromal cells as constituents of the microenvironment, the main determinants for malignant differentiation status of cancer cells in such a clinical subtype might be intracellular genetic/epigenetic alteration, which may be comparable to the monoculture situation *in vitro*. In this case, KRAS mutations could be one of the most potent genetic/epigenetic alterations for making the cancer cells more malignant.

In the general discussion, I address the role of the JAG1-Notch signaling pathway in liver cancer and CRC. Recent reports have provided evidence that Notch signaling is activated and oncogenic in hepatocellular carcinoma (Dill et al., 2013; Tschaharganeh et al., 2013; Villanueva et al., 2012), and might be important for the development of tumors following hepatitis B virus infection (Jeliazkova et al., 2013). Moreover, accumulating evidence supports a pro-tumorigenic role for Notch signaling in cholangiocarcinoma (Akhoondi et al., 2007; Jeliazkova et al., 2013; Zender et al., 2013). There seems to be a consensus that higher Notch signaling levels in liver progenitors favor bile duct differentiation over hepatocytic differentiation. Activation of Notch in these progenitors might promote cholangiocarcinoma. Thus, crosstalk between autophagy and Notch related signaling pathways with regards to stemness and hepatic differentiation in LPCs is of my interest. On the other hand, in CRC, although mutations

in *NOTCH* genes are rare, Notch signaling is constitutively activated in CRC, partly because of mutations in regulators of Notch signaling, including FBXW7 (Akhoondi et al., 2007; Babaei-Jadidi et al., 2011; Miyaki et al., 2009; Sancho et al., 2010; Zhu et al., 2013). In addition, Notch activation has been linked to the regulation of varying signaling pathways such as Hippo/YAP signaling and miRNA related mechanisms as described in previous reports and in my work (Bu et al., 2013; Camargo et al., 2007; Fre et al., 2009; Kim et al., 2012; Kwon et al., 2011; Lu et al., 2013; Peignon et al., 2011; Rodilla et al., 2009; Tschaharganeh et al., 2013). Thus, Notch signaling may play a crucial role in the early stages of CRC development by controlling the fate of stem cells and cancer stem cells, and also in the later stages of tumor invasion and metastasis (Sonoshita et al., 2011). Altogether, the JAG1-Notch pathway signaling seems to be an important target for antitumor treatment in liver cancer (particularly cholangiocarcinoma) as well as CRC.

In conclusion, the findings obtained from my study in Part 1 suggest that LPCs or mature hepatocyte-derived LPCs-like cells could differentiate toward hepatocytes via autophagy inhibition and/or p62 dependent amino acid sensitive mTOR signaling pathway activation. This new finding may provide a clue to clarify the mechanism for biliary plasticity of hepatocytes (hepatocyte reprogramming theory), which is relevant to liver cancer, particularly cholangiocarcinoma. As shown in Part 2, JAG1 is a key Notch ligand in CRC and is connected with the differentiation status and the depth of invasion among the clinical characteristics in CRC patients. JAG1 expression levels are regulated by Wnt-β catenin, p53, and KRAS-MEK-Map kinase signaling pathway and are associated with EMT status. Therefore, my study suggests that JAG1 is an attractive target for novel anticancer treatments to suppress EMT, invasive potential, and

metastasis in CRC. These mechanisms for regulating the differentiation status in normal and cancer cells should provide significant insights for the development of novel and effective therapeutic approaches in cancers of the gastrointestinal tract and the liver.

Acknowledgement

I am deeply grateful to Associate Professor Hidekazu Kuwayama, Faculty of Life and Environmental Sciences, University of Tsukuba, for guiding my work and valuable discussions through this doctoral program.

I gratefully acknowledges Drs. Yoshihiko Maehara, Tomoharu Yoshizumi, Yoshihiro Yoshida, Yuki Bekki, Yoshihiro Matsumoto, Shohei Yoshiya, Takeo Toshima, Toru Ikegami, Shinji Itoh, Norifumi Harimoto, Shinji Okano, Yuji Soejima, Graduate School of Medical Sciences, Kyushu University, Dr. Ken Shirabe, Gunma University, Graduate School of Medicine, for their helpful discussions and support throughout the study in part1.

I would like to thank Ms. Takako Shishino, Noriko Makikusa, Yukiko Nagatomo, Natsumi Maeda, Saori Tsurumaru, Ruriko Aoki, Michi Amago, and Shigemi Takami, Graduate School of Medical Sciences, Kyushu University, for their expert technical assistance in part1.

I gratefully acknowledges Drs. Yoshihiko Maehara, Eiji Oki, Yu Nakaji, Satoshi Tsutsumi, Naomi Ono, Ryota Nakanishi, Masahiko Sugiyama, Yuichiro Nakashima, Hideto Sonoda, Kippei Ohgaki, Nami Yamashita, Hiroshi Saeki, Shinji Okano, Masaru Morita, Hiroyuki Kitao, and Yoshinao Oda, Graduate School of Medical Sciences, Kyushu University, for their helpful discussions and support throughout the study in part2.

I would like to thank Dr. Makoto Iimori, Graduate School of Medical Sciences, Kyushu University, for scientific advice, especially regarding experimental technique. I would like to thank Ms. Yuko Kubota, Takako Shishino, Miki Nakashima, Saori Tsurumaru, Ruriko Aoki, and Shigemi Takami, Graduate School of Medical Sciences, Kyushu University, for their expert technical assistance in part2.

I also express my gratitude to Drs. Yoshiki Kawabe, Thoshihiko Makino, current supervisor, Drs. Kazumi Morikawa, Yoshiyuki Suzuki, previous supervisor, at Chugai Pharmaceutical Co., Ltd. for endorsement of participation in this doctoral program.

I would like to thank my coworkers at Research Division of Chugai Pharmaceutical Co., Ltd. for their encouragement during the preparation of this dissertation.

Finally, I would like to appreciate my family for supporting my life during the preparation of this dissertation in University of Tsukuba.

References

Ahmed D, Eide PW, Eilertsen IA, Danielsen SA, Eknaes M, Hektoen M, Lind GE, Lothe RA. 2013. Epigenetic and genetic features of 24 colon cancer cell lines. Oncogenesis 2:e71.

Akhoondi S, Sun D, von der Lehr N, Apostolidou S, Klotz K, Maljukova A, Cepeda D, Fiegl H, Dafou D, Marth C, Mueller-Holzner E, Corcoran M, Dagnell M, Nejad SZ, Nayer BN, Zali MR, Hansson J, Egyhazi S, Petersson F, Sangfelt P, Nordgren H, Grander D, Reed SI, Widschwendter M, Sangfelt O, Spruck C. 2007. FBXW7/hCDC4 is a general tumor suppressor in human cancer. Cancer Res 67:9006-9012.

Allred DC, Harvey JM, Berardo M, Clark GM. 1998. Prognostic and predictive factors in breast cancer by immunohistochemical analysis. Mod Pathol 11:155-168.

Arcaroli JJ, Tai WM, McWilliams R, Bagby S, Blatchford PJ, Varella-Garcia M, Purkey A, Quackenbush KS, Song EK, Pitts TM, Gao D, Lieu C, McManus M, Tan AC, Zheng X, Zhang Q, Ozeck M, Olson P, Jiang ZQ, Kopetz S, Jimeno A, Keysar S, Eckhardt G, Messersmith WA. 2016. A NOTCH1 gene copy number gain is a prognostic indicator of worse survival and a predictive biomarker to a Notch1 targeting antibody in colorectal cancer. Int J Cancer 138:195-205.

Babaei-Jadidi R, Li N, Saadeddin A, Spencer-Dene B, Jandke A, Muhammad B, Ibrahim EE, Muraleedharan R, Abuzinadah M, Davis H, Lewis A, Watson S, Behrens A, Tomlinson I, Nateri AS. 2011. FBXW7 influences murine intestinal homeostasis and cancer, targeting Notch, Jun, and DEK for degradation. J Exp Med 208:295-312.

Becht E, de Reynies A, Giraldo NA, Pilati C, Buttard B, Lacroix L, Selves J, Sautes-Fridman C, Laurent-Puig P, Fridman WH. 2016. Immune and Stromal Classification of Colorectal Cancer Is Associated with Molecular Subtypes and Relevant for Precision Immunotherapy. Clin Cancer Res 22:4057-4066.

Berardi DE, Flumian C, Rodriguez CE, Bessone MI, Cirigliano SM, Joffe ED, Fiszman GL, Urtreger AJ, Todaro LB. 2016. PKCdelta Inhibition Impairs Mammary Cancer Proliferative Capacity But Selects Cancer Stem Cells, Involving Autophagy. J Cell Biochem 117:730-740.

Boulter L, Govaere O, Bird TG, Radulescu S, Ramachandran P, Pellicoro A, Ridgway RA, Seo SS, Spee B, Van Rooijen N, Sansom OJ, Iredale JP, Lowell S, Roskams T, Forbes SJ. 2012. Macrophage-derived Wnt opposes Notch signaling to specify hepatic progenitor cell fate in chronic liver disease. Nat Med 18:572-579.

Bu P, Chen KY, Chen JH, Wang L, Walters J, Shin YJ, Goerger JP, Sun J, Witherspoon M, Rakhilin N, Li J, Yang H, Milsom J, Lee S, Zipfel W, Jin MM, Gumus ZH, Lipkin SM, Shen X. 2013. A microRNA miR-34a-regulated bimodal switch targets Notch in colon cancer stem cells. Cell Stem Cell 12:602-615.

Camargo FD, Gokhale S, Johnnidis JB, Fu D, Bell GW, Jaenisch R, Brummelkamp TR. 2007. YAP1 increases organ size and expands undifferentiated progenitor cells. Curr Biol 17:2054-2060.

Carethers JM, Jung BH. 2015. Genetics and Genetic Biomarkers in Sporadic Colorectal Cancer. Gastroenterology 149:1177-1190.e1173.

Chanrion M, Kuperstein I, Barriere C, El Marjou F, Cohen D, Vignjevic D, Stimmer L, Paul-Gilloteaux P, Bieche I, Tavares Sdos R, Boccia GF, Cacheux W, Meseure D, Fre S, Martignetti L, Legoix-Ne P, Girard E, Fetler L, Barillot E, Louvard D, Zinovyev A, Robine S. 2014. Concomitant Notch activation and p53 deletion trigger epithelial-to-mesenchymal transition and metastasis in mouse gut. Nat Commun 5:5005.

Chen X, Stoeck A, Lee SJ, Shih Ie M, Wang MM, Wang TL. 2010. Jagged1 expression regulated by Notch3 and Wnt/beta-catenin signaling pathways in ovarian cancer. Oncotarget 1:210-218.

Chu D, Li Y, Wang W, Zhao Q, Li J, Lu Y, Li M, Dong G, Zhang H, Xie H, Ji G. 2010. High level of Notch1 protein is associated with poor overall survival in colorectal cancer. Ann Surg Oncol 17:1337-1342.

Clouston AD, Powell EE, Walsh MJ, Richardson MM, Demetris AJ, Jonsson JR. 2005. Fibrosis correlates with a ductular reaction in hepatitis C: roles of impaired replication, progenitor cells and steatosis. Hepatology 41:809-818.

Dai Y, Wilson G, Huang B, Peng M, Teng G, Zhang D, Zhang R, Ebert MP, Chen J, Wong BC, Chan KW, George J, Qiao L. 2014. Silencing of Jagged1 inhibits cell growth and invasion in colorectal cancer. Cell Death Dis 5:e1170.

Deugnier YM, Guyader D, Crantock L, Lopez JM, Turlin B, Yaouanq J, Jouanolle H, Campion JP, Launois B, Halliday JW, et al. 1993. Primary liver cancer in genetic hemochromatosis: a clinical, pathological, and pathogenetic study of 54 cases. Gastroenterology 104:228-234.

Dill MT, Tornillo L, Fritzius T, Terracciano L, Semela D, Bettler B, Heim MH, Tchorz JS. 2013. Constitutive Notch2 signaling induces hepatic tumors in mice. Hepatology 57:1607-1619.

Dorrell C, Erker L, Schug J, Kopp JL, Canaday PS, Fox AJ, Smirnova O, Duncan AW, Finegold MJ, Sander M, Kaestner KH, Grompe M. 2011. Prospective isolation of

a bipotential clonogenic liver progenitor cell in adult mice. Genes Dev 25:1193-1203.

Dotto GP. 2009. Crosstalk of Notch with p53 and p63 in cancer growth control. Nat Rev Cancer 9:587-595.

Dumble ML, Croager EJ, Yeoh GC, Quail EA. 2002. Generation and characterization of p53 null transformed hepatic progenitor cells: oval cells give rise to hepatocellular carcinoma. Carcinogenesis 23:435-445.

Duncan AW, Dorrell C, Grompe M. 2009. Stem cells and liver regeneration. Gastroenterology 137:466-481.

Duran A, Amanchy R, Linares JF, Joshi J, Abu-Baker S, Porollo A, Hansen M, Moscat J, Diaz-Meco MT. 2011. p62 is a key regulator of nutrient sensing in the mTORC1 pathway. Mol Cell 44:134-146.

Duran A, Serrano M, Leitges M, Flores JM, Picard S, Brown JP, Moscat J, Diaz-Meco MT. 2004. The atypical PKC-interacting protein p62 is an important mediator of RANK-activated osteoclastogenesis. Dev Cell 6:303-309.

Duran RV, Oppliger W, Robitaille AM, Heiserich L, Skendaj R, Gottlieb E, Hall MN. 2012. Glutaminolysis activates Rag-mTORC1 signaling. Mol Cell 47:349-358.

Espeillac C, Mitchell C, Celton-Morizur S, Chauvin C, Koka V, Gillet C, Albrecht JH, Desdouets C, Pende M. 2011. S6 kinase 1 is required for rapamycin-sensitive liver proliferation after mouse hepatectomy. J Clin Invest 121:2821-2832.

Espinoza I, Miele L. 2013. Notch inhibitors for cancer treatment. Pharmacol Ther 139:95-110.

Fan B, Malato Y, Calvisi DF, Naqvi S, Razumilava N, Ribback S, Gores GJ, Dombrowski F, Evert M, Chen X, Willenbring H. 2012. Cholangiocarcinomas can originate from hepatocytes in mice. J Clin Invest 122:2911-2915.

Fender AW, Nutter JM, Bertrand FE, Sigounas G. 2015. Notch-1 Promotes Stemness and Epithelial to Mesenchymal Transition in Colorectal Cancer. J Cell Biochem 116:2517-2527.

Fre S, Pallavi SK, Huyghe M, Lae M, Janssen KP, Robine S, Artavanis-Tsakonas S, Louvard D. 2009. Notch and Wnt signals cooperatively control cell proliferation and tumorigenesis in the intestine. Proc Natl Acad Sci U S A 106:6309-6314.

Fujita K, Maeda D, Xiao Q, Srinivasula SM. 2011. Nrf2-mediated induction of p62 controls Toll-like receptor-4-driven aggresome-like induced structure formation and autophagic degradation. Proc Natl Acad Sci U S A 108:1427-1432.

Furuyama K, Kawaguchi Y, Akiyama H, Horiguchi M, Kodama S, Kuhara T, Hosokawa S, Elbahrawy A, Soeda T, Koizumi M, Masui T, Kawaguchi M, Takaori K, Doi R,

Nishi E, Kakinoki R, Deng JM, Behringer RR, Nakamura T, Uemoto S. 2011. Continuous cell supply from a Sox9-expressing progenitor zone in adult liver, exocrine pancreas and intestine. Nat Genet 43:34-41.

Galluzzi L, Bravo-San Pedro JM, Kroemer G. 2016. Autophagy Mediates Tumor Suppression via Cellular Senescence. Trends Cell Biol 26:1-3.

Gopinathan G, Milagre C, Pearce OM, Reynolds LE, Hodivala-Dilke K, Leinster DA, Zhong H, Hollingsworth RE, Thompson R, Whiteford JR, Balkwill F. 2015. Interleukin-6 Stimulates Defective Angiogenesis. Cancer Res 75:3098-3107.

Gu JW, Rizzo P, Pannuti A, Golde T, Osborne B, Miele L. 2012. Notch signals in the endothelium and cancer "stem-like" cells: opportunities for cancer therapy. Vasc Cell 4:7.

Gu W, Wan D, Qian Q, Yi B, He Z, Gu Y, Wang L, He S. 2014. Ambra1 is an essential regulator of autophagy and apoptosis in SW620 cells: pro-survival role of Ambra1. PLoS One 9:e90151.

Guilmeau S, Flandez M, Mariadason JM, Augenlicht LH. 2010. Heterogeneity of Jagged1 expression in human and mouse intestinal tumors: implications for targeting Notch signaling. Oncogene 29:992-1002.

Guinney J, Dienstmann R, Wang X, de Reynies A, Schlicker A, Soneson C, Marisa L, Roepman P, Nyamundanda G, Angelino P, Bot BM, Morris JS, Simon IM, Gerster S, Fessler E, De Sousa EMF, Missiaglia E, Ramay H, Barras D, Homicsko K, Maru D, Manyam GC, Broom B, Boige V, Perez-Villamil B, Laderas T, Salazar R, Gray JW, Hanahan D, Tabernero J, Bernards R, Friend SH, Laurent-Puig P, Medema JP, Sadanandam A, Wessels L, Delorenzi M, Kopetz S, Vermeulen L, Tejpar S. 2015. The consensus molecular subtypes of colorectal cancer. Nat Med 21:1350-1356.

Gupta PB, Chaffer CL, Weinberg RA. 2009. Cancer stem cells: mirage or reality? Nat Med 15:1010-1012.

Haegebarth A, Clevers H. 2009. Wnt signaling, lgr5, and stem cells in the intestine and skin. Am J Pathol 174:715-721.

Hagiwara A, Nishiyama M, Ishizaki S. 2012. Branched-chain amino acids prevent insulin-induced hepatic tumor cell proliferation by inducing apoptosis through mTORC1 and mTORC2-dependent mechanisms. J Cell Physiol 227:2097-2105.

Hanahan D, Weinberg RA. 2011. Hallmarks of cancer: the next generation. Cell 144:646-674.

Hori K, Sen A, Artavanis-Tsakonas S. 2013. Notch signaling at a glance. J Cell Sci 126:2135-2140.

Huch M, Dorrell C, Boj SF, van Es JH, Li VS, van de Wetering M, Sato T, Hamer K, Sasaki N, Finegold MJ, Haft A, Vries RG, Grompe M, Clevers H. 2013. In vitro expansion of single Lgr5+ liver stem cells induced by Wnt-driven regeneration. Nature 494:247-250.

Hung TM, Yuan RH, Huang WP, Chen YH, Lin YC, Lin CW, Lai HS, Lee PH. 2015. Increased Autophagy Markers Are Associated with Ductular Reaction during the Development of Cirrhosis. Am J Pathol 185:2454-2467.

Ijichi C, Matsumura T, Tsuji T, Eto Y. 2003. Branched-chain amino acids promote albumin synthesis in rat primary hepatocytes through the mTOR signal transduction system. Biochem Biophys Res Commun 303:59-64.

Ishida Y, Yamamoto A, Kitamura A, Lamande SR, Yoshimori T, Bateman JF, Kubota H, Nagata K. 2009. Autophagic elimination of misfolded procollagen aggregates in the endoplasmic reticulum as a means of cell protection. Mol Biol Cell 20:2744-2754.

Iwasa J, Shimizu M, Shiraki M, Shirakami Y, Sakai H, Terakura Y, Takai K, Tsurumi H, Tanaka T, Moriwaki H. 2010. Dietary supplementation with branched-chain amino acids suppresses diethylnitrosamine-induced liver tumorigenesis in obese and diabetic C57BL/KsJ-db/db mice. Cancer Sci 101:460-467.

Jass JR, Sobin LH. 1989. Histological typing of intestinal tumors. WHO international histological classification of tumours. no. 15, 2nd edn.: Springer, Berlin.

Jeliazkova P, Jors S, Lee M, Zimber-Strobl U, Ferrer J, Schmid RM, Siveke JT, Geisler F. 2013. Canonical Notch2 signaling determines biliary cell fates of embryonic hepatoblasts and adult hepatocytes independent of Hes1. Hepatology 57:2469-2479.

Jewell JL, Kim YC, Russell RC, Yu FX, Park HW, Plouffe SW, Tagliabracci VS, Guan KL. 2015. Metabolism. Differential regulation of mTORC1 by leucine and glutamine. Science 347:194-198.

Jewell JL, Russell RC, Guan KL. 2013. Amino acid signalling upstream of mTOR. Nat Rev Mol Cell Biol 14:133-139.

Johnston DA, Dong B, Hughes CC. 2009. TNF induction of jagged-1 in endothelial cells is NFkappaB-dependent. Gene 435:36-44.

Kalluri R, Weinberg RA. 2009. The basics of epithelial-mesenchymal transition. J Clin Invest 119:1420-1428.

Kamiya A, Kakinuma S, Yamazaki Y, Nakauchi H. 2009. Enrichment and clonal culture of progenitor cells during mouse postnatal liver development in mice. Gastroenterology 137:1114-1126, 1126.e1111-1114.

Katsuda T, Kawamata M, Hagiwara K, Takahashi RU, Yamamoto Y, Camargo FD, Ochiya T. 2017. Conversion of Terminally Committed Hepatocytes to Culturable Bipotent Progenitor Cells with Regenerative Capacity. Cell Stem Cell 20:41-55.

Kaur J, Debnath J. 2015. Autophagy at the crossroads of catabolism and anabolism. Nat Rev Mol Cell Biol 16:461-472.

Kawaguchi T, Izumi N, Charlton MR, Sata M. 2011. Branched-chain amino acids as pharmacological nutrients in chronic liver disease. Hepatology 54:1063-1070.

Kim HA, Koo BK, Cho JH, Kim YY, Seong J, Chang HJ, Oh YM, Stange DE, Park JG, Hwang D, Kong YY. 2012. Notch1 counteracts WNT/beta-catenin signaling through chromatin modification in colorectal cancer. J Clin Invest 122:3248-3259.

Kim MH, Kim HB, Yoon SP, Lim SC, Cha MJ, Jeon YJ, Park SG, Chang IY, You HJ. 2013. Colon cancer progression is driven by APEX1-mediated upregulation of Jagged. J Clin Invest 123:3211-3230.

Kim NH, Kim HS, Li XY, Lee I, Choi HS, Kang SE, Cha SY, Ryu JK, Yoon D, Fearon ER, Rowe RG, Lee S, Maher CA, Weiss SJ, Yook JI. 2011. A p53/miRNA-34 axis regulates Snail1-dependent cancer cell epithelial-mesenchymal transition. J Cell Biol 195:417-433.

Kitade M, Factor VM, Andersen JB, Tomokuni A, Kaji K, Akita H, Holczbauer A, Seo D, Marquardt JU, Conner EA, Lee SB, Lee YH, Thorgeirsson SS. 2013. Specific fate decisions in adult hepatic progenitor cells driven by MET and EGFR signaling. Genes Dev 27:1706-1717.

Kokudo T, Suzuki Y, Yoshimatsu Y, Yamazaki T, Watabe T, Miyazono K. 2008. Snail is required for TGFbeta-induced endothelial-mesenchymal transition of embryonic stem cell-derived endothelial cells. J Cell Sci 121:3317-3324.

Komatsu M, Kurokawa H, Waguri S, Taguchi K, Kobayashi A, Ichimura Y, Sou YS, Ueno I, Sakamoto A, Tong KI, Kim M, Nishito Y, Iemura S, Natsume T, Ueno T, Kominami E, Motohashi H, Tanaka K, Yamamoto M. 2010. The selective autophagy substrate p62 activates the stress responsive transcription factor Nrf2 through inactivation of Keap1. Nat Cell Biol 12:213-223.

Kong D, Li Y, Wang Z, Sarkar FH. 2011. Cancer Stem Cells and Epithelial-to-Mesenchymal Transition (EMT)-Phenotypic Cells: Are They Cousins or Twins? Cancers (Basel) 3:716-729.

Kwon C, Cheng P, King IN, Andersen P, Shenje L, Nigam V, Srivastava D. 2011. Notch post-translationally regulates beta-catenin protein in stem and progenitor cells. Nat Cell Biol 13:1244-1251.

Lamouille S, Xu J, Derynck R. 2014. Molecular mechanisms of epithelial-mesenchymal transition. Nat Rev Mol Cell Biol 15:178-196.

Lampropoulos P, Zizi-Sermpetzoglou A, Rizos S, Kostakis A, Nikiteas N, Papavassiliou AG. 2012. TGF-beta signalling in colon carcinogenesis. Cancer Lett 314:1-7.

Lei Y, Zhang D, Yu J, Dong H, Zhang J, Yang S. 2017. Targeting autophagy in cancer stem cells as an anticancer therapy. Cancer Lett 393:33-39.

Leong KG, Niessen K, Kulic I, Raouf A, Eaves C, Pollet I, Karsan A. 2007. Jagged1-mediated Notch activation induces epithelial-to-mesenchymal transition through Slug-induced repression of E-cadherin. J Exp Med 204:2935-2948.

Li J, Hu SB, Wang LY, Zhang X, Zhou X, Yang B, Li JH, Xiong J, Liu N, Li Y, Wu YZ, Zheng QC. 2017. Autophagy-dependent generation of Axin2+ cancer stem-like cells promotes hepatocarcinogenesis in liver cirrhosis. Oncogene.

Lin JT, Chen MK, Yeh KT, Chang CS, Chang TH, Lin CY, Wu YC, Su BW, Lee KD, Chang PJ. 2010. Association of high levels of Jagged-1 and Notch-1 expression with poor prognosis in head and neck cancer. Ann Surg Oncol 17:2976-2983.

Linares JF, Duran A, Reina-Campos M, Aza-Blanc P, Campos A, Moscat J, Diaz-Meco MT. 2015. Amino Acid Activation of mTORC1 by a PB1-Domain-Driven Kinase Complex Cascade. Cell Rep 12:1339-1352.

Linares JF, Duran A, Yajima T, Pasparakis M, Moscat J, Diaz-Meco MT. 2013. K63 polyubiquitination and activation of mTOR by the p62-TRAF6 complex in nutrient-activated cells. Mol Cell 51:283-296.

Linnekamp JF, Wang X, Medema JP, Vermeulen L. 2015. Colorectal cancer heterogeneity and targeted therapy: a case for molecular disease subtypes. Cancer Res 75:245-249.

Lowes KN, Brennan BA, Yeoh GC, Olynyk JK. 1999. Oval cell numbers in human chronic liver diseases are directly related to disease severity. Am J Pathol 154:537-541.

Lu J, Ye X, Fan F, Xia L, Bhattacharya R, Bellister S, Tozzi F, Sceusi E, Zhou Y, Tachibana I, Maru DM, Hawke DH, Rak J, Mani SA, Zweidler-McKay P, Ellis LM. 2013. Endothelial cells promote the colorectal cancer stem cell phenotype through a soluble form of Jagged-1. Cancer Cell 23:171-185.

Magami Y, Azuma T, Inokuchi H, Kokuno S, Moriyasu F, Kawai K, Hattori T. 2002. Cell proliferation and renewal of normal hepatocytes and bile duct cells in adult mouse liver. Liver 22:419-425.

Malato Y, Naqvi S, Schurmann N, Ng R, Wang B, Zape J, Kay MA, Grimm D, Willenbring H. 2011. Fate tracing of mature hepatocytes in mouse liver

homeostasis and regeneration. J Clin Invest 121:4850-4860.

Marchesini G, Bianchi G, Merli M, Amodio P, Panella C, Loguercio C, Rossi Fanelli F, Abbiati R. 2003. Nutritional supplementation with branched-chain amino acids in advanced cirrhosis: a double-blind, randomized trial. Gastroenterology 124:1792-1801.

Markowitz SD, Bertagnolli MM. 2009. Molecular origins of cancer: Molecular basis of colorectal cancer. N Engl J Med 361:2449-2460.

Martin P, Diaz-Meco MT, Moscat J. 2006. The signaling adapter p62 is an important mediator of T helper 2 cell function and allergic airway inflammation. Embo j 25:3524-3533.

Matsuoka K, Iimori M, Niimi S, Tsukihara H, Watanabe S, Kiyonari S, Kiniwa M, Ando K, Tokunaga E, Saeki H, Oki E, Maehara Y, Kitao H. 2015. Trifluridine Induces p53-Dependent Sustained G2 Phase Arrest with Its Massive Misincorporation into DNA and Few DNA Strand Breaks. Mol Cancer Ther 14:1004-1013.

Medici D, Hay ED, Olsen BR. 2008. Snail and Slug promote epithelial-mesenchymal transition through beta-catenin-T-cell factor-4-dependent expression of transforming growth factor-beta3. Mol Biol Cell 19:4875-4887.

Michalopoulos GK, Barua L, Bowen WC. 2005. Transdifferentiation of rat hepatocytes into biliary cells after bile duct ligation and toxic biliary injury. Hepatology 41:535-544.

Michalopoulos GK, DeFrances MC. 1997. Liver regeneration. Science 276:60-66.

Miyajima A, Tanaka M, Itoh T. 2014. Stem/progenitor cells in liver development, homeostasis, regeneration, and reprogramming. Cell Stem Cell 14:561-574.

Miyaki M, Yamaguchi T, Iijima T, Takahashi K, Matsumoto H, Mori T. 2009. Somatic mutations of the CDC4 (FBXW7) gene in hereditary colorectal tumors. Oncology 76:430-434.

Mizushima N, Komatsu M. 2011. Autophagy: renovation of cells and tissues. Cell 147:728-741.

Muto Y, Sato S, Watanabe A, Moriwaki H, Suzuki K, Kato A, Kato M, Nakamura T, Higuchi K, Nishiguchi S, Kumada H. 2005. Effects of oral branched-chain amino acid granules on event-free survival in patients with liver cirrhosis. Clin Gastroenterol Hepatol 3:705-713.

Muto Y, Sato S, Watanabe A, Moriwaki H, Suzuki K, Kato A, Kato M, Nakamura T, Higuchi K, Nishiguchi S, Kumada H, Ohashi Y. 2006. Overweight and obesity increase the risk for liver cancer in patients with liver cirrhosis and long-term oral supplementation with branched-chain amino acid granules inhibits liver

carcinogenesis in heavier patients with liver cirrhosis. Hepatol Res 35:204-214.

Nakanishi R, Harada J, Tuul M, Zhao Y, Ando K, Saeki H, Oki E, Ohga T, Kitao H, Kakeji Y, Maehara Y. 2013. Prognostic relevance of KRAS and BRAF mutations in Japanese patients with colorectal cancer. Int J Clin Oncol 18:1042-1048.

Niessen K, Fu Y, Chang L, Hoodless PA, McFadden D, Karsan A. 2008. Slug is a direct Notch target required for initiation of cardiac cushion cellularization. J Cell Biol 182:315-325.

Nieto MA. 2013. Epithelial plasticity: a common theme in embryonic and cancer cells. Science 342:1234850.

Nishikawa H, Osaki Y. 2014. Clinical significance of therapy using branched-chain amino acid granules in patients with liver cirrhosis and hepatocellular carcinoma. Hepatol Res 44:149-158.

Nishitani S, Horie M, Ishizaki S, Yano H. 2013. Branched chain amino acid suppresses hepatocellular cancer stem cells through the activation of mammalian target of rapamycin. PLoS One 8:e82346.

Nishitani S, Ijichi C, Takehana K, Fujitani S, Sonaka I. 2004. Pharmacological activities of branched-chain amino acids: specificity of tissue and signal transduction. Biochem Biophys Res Commun 313:387-389.

Ohno T, Tanaka Y, Sugauchi F, Orito E, Hasegawa I, Nukaya H, Kato A, Matunaga S, Endo M, Tanaka Y, Sakakibara K, Mizokami M. 2008. Suppressive effect of oral administration of branched-chain amino acid granules on oxidative stress and inflammation in HCV-positive patients with liver cirrhosis. Hepatol Res 38:683-688.

Okabe M, Tsukahara Y, Tanaka M, Suzuki K, Saito S, Kamiya Y, Tsujimura T, Nakamura K, Miyajima A. 2009. Potential hepatic stem cells reside in EpCAM+ cells of normal and injured mouse liver. Development 136:1951-1960.

Okuno M, Moriwaki H, Kato M, Muto Y, Kojima S. 1995. Changes in the ratio of branched-chain to aromatic amino acids affect the secretion of albumin in cultured rat hepatocytes. Biochem Biophys Res Commun 214:1045-1050.

Ozawa T, Kazama S, Akiyoshi T, Murono K, Yoneyama S, Tanaka T, Tanaka J, Kiyomatsu T, Kawai K, Nozawa H, Kanazawa T, Yamaguchi H, Ishihara S, Sunami E, Kitayama J, Morikawa T, Fukayama M, Watanabe T. 2014. Nuclear Notch3 Expression is Associated with Tumor Recurrence in Patients with Stage II and III Colorectal Cancer. Ann Surg Oncol 21:2650-2658.

Paiva TF, Jr., de Jesus VH, Marques RA, da Costa AA, de Macedo MP, Peresi PM, Damascena A, Rossi BM, Begnami MD, de Lima VC. 2015.

Angiogenesis-related protein expression in bevacizumab-treated metastatic colorectal cancer: NOTCH1 detrimental to overall survival. BMC Cancer 15:643.

Pannequin J, Bonnans C, Delaunay N, Ryan J, Bourgaux JF, Joubert D, Hollande F. 2009. The wnt target jagged-1 mediates the activation of notch signaling by progastrin in human colorectal cancer cells. Cancer Res 69:6065-6073.

Peignon G, Durand A, Cacheux W, Ayrault O, Terris B, Laurent-Puig P, Shroyer NF, Van Seuningen I, Honjo T, Perret C, Romagnolo B. 2011. Complex interplay between beta-catenin signalling and Notch effectors in intestinal tumorigenesis. Gut 60:166-176.

Peinado H, Olmeda D, Cano A. 2007. Snail, Zeb and bHLH factors in tumour progression: an alliance against the epithelial phenotype? Nat Rev Cancer 7:415-428.

Pellegrinet L, Rodilla V, Liu Z, Chen S, Koch U, Espinosa L, Kaestner KH, Kopan R, Lewis J, Radtke F. 2011. Dll1- and dll4-mediated notch signaling are required for homeostasis of intestinal stem cells. Gastroenterology 140:1230-1240.e1231-1237.

Preisegger KH, Factor VM, Fuchsbichler A, Stumptner C, Denk H, Thorgeirsson SS. 1999. Atypical ductular proliferation and its inhibition by transforming growth factor beta1 in the 3,5-diethoxycarbonyl-1,4-dihydrocollidine mouse model for chronic alcoholic liver disease. Lab Invest 79:103-109.

Prior P. 1988. Long-term cancer risk in alcoholism. Alcohol Alcohol 23:163-171.

Purow BW, Haque RM, Noel MW, Su Q, Burdick MJ, Lee J, Sundaresan T, Pastorino S, Park JK, Mikolaenko I, Maric D, Eberhart CG, Fine HA. 2005. Expression of Notch-1 and its ligands, Delta-like-1 and Jagged-1, is critical for glioma cell survival and proliferation. Cancer Res 65:2353-2363.

Reedijk M, Odorcic S, Chang L, Zhang H, Miller N, McCready DR, Lockwood G, Egan SE. 2005. High-level coexpression of JAG1 and NOTCH1 is observed in human breast cancer and is associated with poor overall survival. Cancer Res 65:8530-8537.

Richardson MM, Jonsson JR, Powell EE, Brunt EM, Neuschwander-Tetri BA, Bhathal PS, Dixon JB, Weltman MD, Tilg H, Moschen AR, Purdie DM, Demetris AJ, Clouston AD. 2007. Progressive fibrosis in nonalcoholic steatohepatitis: association with altered regeneration and a ductular reaction. Gastroenterology 133:80-90.

Rodilla V, Villanueva A, Obrador-Hevia A, Robert-Moreno A, Fernandez-Majada V, Grilli A, Lopez-Bigas N, Bellora N, Alba MM, Torres F, Dunach M, Sanjuan X,

Gonzalez S, Gridley T, Capella G, Bigas A, Espinosa L. 2009. Jagged1 is the pathological link between Wnt and Notch pathways in colorectal cancer. Proc Natl Acad Sci U S A 106:6315-6320.

Rodriguez A, Duran A, Selloum M, Champy MF, Diez-Guerra FJ, Flores JM, Serrano M, Auwerx J, Diaz-Meco MT, Moscat J. 2006. Mature-onset obesity and insulin resistance in mice deficient in the signaling adapter p62. Cell Metab 3:211-222.

Rogov V, Dotsch V, Johansen T, Kirkin V. 2014. Interactions between autophagy receptors and ubiquitin-like proteins form the molecular basis for selective autophagy. Mol Cell 53:167-178.

Sahlgren C, Gustafsson MV, Jin S, Poellinger L, Lendahl U. 2008. Notch signaling mediates hypoxia-induced tumor cell migration and invasion. Proc Natl Acad Sci U S A 105:6392-6397.

Sancho-Bru P, Altamirano J, Rodrigo-Torres D, Coll M, Millan C, Jose Lozano J, Miquel R, Arroyo V, Caballeria J, Gines P, Bataller R. 2012. Liver progenitor cell markers correlate with liver damage and predict short-term mortality in patients with alcoholic hepatitis. Hepatology 55:1931-1941.

Sancho R, Cremona CA, Behrens A. 2015. Stem cell and progenitor fate in the mammalian intestine: Notch and lateral inhibition in homeostasis and disease. EMBO Rep 16:571-581.

Sancho R, Jandke A, Davis H, Diefenbacher ME, Tomlinson I, Behrens A. 2010. F-box and WD repeat domain-containing 7 regulates intestinal cell lineage commitment and is a haploinsufficient tumor suppressor. Gastroenterology 139:929-941.

Sansone P, Storci G, Tavolari S, Guarnieri T, Giovannini C, Taffurelli M, Ceccarelli C, Santini D, Paterini P, Marcu KB, Chieco P, Bonafe M. 2007. IL-6 triggers malignant features in mammospheres from human ductal breast carcinoma and normal mammary gland. J Clin Invest 117:3988-4002.

Santagata S, Demichelis F, Riva A, Varambally S, Hofer MD, Kutok JL, Kim R, Tang J, Montie JE, Chinnaiyan AM, Rubin MA, Aster JC. 2004. JAGGED1 expression is associated with prostate cancer metastasis and recurrence. Cancer Res 64:6854-6857.

Sato R, Semba T, Saya H, Arima Y. 2016. Concise Review: Stem Cells and Epithelial-Mesenchymal Transition in Cancer: Biological Implications and Therapeutic Targets. Stem Cells 34:1997-2007.

Seglen PO, Gordon PB. 1982. 3-Methyladenine: specific inhibitor of autophagic/lysosomal protein degradation in isolated rat hepatocytes. Proc Natl Acad Sci U S A 79:1889-1892.

Sekiya S, Suzuki A. 2012. Intrahepatic cholangiocarcinoma can arise from Notch-mediated conversion of hepatocytes. J Clin Invest 122:3914-3918.

Sekiya S, Suzuki A. 2014. Hepatocytes, rather than cholangiocytes, can be the major source of primitive ductules in the chronically injured mouse liver. Am J Pathol 184:1468-1478.

Sell S. 2001. Heterogeneity and plasticity of hepatocyte lineage cells. Hepatology 33:738-750.

Serafin V, Persano L, Moserle L, Esposito G, Ghisi M, Curtarello M, Bonanno L, Masiero M, Ribatti D, Sturzl M, Naschberger E, Croner RS, Jubb AM, Harris AL, Koeppen H, Amadori A, Indraccolo S. 2011. Notch3 signalling promotes tumour growth in colorectal cancer. J Pathol 224:448-460.

Sethi N, Dai X, Winter CG, Kang Y. 2011. Tumor-derived JAGGED1 promotes osteolytic bone metastasis of breast cancer by engaging notch signaling in bone cells. Cancer Cell 19:192-205.

Shi Y, Massague J. 2003. Mechanisms of TGF-beta signaling from cell membrane to the nucleus. Cell 113:685-700.

Shinozuka H, Lombardi B, Sell S, Iammarino RM. 1978. Early histological and functional alterations of ethionine liver carcinogenesis in rats fed a choline-deficient diet. Cancer Res 38:1092-1098.

Sikandar SS, Pate KT, Anderson S, Dizon D, Edwards RA, Waterman ML, Lipkin SM. 2010. NOTCH signaling is required for formation and self-renewal of tumor-initiating cells and for repression of secretory cell differentiation in colon cancer. Cancer Res 70:1469-1478.

Sobin LH, Wittekind Ce. 2002. TMN classification of malignant tumors no. 15, 2nd edn.: Wiley-Liss, New Yorlk.

Song YJ, Zhang SS, Guo XL, Sun K, Han ZP, Li R, Zhao QD, Deng WJ, Xie XQ, Zhang JW, Wu MC, Wei LX. 2013. Autophagy contributes to the survival of CD133+ liver cancer stem cells in the hypoxic and nutrient-deprived tumor microenvironment. Cancer Lett 339:70-81.

Sonoshita M, Aoki M, Fuwa H, Aoki K, Hosogi H, Sakai Y, Hashida H, Takabayashi A, Sasaki M, Robine S, Itoh K, Yoshioka K, Kakizaki F, Kitamura T, Oshima M, Taketo MM. 2011. Suppression of colon cancer metastasis by Aes through inhibition of Notch signaling. Cancer Cell 19:125-137.

Steigmann F, Szanto PB, Poulos A, Lim PE, Dubin A. 1984. Significance of serum aminograms in diagnosis and prognosis of liver diseases. J Clin Gastroenterol 6:453-460.

Suresh R, Ali S, Ahmad A, Philip PA, Sarkar FH. 2016. The Role of Cancer Stem Cells in Recurrent and Drug-Resistant Lung Cancer. Adv Exp Med Biol 890:57-74.

Suzuki A, Sekiya S, Onishi M, Oshima N, Kiyonari H, Nakauchi H, Taniguchi H. 2008. Flow cytometric isolation and clonal identification of self-renewing bipotent hepatic progenitor cells in adult mouse liver. Hepatology 48:1964-1978.

Tada T, Kumada T, Toyoda H, Kiriyama S, Tanikawa M, Hisanaga Y, Kanamori A, Kitabatake S, Niinomi T, Ito T, Hasegawa R, Ando Y, Yamamoto K, Tanaka T. 2014. Oral supplementation with branched-chain amino acid granules prevents hepatocarcinogenesis in patients with hepatitis C-related cirrhosis: A propensity score analysis. Hepatol Res 44:288-295.

Takegoshi K, Honda M, Okada H, Takabatake R, Matsuzawa-Nagata N, Campbell JS, Nishikawa M, Shimakami T, Shirasaki T, Sakai Y, Yamashita T, Takamura T, Tanaka T, Kaneko S. 2017. Branched-chain amino acids prevent hepatic fibrosis and development of hepatocellular carcinoma in a non-alcoholic steatohepatitis mouse model. Oncotarget 8:18191-18205.

Tanaka S, Shiraha H, Nakanishi Y, Nishina S, Matsubara M, Horiguchi S, Takaoka N, Iwamuro M, Kataoka J, Kuwaki K, Hagihara H, Toshimori J, Ohnishi H, Takaki A, Nakamura S, Nouso K, Yagi T, Yamamoto K. 2012. Runt-related transcription factor 3 reverses epithelial-mesenchymal transition in hepatocellular carcinoma. Int J Cancer 131:2537-2546.

Tarlow BD, Pelz C, Naugler WE, Wakefield L, Wilson EM, Finegold MJ, Grompe M. 2014. Bipotential adult liver progenitors are derived from chronically injured mature hepatocytes. Cell Stem Cell 15:605-618.

Theise ND, Saxena R, Portmann BC, Thung SN, Yee H, Chiriboga L, Kumar A, Crawford JM. 1999. The canals of Hering and hepatic stem cells in humans. Hepatology 30:1425-1433.

Thiery JP. 2002. Epithelial-mesenchymal transitions in tumour progression. Nat Rev Cancer 2:442-454.

Toshima T, Shirabe K, Fukuhara T, Ikegami T, Yoshizumi T, Soejima Y, Ikeda T, Okano S, Maehara Y. 2014. Suppression of autophagy during liver regeneration impairs energy charge and hepatocyte senescence in mice. Hepatology 60:290-300.

Tschaharganeh DF, Chen X, Latzko P, Malz M, Gaida MM, Felix K, Ladu S, Singer S, Pinna F, Gretz N, Sticht C, Tomasi ML, Delogu S, Evert M, Fan B, Ribback S, Jiang L, Brozzetti S, Bergmann F, Dombrowski F, Schirmacher P, Calvisi DF, Breuhahn K. 2013. Yes-associated protein up-regulates Jagged-1 and activates the Notch pathway in human hepatocellular carcinoma. Gastroenterology

144:1530-1542.e1512.

Tse JC, Kalluri R. 2007. Mechanisms of metastasis: epithelial-to-mesenchymal transition and contribution of tumor microenvironment. J Cell Biochem 101:816-829.

Tsukuma H, Hiyama T, Tanaka S, Nakao M, Yabuuchi T, Kitamura T, Nakanishi K, Fujimoto I, Inoue A, Yamazaki H, et al. 1993. Risk factors for hepatocellular carcinoma among patients with chronic liver disease. N Engl J Med 328:1797-1801.

Turner R, Lozoya O, Wang Y, Cardinale V, Gaudio E, Alpini G, Mendel G, Wauthier E, Barbier C, Alvaro D, Reid LM. 2011. Human hepatic stem cell and maturational liver lineage biology. Hepatology 53:1035-1045.

Umemura A, Park EJ, Taniguchi K, Lee JH, Shalapour S, Valasek MA, Aghajan M, Nakagawa H, Seki E, Hall MN, Karin M. 2014. Liver damage, inflammation, and enhanced tumorigenesis after persistent mTORC1 inhibition. Cell Metab 20:133-144.

Villanueva A, Alsinet C, Yanger K, Hoshida Y, Zong Y, Toffanin S, Rodriguez-Carunchio L, Sole M, Thung S, Stanger BZ, Llovet JM. 2012. Notch signaling is activated in human hepatocellular carcinoma and induces tumor formation in mice. Gastroenterology 143:1660-1669.e1667.

Yamamoto M, Taguchi Y, Ito-Kureha T, Semba K, Yamaguchi N, Inoue J. 2013. NF-kappaB non-cell-autonomously regulates cancer stem cell populations in the basal-like breast cancer subtype. Nat Commun 4:2299.

Yanger K, Zong Y, Maggs LR, Shapira SN, Maddipati R, Aiello NM, Thung SN, Wells RG, Greenbaum LE, Stanger BZ. 2013. Robust cellular reprogramming occurs spontaneously during liver regeneration. Genes Dev 27:719-724.

Yeh TS, Wu CW, Hsu KW, Liao WJ, Yang MC, Li AF, Wang AM, Kuo ML, Chi CW. 2009. The activated Notch1 signal pathway is associated with gastric cancer progression through cyclooxygenase-2. Cancer Res 69:5039-5048.

Yimlamai D, Christodoulou C, Galli GG, Yanger K, Pepe-Mooney B, Gurung B, Shrestha K, Cahan P, Stanger BZ, Camargo FD. 2014. Hippo pathway activity influences liver cell fate. Cell 157:1324-1338.

Yoshiji H, Noguchi R, Kitade M, Kaji K, Ikenaka Y, Namisaki T, Yoshii J, Yanase K, Yamazaki M, Tsujimoto T, Akahane T, Kawaratani H, Uemura M, Fukui H. 2009. Branched-chain amino acids suppress insulin-resistance-based hepatocarcinogenesis in obese diabetic rats. J Gastroenterol 44:483-491.

Zavadil J, Cermak L, Soto-Nieves N, Bottinger EP. 2004. Integration of TGF-beta/Smad and Jagged1/Notch signalling in epithelial-to-mesenchymal transition. Embo j

23:1155-1165.

Zender S, Nickeleit I, Wuestefeld T, Sorensen I, Dauch D, Bozko P, El-Khatib M, Geffers R, Bektas H, Manns MP, Gossler A, Wilkens L, Plentz R, Zender L, Malek NP. 2013. A critical role for notch signaling in the formation of cholangiocellular carcinomas. Cancer Cell 23:784-795.

Zeng Q, Li S, Chepeha DB, Giordano TJ, Li J, Zhang H, Polverini PJ, Nor J, Kitajewski J, Wang CY. 2005. Crosstalk between tumor and endothelial cells promotes tumor angiogenesis by MAPK activation of Notch signaling. Cancer Cell 8:13-23.

Zeuner A, Todaro M, Stassi G, De Maria R. 2014. Colorectal cancer stem cells: from the crypt to the clinic. Cell Stem Cell 15:692-705.

Zhang D, Zhao Q, Sun H, Yin L, Wu J, Xu J, He T, Yang C, Liang C. 2016. Defective autophagy leads to the suppression of stem-like features of CD271+ osteosarcoma cells. J Biomed Sci 23:82.

Zhang L, Liu L, He Z, Li G, Liu J, Song Z, Jin H, Rudolph KL, Yang H, Mao Y, Zhang L, Zhang H, Xiao Z, Ju Z. 2015. Inhibition of wild-type p53-induced phosphatase 1 promotes liver regeneration in mice by direct activation of mammalian target of rapamycin. Hepatology 61:2030-2041.

Zhang L, Xu L, Zhang F, Vlashi E. 2017. Doxycycline inhibits the cancer stem cell phenotype and epithelial-to-mesenchymal transition in breast cancer. Cell Cycle 16:737-745.

Zhao Y, Miyashita K, Ando T, Kakeji Y, Yamanaka T, Taguchi K, Ushijima T, Oda S, Maehara Y. 2008. Exclusive KRAS mutation in microsatellite-unstable human colorectal carcinomas with sequence alterations in the DNA mismatch repair gene, MLH1. Gene 423:188-193.

Zheng H, Kang Y. 2014. Multilayer control of the EMT master regulators. Oncogene 33:1755-1763.

Zhou BP, Deng J, Xia W, Xu J, Li YM, Gunduz M, Hung MC. 2004. Dual regulation of Snail by GSK-3beta-mediated phosphorylation in control of epithelial-mesenchymal transition. Nat Cell Biol 6:931-940.

Zhu J, Wang J, Shi Z, Franklin JL, Deane NG, Coffey RJ, Beauchamp RD, Zhang B. 2013. Deciphering genomic alterations in colorectal cancer through transcriptional subtype-based network analysis. PLoS One 8:e79282.

List of Publications

1. **Sugiyama M**, Yoshizumi T, Yoshida Y, Bekki Y, Matsumoto Y, Yoshiya S, Toshima T, Ikegami T, Itoh S, Harimoto N, Okano S, Soejima Y, Shirabe K, Maehara Y,
   p62 promotes amino acid sensitivity of mTOR pathway and hepatic differentiation in adult liver stem/progenitor cells.
   J Cell Physiol 2017; 232 (8): 2112-2124

2. **Sugiyama M**, Oki E, Nakaji Y, Tsutsumi S, Ono N, Nakanishi R, Sugiyama M, Nakashima Y, Sonoda H, Ohgaki K, Yamashita N, Saeki H, Okano S, Kitao H, Morita M, Oda Y, Maehara Y,
   High expression of the Notch ligand Jagged-1 is associated with poor prognosis after surgery for colorectal cancer.
   Cancer Sci 2016; 107 (11): 1705-1716